




Cite this: *Phys. Chem. Chem. Phys.*,  
2019, 21, 16949

# On the formation of complex organic molecules in the interstellar medium: untangling the chemical complexity of carbon monoxide–hydrocarbon containing ice analogues exposed to ionizing radiation *via* a combined infrared and reflectron time-of-flight analysis†

Matthew J. Abplanalp<sup>ab</sup> and Ralf I. Kaiser<sup>ib</sup>  <sup>★ab</sup>

Recently, over 200 molecules have been detected in the interstellar medium (ISM), with about one third being complex organic molecules (COMs), molecules containing six or more atoms. Over the last few decades, astrophysical laboratory experiments have shown that several COMs are formed *via* interaction of ionizing radiation within ices deposited on interstellar dust particles at 10 K (H<sub>2</sub>O, CH<sub>3</sub>OH, CO, CO<sub>2</sub>, CH<sub>4</sub>, NH<sub>3</sub>). However, there is still a lack of understanding of the chemical complexity that is available through individual ice constituents. The present research investigates experimentally the synthesis of carbon, hydrogen, and oxygen bearing COMs from interstellar ice analogues containing carbon monoxide (CO) and methane (CH<sub>4</sub>), ethane (C<sub>2</sub>H<sub>6</sub>), ethylene (C<sub>2</sub>H<sub>4</sub>), or acetylene (C<sub>2</sub>H<sub>2</sub>) exposed to ionizing radiation. Utilizing online and *in situ* techniques, such as infrared spectroscopy and tunable photoionization reflectron time-of-flight mass spectrometry (PI-ReTOF-MS), specific isomers produced could be characterized. A total of 12 chemically different groups were detected corresponding to C<sub>2</sub>H<sub>n</sub>O ( $n = 2, 4, 6$ ), C<sub>3</sub>H<sub>n</sub>O ( $n = 2, 4, 6, 8$ ), C<sub>4</sub>H<sub>n</sub>O ( $n = 4, 6, 8, 10$ ), C<sub>5</sub>H<sub>n</sub>O ( $n = 4, 6, 8, 10$ ), C<sub>6</sub>H<sub>n</sub>O ( $n = 4, 6, 8, 10, 12, 14$ ), C<sub>2</sub>H<sub>n</sub>O<sub>2</sub> ( $n = 2, 4$ ), C<sub>3</sub>H<sub>n</sub>O<sub>2</sub> ( $n = 4, 6, 8$ ), C<sub>4</sub>H<sub>n</sub>O<sub>2</sub> ( $n = 4, 6, 8, 10$ ), C<sub>5</sub>H<sub>n</sub>O<sub>2</sub> ( $n = 6, 8$ ), C<sub>6</sub>H<sub>n</sub>O<sub>2</sub> ( $n = 8, 10, 12$ ), C<sub>4</sub>H<sub>n</sub>O<sub>3</sub> ( $n = 4, 6, 8$ ), and C<sub>5</sub>H<sub>n</sub>O<sub>3</sub> ( $n = 6, 8$ ). More than half of these isomer specifically identified molecules have been identified in the ISM, and the remaining COMs detected here can be utilized to guide future astronomical observations. Of these isomers, three groups – alcohols, aldehydes, and molecules containing two of these functional groups – displayed varying degrees of unsaturation. Also, the detection of 1-propanol, 2-propanol, 1-butanal, and 2-methylpropanal has significant implications as the propyl and isopropyl moieties (C<sub>3</sub>H<sub>7</sub>), which have already been detected in the ISM *via* propyl cyanide and isopropyl cyanide, could be detected in our laboratory studies. General reaction mechanisms for their formation are also proposed, with distinct follow-up studies being imperative to elucidate the complexity of COMs synthesized in these ices.

Received 30th March 2019,  
Accepted 4th July 2019

DOI: 10.1039/c9cp01793c

rsc.li/pccp

## 1. Introduction

Complex organic molecules (COMs) – molecules containing six or more atoms of carbon, hydrogen, oxygen, and nitrogen such as aldehydes (HCOR), ketones (RCOR'), carboxylic acids (RCOOH), esters (RCOOR'), amides (RCONH<sub>2</sub>), and nitriles (RCN), with R and R' being an alkyl group – are ubiquitous throughout the

interstellar medium (ISM) (Fig. 1).<sup>1,2</sup> A detailed understanding of the synthetic routes of structural isomers – molecules with the same molecular formula but different orders of atoms – of COMs is of fundamental significance to the laboratory astrophysics and astronomy communities. These unique isomers are utilized as tracers to determine the physical and chemical conditions of interstellar environments and can be used to test chemical models of molecular clouds and star forming regions.<sup>3</sup> Despite the vital role of structural isomers of COMs as evolutionary fingerprints in astronomy to constrain the evolutionary stage of molecular clouds and star forming regions together with their chemical and physical boundary conditions, definitive evidence for their formation mechanisms is lacking.<sup>2,4</sup>

<sup>a</sup> W. M. Keck Research Laboratory in Astrochemistry, University of Hawaii at Manoa, Honolulu, HI, 96822, USA. E-mail: ralfk@hawaii.edu

<sup>b</sup> Department of Chemistry, University of Hawaii at Manoa, Honolulu, HI, 96822, USA

† Electronic supplementary information (ESI) available. See DOI: 10.1039/c9cp01793c

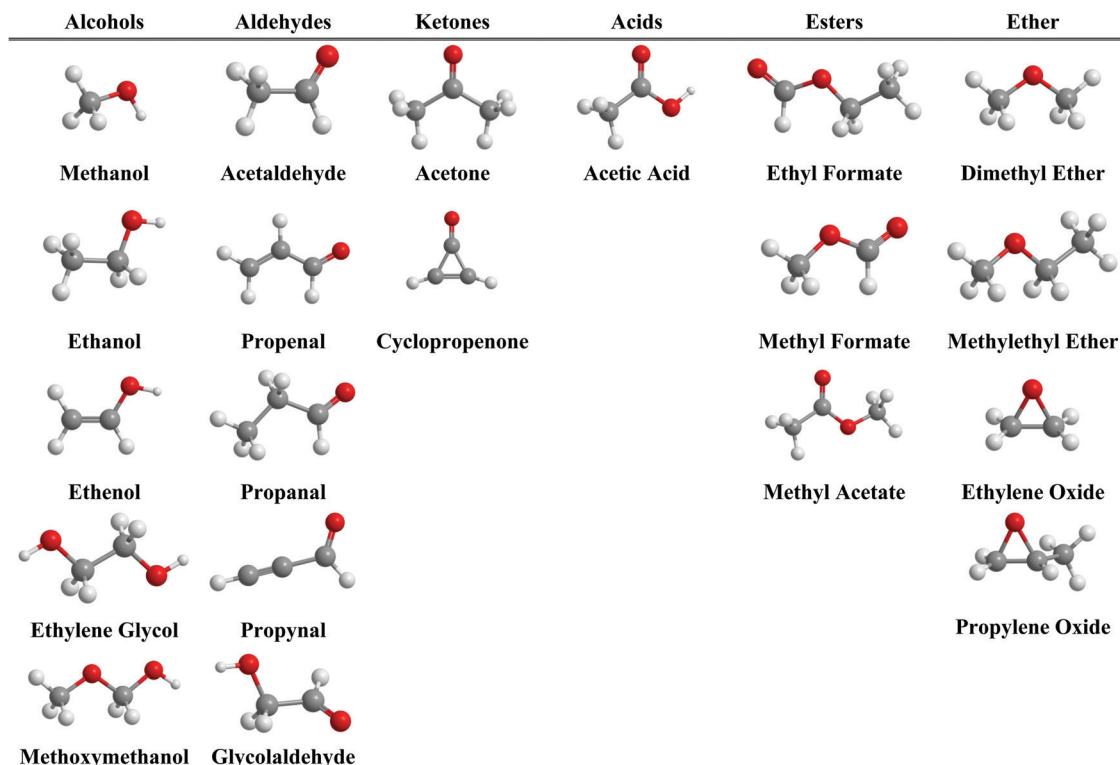


Fig. 1 Selected complex organic molecules (COMs) detected in the ISM containing carbon, hydrogen, and oxygen atoms.

Initially, astrochemical models of gas-phase-only-chemistry were utilized to explain observed COMs, but these models yielded abundances with discrepancies of more than an order of magnitude with respect to observations.<sup>2,5–9</sup> For example, acetaldehyde has been detected toward SgrB2 with a column density of  $2.2 \times 10^{14}$  molecules  $\text{cm}^{-2}$ , with respect to hydrogen, but gas-phase astrochemical models produced column densities almost four orders of magnitude less of  $5.6 \times 10^{11}$  molecules  $\text{cm}^{-2}$ .<sup>10</sup> Therefore, these ‘gas-phase only’ models have been modified in multiple ways such as by including gas phase neutral–neutral reactions, grain-surface reactions, multi-phase temperature procedures, photodesorption, and reactive desorption and by injecting complex molecules formed on the surfaces of ice-coated grains.<sup>2,6,11</sup> Nonetheless, even these improved models could not duplicate observed relative abundances of structural isomers of COMs.<sup>2,10,12</sup> However, interstellar ices comprised of water ( $\text{H}_2\text{O}$ ), methanol ( $\text{CH}_3\text{OH}$ ), carbon monoxide ( $\text{CO}$ ), carbon dioxide ( $\text{CO}_2$ ), formaldehyde ( $\text{H}_2\text{CO}$ ), methane ( $\text{CH}_4$ ), and ammonia ( $\text{NH}_3$ ) are present in molecular clouds,<sup>13</sup> and the synthesis of COMs has been linked to the processing of icy interstellar grains with ionizing radiation *via* galactic cosmic rays (GCRs) and the internal ultraviolet photon field in cold molecular clouds – the nurseries of stars and planetary systems – and in star forming regions.<sup>2,3,10,12,14–17</sup> The inclusion of solid laboratory data – rate constants, reaction products, branching ratios, temperature dependence, and chemical composition – into astrochemical reaction networks has allowed these models to more accurately match ISM abundances, which suggests that key production routes to COMs on interstellar

grains have been missing.<sup>10,12,14,15,18</sup> Incorporating the respective solid state data into models for the COMs acetaldehyde ( $\text{CH}_3\text{CHO}$ ), ethenol ( $\text{CH}_2\text{CHOH}$ ), and propylene oxide ( $\text{c-C}_3\text{H}_6\text{O}$ ) resulted in the production of column densities of  $2.75 \times 10^{14}$  molecules  $\text{cm}^{-2}$ ,  $1.55 \times 10^{14}$  molecules  $\text{cm}^{-2}$ , and  $1 \times 10^{13}$  molecules  $\text{cm}^{-2}$ , respectively. These new model abundances are very similar to observed values of  $2.2 \times 10^{14}$  molecules  $\text{cm}^{-2}$ ,  $2.2 \times 10^{14}$  molecules  $\text{cm}^{-2}$ , and  $1 \times 10^{13}$  molecules  $\text{cm}^{-2}$ , for acetaldehyde, ethenol, and propylene oxide, respectively. Therefore, novel laboratory experiments exploiting experimental techniques able to probe the formation of COMs in interstellar ice analogues *via* interaction of ionizing radiation are clearly necessary to unravel comprehensively the complex organic chemistry occurring within interstellar ices. These simulation experiments also allow identifying COMs, which have not been detected in the ISM to date, which can then be searched for in future astronomical observations *via*, for instance, the Atacama Large Millimeter/Submillimeter Array (ALMA). Although studies of the interaction of ionizing radiation with interstellar ice analogues have been carried out for the past five decades, the understanding of the synthesis of COMs in interstellar ice analogues subjected to ionizing radiation is still in its infancy.<sup>7,19,20</sup>

Previous studies have been limited by the analytical tools used to identify newly formed molecules, such as with Fourier transform infrared (FTIR) spectroscopy<sup>21–24</sup> and electron impact ionization quadrupole mass spectrometry (EI-QMS).<sup>16,25–27</sup> Here, FTIR spectroscopy of the solid state may identify functional groups of molecules, and small molecules themselves, but is

incapable of definitively identifying individual COMs.<sup>24,28,29</sup> Often these processed ices are then heated, causing the synthesized molecules to sublime into the gas phase, which simulates the transition of a cold molecular cloud into a star forming region such as Sagittarius B2.<sup>17,30–34</sup> The subliming molecules are then traditionally studied with EI-QMS, but often this causes fragmentation of the products into overlapping fragments that make it very difficult, if not impossible, to determine what parent molecule was actually produced in particular in complex gas mixtures.<sup>27,35</sup> To circumvent these drawbacks, novel analytical techniques need to be employed. Utilizing tunable vacuum-ultraviolet (VUV) single photon photoionization coupled to a reflectron time-of-flight mass spectrometer (PI-ReTOF-MS) allows a definitive isomer specific detection of complex organic molecules based on their known ionization energies (IEs).<sup>36,37</sup> Since individual COMs, as well as isomers, have discrete ionization energies, a correlation of the ionization energy with the mass-to-charge of the product helps in uniquely identifying specific COMs.<sup>38–47</sup> Note that the warm up phase is also monitored by FTIR spectroscopy in the condensed phase so that the temperature-dependent evolution of the functional groups of the COMs can be traced in the ices and correlated with their corresponding sublimation profiles.<sup>24,48</sup> Here, decays of the absorption intensities of the functional groups of the COMs in the ices can be correlated with increases of the signals of individual COMs in the gas-phase upon sublimation.<sup>49</sup>

As discussed above, ices containing carbon monoxide and methane at levels up to 50% and 11%, respectively, have been detected in the ISM.<sup>13</sup> The processing of pure methane ices at ISM temperatures has been shown to produce the C2 hydrocarbons ethane (C<sub>2</sub>H<sub>6</sub>), ethylene (C<sub>2</sub>H<sub>4</sub>), and acetylene (C<sub>2</sub>H<sub>2</sub>) as major products, as well as more complex hydrocarbons up to C<sub>22</sub>H<sub>x</sub>.<sup>16,29,46,50–54</sup> Therefore, ice analogues containing binary ice mixtures of carbon monoxide and methane, ethane, ethylene, and acetylene have been selected to study the chemical complexity of COMs that can be produced. Although interstellar ices are typically comprised of more complex mixtures as noted above – water (H<sub>2</sub>O), methanol (CH<sub>3</sub>OH), carbon monoxide (CO), carbon dioxide (CO<sub>2</sub>), formaldehyde (H<sub>2</sub>CO), methane (CH<sub>4</sub>), and ammonia (NH<sub>3</sub>) – these simplified ices are necessary to provide a thorough understanding of the chemical complexity available from these individual constituents, and the results obtained from these ice analogues can be utilized to untangle the complex chemistry occurring in more realistic ice mixtures. Although ethane, ethylene, and acetylene have not been detected in interstellar ices, their production from methane ices allows them to be utilized as proxies for different amounts of processing of ISM ices containing carbon monoxide–methane, and the unique products detected from the different carbon monoxide–hydrocarbon systems can be utilized in constraining the chemical complexity available.<sup>4,55–57</sup> Furthermore, 18 of these COMs, out of the 20 detected C, H, and O containing molecules in the ISM, are part of some groups of isomers already detected in the ISM corresponding to the molecular formulae C<sub>2</sub>H<sub>4</sub>O, C<sub>2</sub>H<sub>6</sub>O, C<sub>3</sub>H<sub>2</sub>O, C<sub>3</sub>H<sub>6</sub>O, C<sub>2</sub>H<sub>4</sub>O<sub>2</sub>, C<sub>2</sub>H<sub>6</sub>O<sub>2</sub>, and C<sub>3</sub>H<sub>6</sub>O<sub>2</sub>. Therefore, unraveling the synthetic routes to COMs by studying

only carbon, hydrogen, and oxygen containing COMs and their isomers is an important first step in understanding the chemical complexity available *via* ice phase chemistry in the ISM.

## 2. Experimental details

The experimental apparatus consists of a contamination free stainless steel ultrahigh vacuum (UHV) chamber operated at a base pressure of a few 10<sup>−11</sup> Torr.<sup>58,59</sup> A silver mirror acts as the substrate and is mounted within the UHV chamber to a cryostat that is cooled to 5.0 ± 0.1 K. The closed cycle helium cryostat (Sumitomo, RDK-415E) can be rotated in the horizontal plane or repositioned in the vertical plane of the UHV chamber utilizing its differentially pumped rotary-feedthrough (Thermionics Vacuum Products, RNN-600/FA/MCO) and UHV compatible bellow (McAllister, BLT106), respectively.<sup>60–62</sup> After the substrate was cooled, a premixed system of methane (CH<sub>4</sub>, Specialty Gases of America, 99.999%), ethane (C<sub>2</sub>H<sub>6</sub>, GasPro, 99.999%), ethylene (C<sub>2</sub>H<sub>4</sub>, Linde, 99.999%), or acetylene (C<sub>2</sub>H<sub>2</sub>, AirGas) and carbon monoxide (CO, Aldrich, 99.99%) was deposited onto the substrate *via* a glass capillary array, positioned 30 mm away, using a background pressure of 5 × 10<sup>−8</sup> Torr over a few minutes (Table 1).<sup>33</sup> To remove even trace amounts of the acetone (CH<sub>3</sub>C(O)CH<sub>3</sub>) stabilizer from the acetylene gas, a dry ice–ethanol slush bath combined with a zeolite absorber cartridge (Chromatography Research Systems, Model 300) was utilized prior to mixing the acetylene gas with the carbon monoxide gas. The deposition of each carbon monoxide–hydrocarbon mixture was monitored online and *in situ via* laser interferometry by reflecting a HeNe laser (λ = 632.8 nm; CVI Melles-Griot; 25-LHP-230) off the silver mirror into a photodiode.<sup>63–65</sup> By utilizing refractive indices (*n*) of 1.31, 1.30, 1.32, and 1.32 for carbon monoxide–methane/ethane/ethylene/acetylene ices, respectively, interference fringes were recorded, and they allow for a precise determination of the ice thickness.<sup>10,17,66</sup> The total thicknesses of the carbon monoxide–methane, –ethane, –ethylene, and –acetylene ices were calculated to be 520 ± 50 nm, 500 ± 10 nm, 550 ± 20 nm, and 800 ± 50 nm, respectively.<sup>67–69</sup> These ices had ratios of 1.4 ± 0.5 : 1.0 ± 0.4, 1.0 ± 0.3 : 1.5 ± 0.4, 1.0 ± 0.2 : 1.7 ± 0.6, and 1.0 ± 0.3 : 1.1 ± 0.5 for carbon monoxide to methane, ethane, ethylene, and acetylene, respectively. These ratios were determined by utilizing unique infrared features at 2139 cm<sup>−1</sup> (ν<sub>1</sub>, CO), 2090 cm<sup>−1</sup> (ν<sub>1</sub>, <sup>13</sup>CO), 3010 cm<sup>−1</sup> (ν<sub>3</sub>, CH<sub>4</sub>), 4203 cm<sup>−1</sup> (ν<sub>1</sub> + ν<sub>4</sub>, CH<sub>4</sub>), 2974 cm<sup>−1</sup> (ν<sub>10</sub>, C<sub>2</sub>H<sub>6</sub>), 4322 cm<sup>−1</sup> (ν<sub>6</sub> + ν<sub>10</sub>, C<sub>2</sub>H<sub>6</sub>), 949 cm<sup>−1</sup> (ν<sub>7</sub>, C<sub>2</sub>H<sub>4</sub>), 4710 cm<sup>−1</sup> (ν<sub>2</sub> + ν<sub>9</sub>, C<sub>2</sub>H<sub>4</sub>), 3240 cm<sup>−1</sup> (ν<sub>3</sub>, C<sub>2</sub>H<sub>2</sub>), and 4072 cm<sup>−1</sup> (ν<sub>1</sub> + ν<sub>5</sub>, C<sub>2</sub>H<sub>2</sub>), and their corresponding absorption coefficients of 1.1 × 10<sup>−17</sup> cm molecules<sup>−1</sup>,<sup>70</sup> 1.3 × 10<sup>−17</sup> cm molecules<sup>−1</sup>,<sup>70</sup> 1.4 × 10<sup>−17</sup> cm molecules<sup>−1</sup>,<sup>67</sup> 3.9 × 10<sup>−19</sup> cm molecules<sup>−1</sup>,<sup>67</sup> 2.2 × 10<sup>−17</sup> cm molecules<sup>−1</sup>,<sup>68</sup> 2.2 × 10<sup>−19</sup> cm molecules<sup>−1</sup>,<sup>68</sup> 1.3 × 10<sup>−17</sup> cm molecules<sup>−1</sup>,<sup>68</sup> 1.0 × 10<sup>−19</sup> cm molecules<sup>−1</sup>,<sup>68</sup> 2.4 × 10<sup>−17</sup> cm molecules<sup>−1</sup>,<sup>69</sup> and 2.3 × 10<sup>−19</sup> cm molecules<sup>−1</sup>,<sup>69</sup> respectively. Isotopically substituted starting mixtures were also utilized *via* deuterated-carbon-13-methane (<sup>13</sup>CD<sub>4</sub>, Isotec, 99% <sup>13</sup>C, 99% D), deuterated-ethylene (C<sub>2</sub>D<sub>4</sub>, C.D.N. Isotopes, 99.8% D), deuterated-acetylene

**Table 1** List of experiments and experimental parameters for each ice mixture

Ice composition	Processing	Dose (eV molecule <sup>-1</sup> )	Photoionization energy (eV)	Experiment type
CO-CH <sub>4</sub>	30 nA of 5 keV electrons for 60 minutes	3.1 ± 1.0 (CO) 3.5 ± 1.0 (CH <sub>4</sub> )	10.49, 9.8	FTIR analysis during irradiation and PI-ReTOF-MS during TPD
CO-CH <sub>4</sub>	30 nA of 5 keV electrons for 60 minutes	3.1 ± 1.0 (CO) 3.5 ± 1.0 (CH <sub>4</sub> )	—	FTIR analysis during irradiation and TPD
<sup>13</sup> CO- <sup>13</sup> CD <sub>4</sub>	30 nA of 5 keV electrons for 60 minutes	4.5 ± 0.9 ( <sup>13</sup> CO) 3.3 ± 0.7 ( <sup>13</sup> CD <sub>4</sub> )	10.49, 9.93, 9.75, 9.63	FTIR analysis during irradiation and PI-ReTOF-MS during TPD
CO-C <sub>2</sub> H <sub>6</sub>	30 nA of 5 keV electrons for 60 minutes	3.7 ± 1.0 (CO) 5.6 ± 1.3 (C <sub>2</sub> H <sub>6</sub> )	10.49	FTIR analysis during irradiation and PI-ReTOF-MS during TPD
CO-C <sub>2</sub> H <sub>6</sub>	30 nA of 5 keV electrons for 60 minutes	3.7 ± 1.0 (CO) 5.6 ± 1.3 (C <sub>2</sub> H <sub>6</sub> )	—	FTIR analysis during irradiation and TPD
C <sup>18</sup> O-C <sub>2</sub> H <sub>6</sub>	30 nA of 5 keV electrons for 60 minutes	3.9 ± 1.0 (C <sup>18</sup> O) 5.6 ± 1.3 (C <sub>2</sub> H <sub>6</sub> )	10.49, 9.8, 9.6, 8.4	FTIR analysis during irradiation and PI-ReTOF-MS during TPD
CO-C <sub>2</sub> H <sub>4</sub>	30 nA of 5 keV electrons for 60 minutes	3.6 ± 1.0 (CO) 4.9 ± 1.0 (C <sub>2</sub> H <sub>4</sub> )	10.49, 9.00	FTIR analysis during irradiation and PI-ReTOF-MS during TPD
CO-C <sub>2</sub> H <sub>4</sub>	30 nA of 5 keV electrons for 60 minutes	3.6 ± 1.0 (CO) 4.9 ± 1.0 (C <sub>2</sub> H <sub>4</sub> )	—	FTIR analysis during irradiation and TPD
C <sup>18</sup> O-C <sub>2</sub> D <sub>4</sub>	30 nA of 5 keV electrons for 60 minutes	3.9 ± 1.0 (C <sup>18</sup> O) 5.7 ± 1.0 (C <sub>2</sub> H <sub>4</sub> )	10.49, 9.60	FTIR analysis during irradiation and PI-ReTOF-MS during TPD
CO-C <sub>2</sub> H <sub>2</sub>	20 nA of 5 keV electrons for 15 minutes	0.6 ± 0.1 (CO) 0.6 ± 0.1 (C <sub>2</sub> H <sub>2</sub> )	10.49	FTIR analysis during irradiation and PI-ReTOF-MS during TPD
CO-C <sub>2</sub> H <sub>2</sub>	20 nA of 5 keV electrons for 15 minutes	0.6 ± 0.1 (CO) 0.6 ± 0.1 (C <sub>2</sub> H <sub>2</sub> )	—	FTIR analysis during irradiation and TPD
C <sup>18</sup> O-C <sub>2</sub> D <sub>2</sub>	20 nA of 5 keV electrons for 15 minutes	0.7 ± 0.1 (C <sup>18</sup> O) 0.6 ± 0.1 (C <sub>2</sub> D <sub>2</sub> )	10.82, 10.49, 9.15	FTIR analysis during irradiation and PI-ReTOF-MS during TPD



(C<sub>2</sub>D<sub>2</sub>, C.D.N. Isotopes, 99% D), carbon-13-carbon monoxide (<sup>13</sup>CO, Aldrich, 99% <sup>13</sup>C), and oxygen-18-carbon monoxide (C<sup>18</sup>O, Aldrich, 99% <sup>18</sup>O), with similar thicknesses for each system, to observe isotopic shifts in order to confirm both the infrared spectroscopy and mass spectrometry assignments (Tables 2 and 3 and Table S1, ESI†).<sup>45,71,72</sup>

Following the deposition of the binary ice, each ice mixture was analyzed online and *in situ* before, during, and after processing with an FTIR spectrometer (Nicolet 6700). The infrared spectrum was collected in absorption–reflection–absorption mode at a reflection angle of 45°, and the infrared region of 500 to 5000 cm<sup>−1</sup> was examined, using a resolution of 4 cm<sup>−1</sup>, during the irradiation of the ice with 5 keV electrons (Fig. 2 and Fig. S1–S4, ESI†). While monitoring with the FTIR spectrometer, the deposited ice was then irradiated with 5 keV electrons over an area of 1.0 ± 0.1 cm<sup>2</sup> of the ice. These energetic electrons impinge on the ice at an incidence angle of 70° relative to the surface normal of the substrate, mimicking the secondary electrons produced when GCRs penetrate interstellar ices.<sup>59,60,73–76</sup> By utilizing Monte Carlo simulations, *via* CASINO 2.42 software, and supplying the densities of methane (CH<sub>4</sub>, ρ = 0.47 g cm<sup>−3</sup>), ethane (C<sub>2</sub>H<sub>6</sub>, ρ = 0.72 g cm<sup>−3</sup>), ethylene (C<sub>2</sub>H<sub>4</sub>, ρ = 0.75 g cm<sup>−3</sup>), acetylene (C<sub>2</sub>H<sub>2</sub>, ρ = 0.76 g cm<sup>−3</sup>), and carbon monoxide (CO, ρ = 1.03 g cm<sup>−3</sup>), the penetration depths for these ices were found to range from 300 to 400 nm. Note that this penetration of the electrons results in chemistry occurring throughout the bulk of the ice mantle and not only at the surface of the ice. Also, the dose deposited *via* the energetic electrons into the ice was determined (Table 1).<sup>62,77–82</sup> Interstellar ices present in cold molecular clouds of ages 10<sup>6</sup>–10<sup>7</sup> years have been calculated to receive doses of about 0.3–3.0 eV molecule<sup>−1</sup>, respectively.<sup>76</sup> The current experiments utilized doses mimicking the higher end of this range. Although irradiation with a dose comparable to what ISM ices receive is possible, the durations to deliver these amounts of energy are significantly shorter in laboratory experiments than in the ISM, and an experiment replicating ISM irradiation times is simply not feasible. It is crucial to point out that no laboratory astrochemistry experiment worldwide can reproduce the chemical complexity and radiation environment concurrently. Therefore, simulation experiments were conducted with well-defined model ices and irradiation sources to provide a systematic understanding of the fundamental processes leading to COMs in ISM ices.

After irradiating the ice mixture, the substrate was then heated at a rate of 0.5 K min<sup>−1</sup> to 300 K (temperature programmed desorption, TPD).<sup>61,83,84</sup> The subliming molecules were then analyzed *via* EI-QMS (Extrel, Model 5221) and the PI-ReTOF-MS technique (Fig. 3).<sup>80–82</sup> The QMS operated in residual gas analyzer mode using an electron impact ionizer (70 eV) with an emission current of 1 mA to monitor the mass range of 1–200 amu during TPD.<sup>85</sup> Concurrently, the PI-ReTOF-MS system also evaluated the subliming molecules by first using single photon ionization *via* pulsed coherent VUV light to ionize the molecules. Next, these ions were detected utilizing a modified reflectron time-of-flight mass spectrometer (Jordan TOF Products, Inc.).<sup>40,85–87</sup> A series of different photoionization

energies were employed for the ice mixtures, and included 8.40 eV (λ = 147.6 nm), 9.00 eV (λ = 137.8 nm), 9.15 eV (λ = 135.5 nm), 9.60 eV (λ = 129.1 nm), 9.63 eV (λ = 128.7 nm), 9.75 eV (λ = 127.2 nm), 9.80 eV (λ = 126.5 nm), 9.93 eV (λ = 124.9 nm), 10.49 eV (λ = 118.2 nm), and 10.82 eV (λ = 114.6 nm) with fluxes of 2.0 ± 0.5 × 10<sup>12</sup> photons s<sup>−1</sup> measured.<sup>29,53,54</sup>

In detail, the VUV light utilized to photoionize the subliming molecules was generated *via* four-wave mixing. Here, non-resonant four-wave mixing by frequency tripling the third harmonic output (355 nm) of an Nd:YAG laser (Spectra-Physics Pro-250-30/Spectra-Physics Pro-270-30) in xenon gas (99.999% Praxair), used as the non-linear medium, produces 10.49 eV photons.<sup>42</sup> Alternatively, all the other photon energies (8.40 eV, 9.00 eV, 9.15 eV, 9.60 eV, 9.63 eV, 9.75 eV, 9.80 eV, 9.93 eV, 10.82 eV) were generated *via* resonant four-wave mixing by first pumping separate dye lasers (Sirah Cobra-Stretch/Sirah PrecisionScan) with 355 nm or 532 nm light from individual Nd:YAG lasers to produce photons at a resonance of either xenon or krypton and the second wavelength generated was then used to tune the VUV photon energy for each experiment. Once the VUV photons were produced, they were then separated from the input wavelengths with a lithium fluoride (LiF) lens based on their difference in refractive index.<sup>73,88</sup> This LiF separation lens was also designed to focus the VUV photons about 1 cm above the ice to photoionize subliming molecules. The photoionized molecules were then mass analyzed *via* the ReTOF-MS system utilizing a dual chevron configured multichannel plate (MCP). The detected ion signals were then amplified (Ortec 9305) and shaped using a 100 MHz discriminator. The collected mass spectra were recorded with 4 ns bin widths over 3600 sweeps using a personal computer based multichannel scaler (FAST ComTec, P7888-1 E) that was triggered at 30 Hz (Quantum Composers, 9518), resulting in a single mass spectrum per 1 K increase in temperature of the substrate (Fig. 3).

## 3. Results & discussion

### 3.1. Infrared spectroscopy

Processing of the ice mixtures resulted in several new infrared absorptions being detected (Fig. 2). These features can be assigned to ten unique small closed molecules and radicals (Table 2). The small molecules identified in the carbon monoxide–methane irradiated ices include the methyl radical (CH<sub>3</sub>) (3151 cm<sup>−1</sup>, ν<sub>3</sub>; 613 cm<sup>−1</sup>, ν<sub>2</sub>); the formyl radical (HCO) (1853 cm<sup>−1</sup>, ν<sub>3</sub>); the C2 hydrocarbons acetylene (C<sub>2</sub>H<sub>2</sub>) (3253 cm<sup>−1</sup>, ν<sub>3</sub>), ethylene (C<sub>2</sub>H<sub>4</sub>) (3093 cm<sup>−1</sup>, ν<sub>6</sub>; 957 cm<sup>−1</sup>, ν<sub>7</sub>), and ethane (C<sub>2</sub>H<sub>6</sub>) (2978 cm<sup>−1</sup>, ν<sub>10</sub>; 2920 cm<sup>−1</sup>, ν<sub>8</sub> + ν<sub>11</sub>; 2885 cm<sup>−1</sup>, ν<sub>5</sub>; 1466 cm<sup>−1</sup>, ν<sub>11</sub>; 1373 cm<sup>−1</sup>, ν<sub>6</sub>); and even carbon dioxide (CO<sub>2</sub>) (2341 cm<sup>−1</sup>, ν<sub>6</sub>) along with carbon suboxide (C<sub>3</sub>O<sub>2</sub>) (2242 cm<sup>−1</sup>, ν<sub>3</sub>; 2192 cm<sup>−1</sup>, ν<sub>1</sub>) (Fig. S1, ESI†).<sup>10,17,21,22,41</sup> Discrete small molecules identified in the carbon monoxide–ethane irradiated ices include methane (CH<sub>4</sub>) (3008 cm<sup>−1</sup>, ν<sub>3</sub>; 1300 cm<sup>−1</sup>, ν<sub>4</sub>), the formyl radical (HCO) (1855 cm<sup>−1</sup>, ν<sub>3</sub>), the hydrocarboxyl radical (HOCO) (1845 cm<sup>−1</sup>, ν<sub>2</sub>), ethylene (C<sub>2</sub>H<sub>4</sub>) (3092 cm<sup>−1</sup>, ν<sub>9</sub>; 1435 cm<sup>−1</sup>, ν<sub>12</sub>; 950 cm<sup>−1</sup>, ν<sub>7</sub>), carbon dioxide

Table 2 Infrared absorption features recorded before and after the irradiation of each ice mixture at 5 K

CO-CH <sub>4</sub>		CO-C <sub>2</sub> H <sub>6</sub>		CO-C <sub>2</sub> H <sub>4</sub>		CO-C <sub>2</sub> H <sub>2</sub>		Ref.
Before irradiation (cm <sup>-1</sup> )	After irradiation (cm <sup>-1</sup> )	Before irradiation (cm <sup>-1</sup> )	After irradiation (cm <sup>-1</sup> )	Before irradiation (cm <sup>-1</sup> )	After irradiation (cm <sup>-1</sup> )	Before irradiation (cm <sup>-1</sup> )	After irradiation (cm <sup>-1</sup> )	
4534, 4302, 4204		4400, 4357, 4321, 4272, 4251, 4177, 4161, 4126, 4100, 4070		4746, 4710, 4578, 4500, 4426, 4396, 4310, 4275, 4192		6470, 5190, 4076, 3948, 3863		<i>a</i>
		4246		4248				<i>b,c,d</i>
	4248							<i>e,f</i> <i>g,h</i>
		3260		3300				<i>i</i>
3011	3253		3105			4248		<i>a</i>
	3151		3092			3328		<i>j,k</i> <i>h,i,l</i>
	3093		3069					<i>m</i>
			3008					<i>n,o,p</i> <i>a,e,o</i> <i>q</i>
2905						3246		<i>p,r</i>
								<i>h</i>
								<i>e,d</i>
								<i>c,d</i>
2818						3010		<i>e,d</i>
								<i>e,f,o</i>
								<i>e,f,n,o</i>
2595								<i>e,h,o</i>
								<i>e,h,o</i>
								<i>e,h,o</i>
								<i>e,f,o</i>
2137								<i>e,h,o</i>
								<i>h,i,l</i>
								<i>h,i,l</i>
								<i>e,f,o</i>
2090								<i>s,t</i>
								<i>h,i,l</i>
								<i>e,f,o</i>
								<i>l,u</i>
3011								<i>h,i,l,u</i>
								<i>v</i>
								<i>w</i>
								<i>v</i>
2137								<i>i</i>
								<i>i</i>
								<i>i,v</i>
								<i>i</i>

Table 2 (continued)

CO-CH <sub>4</sub>		CO-C <sub>2</sub> H <sub>6</sub>		CO-C <sub>2</sub> H <sub>4</sub>		CO-C <sub>2</sub> H <sub>2</sub>		Assignment	Carrier	Ref.
Before irradiation (cm <sup>-1</sup> )	After irradiation (cm <sup>-1</sup> )	Before irradiation (cm <sup>-1</sup> )	After irradiation (cm <sup>-1</sup> )	Before irradiation (cm <sup>-1</sup> )	After irradiation (cm <sup>-1</sup> )	Before irradiation (cm <sup>-1</sup> )	After irradiation (cm <sup>-1</sup> )			
				2087				$\nu_1$ (C <sup>18</sup> O)	CO stretch	<i>i,w</i>
				2043				$\nu_1$ (C <sup>13</sup> C <sup>18</sup> O)	CO stretch	<i>w</i>
						1989		$\nu_2$ (C <sub>2</sub> H <sub>2</sub> )	C≡C stretch	<i>t</i>
				1965				$\nu_4 + \nu_8$ (C <sub>2</sub> H <sub>4</sub> )	Combination	<i>x</i>
				1899				$\nu_7 + \nu_8$ (C <sub>2</sub> H <sub>4</sub> )	Combination	<i>x</i>
								$\nu_{ab}$	CO stretch	<i>y</i>
1853	1855	1855	1845				1877	$\nu_3$ (HCO)	CO stretch	<i>z</i>
	1845	1845	1823				1853	$\nu_2$ (HOCO)	CO stretch	<i>aa</i>
1800–1600	1800–1600	1800–1600	1800–1600				1800–1600	$\nu_{ab}$	CO stretch	<i>q</i>
1466	1435	1435	1464	1619				$\nu_2$ (C <sub>2</sub> H <sub>4</sub> )	C=C stretch	<i>d</i>
								$\nu_{11}$ (C <sub>2</sub> H <sub>6</sub> )	CH <sub>3</sub> deformation	<i>e,h,o</i>
				1439				$\nu_{12}$ (C <sub>2</sub> H <sub>4</sub> )	CH <sub>2</sub> scissor	<i>q</i>
1373	1371	1371	1377	1339		1375		$\nu_4 + \nu_5$ (C <sub>2</sub> H <sub>2</sub> )/ $\nu_6$ (C <sub>2</sub> H <sub>6</sub> )	CH <sub>3</sub> symmetric deformation	<i>e,h,o,s</i>
								$\nu_3$ (C <sub>2</sub> H <sub>4</sub> )	CH <sub>2</sub> scissor	<i>d</i>
1302	1300	1300						$\nu_4$ (CH <sub>4</sub> )	Degenerate stretch	<i>e,f,o</i>
								$2\nu_{17}$ (C <sub>4</sub> H <sub>4</sub> )/ $\nu_6 + \nu_8$ (C <sub>4</sub> H <sub>2</sub> )	Overtone/combination	<i>m,n,p,t</i>
				1224			1240	$\nu_6$ (C <sub>2</sub> H <sub>4</sub> )	CH <sub>2</sub> rock	<i>d</i>
957	950	950		953				$\nu_7$ (C <sub>2</sub> H <sub>4</sub> )	CH <sub>2</sub> wag	<i>d</i>
821	823	823		823				$\nu_{12}$ (C <sub>2</sub> H <sub>6</sub> )/ $\nu_{10}$ (C <sub>2</sub> H <sub>4</sub> )	Bending	<i>d,h</i>
						748		$\nu_5$ (C <sub>2</sub> H <sub>2</sub> )	CCH bend	<i>a</i>
613								$\nu_2$ (CH <sub>3</sub> )	Out of plane	<i>e,f,o</i>

<sup>a</sup> Hudson *et al.* (2014), <sup>b</sup> Brock *et al.* (1994), <sup>c</sup> Bohn *et al.* (1994), <sup>d</sup> Abplanalp and Kaiser (2017), <sup>e</sup> Bennett *et al.* (2006), <sup>f</sup> Abplanalp *et al.* (2018), <sup>g</sup> Lattanzi *et al.* (2011), <sup>h</sup> Abplanalp and Kaiser (2016), <sup>i</sup> Jamieson *et al.* (2006), <sup>j</sup> Zhou *et al.* (2014), <sup>k</sup> Shimanouchi (1972), <sup>l</sup> Hepp and Herman (1999), <sup>m</sup> Zhou *et al.* (2009), <sup>n</sup> Cuyile *et al.* (2014), <sup>o</sup> Kaiser and Roessler (1998), <sup>p</sup> Zhou *et al.* (2010), <sup>q</sup> Kaiser *et al.* (2014), <sup>r</sup> Allamandola *et al.* (1989), <sup>s</sup> Bottger and Jr. (1964), <sup>t</sup> Doney *et al.* (2018), <sup>u</sup> Kim (2003), <sup>v</sup> Bennett *et al.* (2004), <sup>w</sup> Bennett *et al.* (2009), <sup>x</sup> Ennis *et al.* (2011), <sup>y</sup> Zhou *et al.* (2008), <sup>z</sup> Bennett *et al.* (2005), <sup>aa</sup> Abplanalp *et al.* (2015), <sup>ab</sup> Carbonyl stretching region (saturated/unsaturated aldehydes/ketones with mono-/di-/tri-/tetra-substituted side chains),

**Table 3** Ions detected at different photoionization energies subliming from irradiated ices of (a) CO-CH<sub>4</sub>/<sup>13</sup>CO-<sup>13</sup>CD<sub>4</sub>, (b) CO-C<sub>2</sub>H<sub>6</sub>/C<sup>18</sup>O-C<sub>2</sub>H<sub>6</sub>, (c) CO-C<sub>2</sub>H<sub>4</sub>/C<sup>18</sup>O-C<sub>2</sub>D<sub>4</sub>, and (d) CO-C<sub>2</sub>H<sub>2</sub>/C<sup>18</sup>O-C<sub>2</sub>D<sub>2</sub><sup>a</sup>

(a) Formula	CO-CH <sub>4</sub> ( <i>m/z</i> )		<sup>13</sup> CO- <sup>13</sup> CD <sub>4</sub> ( <i>m/z</i> )			
	10.49 eV	9.8 eV	10.49 eV	9.93 eV	9.75 eV	9.63 eV
C <sub>3</sub> H <sub>4</sub>	40	—	47	47	47	47
C <sub>3</sub> H <sub>6</sub>	42	42	51	51	51	—
C <sub>2</sub> H <sub>2</sub> O	42	42	46	46	46	46
C <sub>2</sub> H <sub>4</sub> O	44	44	50	50	50	50
C <sub>2</sub> H <sub>6</sub> O	46	—	54	—	—	—
C <sub>3</sub> H <sub>2</sub> O	54	—	59	59	59	—
C <sub>4</sub> H <sub>6</sub>	54	—	64	64	64	64
C <sub>3</sub> H <sub>4</sub> O	56	56	63	63	63	63
C <sub>4</sub> H <sub>8</sub>	56	56	68	68	68	68
C <sub>3</sub> H <sub>6</sub> O	58	58	67	67	67	67
C <sub>2</sub> H <sub>2</sub> O <sub>2</sub>	58	58	62	62	62	62
C <sub>3</sub> H <sub>8</sub> O	60	—	71	71	—	—
C <sub>2</sub> H <sub>4</sub> O <sub>2</sub>	60	—	66	66	66	66
C <sub>5</sub> H <sub>8</sub>	68	—	81	81	81	81
C <sub>4</sub> H <sub>4</sub> O	68	—	76	—	—	—
C <sub>5</sub> H <sub>10</sub>	70	70	85	85	85	—
C <sub>4</sub> H <sub>6</sub> O	70	70	80	80	80	80
C <sub>4</sub> H <sub>8</sub> O	72	72	84	84	84	84
C <sub>3</sub> H <sub>4</sub> O <sub>2</sub>	72	72	79	79	79	79
C <sub>4</sub> H <sub>10</sub> O	74	74	88	88	88	88
C <sub>3</sub> H <sub>6</sub> O <sub>2</sub>	74	74	83	83	83	83
C <sub>6</sub> H <sub>10</sub>	82	—	98	98	98	98
C <sub>5</sub> H <sub>6</sub> O	82	—	93	93	93	—
C <sub>5</sub> H <sub>8</sub> O	84	—	97	97	97	97
C <sub>4</sub> H <sub>4</sub> O <sub>2</sub>	84	—	92	92	92	92
C <sub>4</sub> H <sub>6</sub> O <sub>2</sub>	86	86	96	96	96	96
C <sub>5</sub> H <sub>10</sub> O	86	86	101	101	101	101
C <sub>4</sub> H <sub>8</sub> O <sub>2</sub>	88	—	100	100	100	100
C <sub>4</sub> H <sub>10</sub> O <sub>2</sub>	90	—	104	—	—	—
C <sub>6</sub> H <sub>8</sub> O	96	—	110	110	110	110
C <sub>7</sub> H <sub>14</sub>	98	—	119	119	119	—
C <sub>6</sub> H <sub>10</sub> O	98	—	114	114	114	114
C <sub>5</sub> H <sub>6</sub> O <sub>2</sub>	98	—	109	109	109	109
C <sub>7</sub> H <sub>16</sub>	100	—	123	—	—	—
C <sub>6</sub> H <sub>12</sub> O	100	100	118	118	118	118
C <sub>5</sub> H <sub>8</sub> O <sub>2</sub>	100	—	113	113	113	113
C <sub>4</sub> H <sub>4</sub> O <sub>3</sub>	100	—	108	108	108	108
C <sub>6</sub> H <sub>14</sub> O	102	102	122	—	—	—
C <sub>4</sub> H <sub>6</sub> O <sub>3</sub>	102	102	112	112	112	112
C <sub>4</sub> H <sub>8</sub> O <sub>3</sub>	104	—	116	116	116	116
C <sub>6</sub> H <sub>8</sub> O <sub>2</sub>	112	—	126	126	126	126
C <sub>5</sub> H <sub>6</sub> O <sub>3</sub>	114	114	125	125	125	125
C <sub>6</sub> H <sub>10</sub> O <sub>2</sub>	114	114	130	130	130	130
C <sub>5</sub> H <sub>8</sub> O <sub>3</sub>	116	116	129	129	129	129
C <sub>6</sub> H <sub>12</sub> O <sub>2</sub>	116	116	134	134	134	134

(b) Formula	CO-C <sub>2</sub> H <sub>6</sub> ( <i>m/z</i> )		C <sup>18</sup> O-C <sub>2</sub> H <sub>6</sub> ( <i>m/z</i> )			
	10.49 eV	9.8 eV	10.49 eV	9.8 eV	9.6 eV	8.4 eV
C <sub>3</sub> H <sub>4</sub>	40	—	40	—	—	—
C <sub>3</sub> H <sub>6</sub>	42	—	42	42	—	—
C <sub>2</sub> H <sub>2</sub> O	42	—	44	44	44	—
C <sub>2</sub> H <sub>4</sub> O	44	—	46	46	46	—
C <sub>4</sub> H <sub>6</sub>	54	—	54	54	54	—
C <sub>3</sub> H <sub>2</sub> O	54	—	56	56	56	—
C <sub>3</sub> H <sub>4</sub> O	56	—	58	58	58	—
C <sub>4</sub> H <sub>8</sub>	56	—	56	56	56	—
C <sub>3</sub> H <sub>6</sub> O	58	—	60	60	60	—
C <sub>2</sub> H <sub>2</sub> O <sub>2</sub>	58	—	62	—	—	—
C <sub>5</sub> H <sub>8</sub>	68	—	68	68	68	—
C <sub>4</sub> H <sub>4</sub> O	68	—	70	70	70	—
C <sub>5</sub> H <sub>10</sub>	70	—	70	70	70	—
C <sub>4</sub> H <sub>6</sub> O	70	—	72	72	72	—
C <sub>4</sub> H <sub>8</sub> O	72	—	74	74	74	—
C <sub>6</sub> H <sub>10</sub>	82	—	82	82	82	82
C <sub>5</sub> H <sub>6</sub> O	82	—	84	84	84	—

**Table 3** (continued)

(b) Formula	CO-C <sub>2</sub> H <sub>6</sub> ( <i>m/z</i> )		C <sup>18</sup> O-C <sub>2</sub> H <sub>6</sub> ( <i>m/z</i> )			
	10.49 eV	9.8 eV	10.49 eV	9.8 eV	9.6 eV	8.4 eV
C <sub>6</sub> H <sub>12</sub>	84	—	84	84	84	—
C <sub>5</sub> H <sub>8</sub> O	84	—	86	86	86	86
C <sub>4</sub> H <sub>4</sub> O <sub>2</sub>	84	—	88	88	88	88
C <sub>6</sub> H <sub>14</sub>	86	—	86	86	86	86
C <sub>5</sub> H <sub>10</sub> O	86	—	88	88	88	88
C <sub>4</sub> H <sub>6</sub> O <sub>2</sub>	86	—	90	90	90	—
C <sub>4</sub> H <sub>8</sub> O <sub>2</sub>	88	—	92	—	—	—
C <sub>7</sub> H <sub>14</sub>	98	—	98	98	98	—
C <sub>6</sub> H <sub>10</sub> O	98	—	100	100	100	100
C <sub>5</sub> H <sub>6</sub> O <sub>2</sub>	98	—	100	100	100	100
C <sub>8</sub> H <sub>4</sub>	100	—	100	100	100	100
C <sub>6</sub> H <sub>12</sub> O	100	—	102	102	102	—
C <sub>5</sub> H <sub>8</sub> O <sub>2</sub>	100	—	104	104	104	—
C <sub>6</sub> H <sub>14</sub> O	102	—	104	104	104	—
C <sub>8</sub> H <sub>16</sub>	112	—	112	112	112	—
C <sub>6</sub> H <sub>8</sub> O <sub>2</sub>	112	—	116	116	116	—
C <sub>6</sub> H <sub>10</sub> O <sub>2</sub>	114	—	118	118	118	—
C <sub>5</sub> H <sub>6</sub> O <sub>3</sub>	114	—	120	120	120	—
C <sub>6</sub> H <sub>12</sub> O <sub>2</sub>	116	—	120	120	120	—
C <sub>5</sub> H <sub>8</sub> O <sub>3</sub>	116	—	126	126	126	—

(c) Formula	CO-C <sub>2</sub> H <sub>4</sub> ( <i>m/z</i> )		C <sup>18</sup> O-C <sub>2</sub> D <sub>4</sub> ( <i>m/z</i> )	
	10.49 eV	9.00 eV	10.49 eV	9.60 eV
C <sub>3</sub> H <sub>4</sub>	40	—	44	—
C <sub>3</sub> H <sub>6</sub>	42	—	48	—
C <sub>2</sub> H <sub>2</sub> O	42	—	46	—
C <sub>2</sub> H <sub>4</sub> O	44	—	50	50
C <sub>4</sub> H <sub>2</sub>	50	—	52	—
C <sub>4</sub> H <sub>4</sub>	52	—	56	56
C <sub>4</sub> H <sub>6</sub>	54	—	60	60
C <sub>3</sub> H <sub>2</sub> O	54	—	58	—
C <sub>3</sub> H <sub>4</sub> O	56	56	62	62
C <sub>4</sub> H <sub>8</sub>	56	56	64	64
C <sub>2</sub> H <sub>2</sub> O <sub>2</sub>	58	64	64	—
C <sub>3</sub> H <sub>6</sub> O	58	—	66	—
C <sub>5</sub> H <sub>6</sub>	66	66	72	72
C <sub>5</sub> H <sub>8</sub>	68	68	76	76
C <sub>4</sub> H <sub>4</sub> O	68	68	74	—
C <sub>5</sub> H <sub>10</sub>	70	70	80	80
C <sub>4</sub> H <sub>6</sub> O	70	70	78	78
C <sub>5</sub> H <sub>12</sub>	72	—	84	—
C <sub>4</sub> H <sub>8</sub> O	72	—	82	—
C <sub>3</sub> H <sub>4</sub> O <sub>2</sub>	72	—	80	80
C <sub>6</sub> H <sub>6</sub>	78	78	84	—
C <sub>6</sub> H <sub>8</sub>	80	80	88	88
C <sub>5</sub> H <sub>4</sub> O	80	80	86	—
C <sub>6</sub> H <sub>10</sub>	82	82	92	92
C <sub>5</sub> H <sub>6</sub> O	82	82	90	90
C <sub>6</sub> H <sub>12</sub>	84	84	96	96
C <sub>5</sub> H <sub>8</sub> O	84	84	94	94
C <sub>4</sub> H <sub>4</sub> O <sub>2</sub>	84	84	92	92
C <sub>6</sub> H <sub>14</sub>	86	—	100	100
C <sub>5</sub> H <sub>10</sub> O	86	—	98	98
C <sub>4</sub> H <sub>6</sub> O <sub>2</sub>	86	—	96	96
C <sub>7</sub> H <sub>6</sub>	90	—	96	96
C <sub>4</sub> H <sub>10</sub> O <sub>2</sub>	90	—	104	104
C <sub>7</sub> H <sub>8</sub>	92	92	100	100
C <sub>6</sub> H <sub>4</sub> O	92	92	98	98
C <sub>7</sub> H <sub>10</sub>	94	94	104	104
C <sub>6</sub> H <sub>6</sub> O	94	94	102	—
C <sub>7</sub> H <sub>12</sub>	96	96	108	108
C <sub>6</sub> H <sub>8</sub> O	96	96	106	106
C <sub>7</sub> H <sub>14</sub>	98	98	112	112
C <sub>6</sub> H <sub>10</sub> O	98	98	110	110
C <sub>6</sub> H <sub>12</sub> O	100	—	114	—
C <sub>6</sub> H <sub>14</sub> O	102	102	118	—
C <sub>8</sub> H <sub>10</sub>	106	106	116	—

Table 3 (continued)

(c) Formula	CO–C <sub>2</sub> H <sub>4</sub> ( <i>m/z</i> )		C <sup>18</sup> O–C <sub>2</sub> D <sub>4</sub> ( <i>m/z</i> )	
	10.49 eV	9.00 eV	10.49 eV	9.60 eV
C <sub>8</sub> H <sub>12</sub>	108	108	120	120
C <sub>8</sub> H <sub>14</sub>	110	110	124	124
C <sub>8</sub> H <sub>16</sub>	112	112	128	128
C <sub>9</sub> H <sub>6</sub>	114	114	120	120
C <sub>9</sub> H <sub>14</sub>	122	122	136	—
C <sub>9</sub> H <sub>16</sub>	124	124	140	140
C <sub>10</sub> H <sub>18</sub>	138	138	156	156
C <sub>10</sub> H <sub>20</sub>	140	140	160	160

(d) Formula	CO–C <sub>2</sub> H <sub>2</sub> ( <i>m/z</i> )		C <sup>18</sup> O–C <sub>2</sub> D <sub>2</sub> ( <i>m/z</i> )	
	10.49 eV	10.82 eV	10.49 eV	9.15 eV
C <sub>3</sub> H <sub>4</sub>	40	44	44	—
C <sub>2</sub> H <sub>2</sub> O	42	46	46	—
C <sub>4</sub> H <sub>2</sub>	50	52	52	—
C <sub>4</sub> H <sub>4</sub>	52	56	56	—
C <sub>3</sub> H <sub>2</sub> O	54	58	58	—
C <sub>4</sub> H <sub>6</sub>	54	60	60	60
C <sub>3</sub> H <sub>4</sub> O	56	62	62	—
C <sub>4</sub> H <sub>8</sub>	56	64	64	—
C <sub>3</sub> H <sub>6</sub> O	58	66	66	—
C <sub>2</sub> H <sub>2</sub> O <sub>2</sub>	58	64	64	—
C <sub>5</sub> H <sub>4</sub>	64	68	68	68
C <sub>5</sub> H <sub>6</sub>	66	72	72	72
C <sub>4</sub> H <sub>4</sub> O	68	74	74	—
C <sub>5</sub> H <sub>8</sub>	68	76	76	—
C <sub>5</sub> H <sub>10</sub>	70	80	80	80
C <sub>6</sub> H <sub>2</sub>	74	76	76	—
C <sub>3</sub> H <sub>6</sub> O <sub>2</sub>	74	84	84	84
C <sub>6</sub> H <sub>4</sub>	76	80	80	80
C <sub>3</sub> H <sub>8</sub> O <sub>2</sub>	76	88	88	88
C <sub>6</sub> H <sub>6</sub>	78	84	84	84
C <sub>5</sub> H <sub>4</sub> O	80	86	86	86
C <sub>6</sub> H <sub>8</sub>	80	88	88	88
C <sub>5</sub> H <sub>6</sub> O	82	90	90	90
C <sub>6</sub> H <sub>10</sub>	82	92	92	92
C <sub>5</sub> H <sub>8</sub> O	84	94	94	94
C <sub>7</sub> H <sub>6</sub>	90	96	96	96
C <sub>4</sub> H <sub>10</sub> O <sub>2</sub>	90	104	104	104
C <sub>6</sub> H <sub>4</sub> O	92	98	98	—
C <sub>6</sub> H <sub>6</sub> O	94	102	102	—
C <sub>8</sub> H <sub>6</sub>	102	108	108	108
C <sub>8</sub> H <sub>8</sub>	104	112	112	112
C <sub>10</sub> H <sub>8</sub>	128	136	136	136

<sup>a</sup> Italics indicates a tentative detection.

(CO<sub>2</sub>) (2345 cm<sup>−1</sup>,  $\nu_6$ ), and carbon suboxide (C<sub>3</sub>O<sub>2</sub>) (2242 cm<sup>−1</sup>,  $\nu_3$ ; 2192 cm<sup>−1</sup>,  $\nu_1$ ) (Fig. S2, ESI†).<sup>10,54,89,90</sup> The specific small molecules detected in the carbon monoxide–ethylene irradiated ices were the formyl radical (HCO) (1853 cm<sup>−1</sup>,  $\nu_3$ ), the hydrocarboxyl radical (HOCO) (1823 cm<sup>−1</sup>,  $\nu_2$ ), and the C2 hydrocarbons acetylene (C<sub>2</sub>H<sub>2</sub>) (3245 cm<sup>−1</sup>,  $\nu_3$ ; 1377 cm<sup>−1</sup>,  $\nu_4 + \nu_5$ ; 758 cm<sup>−1</sup>,  $\nu_5$ ) and ethane (C<sub>2</sub>H<sub>6</sub>) (2965 cm<sup>−1</sup>,  $\nu_1$ ; 2920 cm<sup>−1</sup>,  $\nu_8 + \nu_{11}$ ; 2880 cm<sup>−1</sup>,  $\nu_5$ ; 2832 cm<sup>−1</sup>,  $\nu_6 + \nu_{11}$ ; 2740 cm<sup>−1</sup>,  $\nu_2 + \nu_6$ ; 1464 cm<sup>−1</sup>,  $\nu_{11}$ ; 1377 cm<sup>−1</sup>,  $\nu_6$ ) (Fig. S3, ESI†).<sup>34,53,66</sup> Finally, the FTIR analysis of the carbon monoxide–acetylene irradiated ices showed the formyl radical (HCO) (1853 cm<sup>−1</sup>,  $\nu_3$ ), ethylene (C<sub>2</sub>H<sub>4</sub>) (2978 cm<sup>−1</sup>,  $\nu_{11}$ ), ethane (C<sub>2</sub>H<sub>6</sub>) (2978 cm<sup>−1</sup>,  $\nu_{10}$ ), diacetylene (C<sub>4</sub>H<sub>2</sub>) (3320 cm<sup>−1</sup>,  $\nu_4$ ; 1240 cm<sup>−1</sup>,  $\nu_6 + \nu_8$ ), vinylacetylene (C<sub>4</sub>H<sub>4</sub>) (3285 cm<sup>−1</sup>,  $\nu_4$ ; 2978 cm<sup>−1</sup>,  $\nu_6 + \nu_7$ ; 1240 cm<sup>−1</sup>,  $2\nu_{17}$ ), and carbon suboxide (C<sub>3</sub>O<sub>2</sub>) (2250 cm<sup>−1</sup>,  $\nu_3$ ) (Fig. S4, ESI†).<sup>91</sup> These assignments were

also confirmed *via* their isotopic shifts<sup>92</sup> in <sup>13</sup>CO–<sup>13</sup>CD<sub>4</sub>, C<sup>18</sup>O–C<sub>2</sub>H<sub>6</sub>, C<sup>18</sup>O–C<sub>2</sub>D<sub>4</sub>, and C<sup>18</sup>O–C<sub>2</sub>D<sub>2</sub> ices, respectively (Table S1, ESI†).

However, several of these features remain past the sublimation of these assigned molecules, proving that they are also related to more complex species formed by irradiation. Furthermore, a broad absorption feature spanning 1600–1800 cm<sup>−1</sup>, which can be correlated with a carbonyl functional group (C=O), was detected in each ice mixture. This infrared detection has been shown to belong to multiple carriers, rather than a single molecule, generally defined as saturated aldehydes, alkylketones,  $\alpha,\beta$ -unsaturated aldehydes/ketones,  $\alpha,\beta$ -dicarbonyl compounds in the keto–enol form,  $\alpha,\beta,\gamma,\delta$ -unsaturated aldehydes/ketones, and/or unsaturated dicarbonyls. In summary, infrared spectroscopy identified ten specific small molecules as well as newly formed molecules carrying the carbonyl group.<sup>93–97</sup>

### 3.2. Mass spectrometry – PI-ReTOF-MS

Although FTIR analysis revealed the presence of several small molecules, it is incapable of definitively identifying more complex species such as the parent molecules of the observed carbonyl stretching band. However, the complementary analytical technique, PI-ReTOF-MS, provides extremely sensitive analysis that allows for the determination of the identity of the molecular formulae of the complex molecules produced, and in some instances even the specific isomers formed. Here, we discuss the detected molecular formulae containing carbon, hydrogen, and oxygen atoms, and molecules formed solely from each of the hydrocarbon reactants – CH<sub>4</sub>, C<sub>2</sub>H<sub>6</sub>, C<sub>2</sub>H<sub>4</sub>, and C<sub>2</sub>H<sub>2</sub> as pure ices – have been investigated and disseminated previously utilizing the same technique.<sup>29,46,53,54</sup>

**3.2.1. C<sub>2</sub>H<sub>n</sub>O ( $n = 2, 4, 6$ ).** PI-ReTOF-MS detected ions at  $m/z = 42$ ,  $m/z = 44$ , and  $m/z = 46$  corresponding to the molecular formulae C<sub>2</sub>H<sub>2</sub>O, C<sub>2</sub>H<sub>4</sub>O, and C<sub>2</sub>H<sub>6</sub>O, respectively (Fig. 4 and Fig. S5–S7, ESI† and Table 3). These assignments were also confirmed *via* isotopic shifts as previously discussed to separate the molecular formulae from overlapping mass-to-charge ratios, for example from C<sub>3</sub>H<sub>6</sub> ( $m/z = 42$ ). The ion signal for C<sub>2</sub>H<sub>2</sub>O ( $m/z = 42$ ) was observed in all the ice mixtures, C<sub>2</sub>H<sub>4</sub>O ( $m/z = 44$ ) was detected in all the systems except for the carbon monoxide–acetylene ices, and C<sub>2</sub>H<sub>6</sub>O ( $m/z = 46$ ) was only seen subliming from the irradiated carbon monoxide–methane ices using a PI energy of 10.49 eV. Here, the sublimation event for the C<sub>2</sub>H<sub>n</sub>O ions, as well as the isotopologues studied, began at 79 K, 101 K, and 100 K in all ices in which they were detected for increasing  $n$ . However, all of these groups, C<sub>2</sub>H<sub>2</sub>O, C<sub>2</sub>H<sub>4</sub>O, and C<sub>2</sub>H<sub>6</sub>O, display a bimodal sublimation profile, suggesting that multiple isomers may have been formed.

The ions corresponding to C<sub>2</sub>H<sub>n</sub>O ( $n = 2, 4, 6$ ) represent the simplest carbon, hydrogen, and oxygen atom containing molecules detected *via* PI-ReTOF-MS in these experiments, but each of these formulae has multiple possible isomers. The possible isomers corresponding to C<sub>2</sub>H<sub>2</sub>O are ketene (H<sub>2</sub>CCO, IE =  $9.61 \pm 0.03$  eV),<sup>98</sup> ethynol (HCCOH, IE = 9.75 eV),<sup>99</sup> and oxirene (c-C<sub>2</sub>H<sub>2</sub>O). To our knowledge, the photoionization energy of oxirene has not been measured, and ethynol's photoionization energy is a calculated value.<sup>99</sup> The ketene isomer, which is also the most stable isomer, has been observed in the



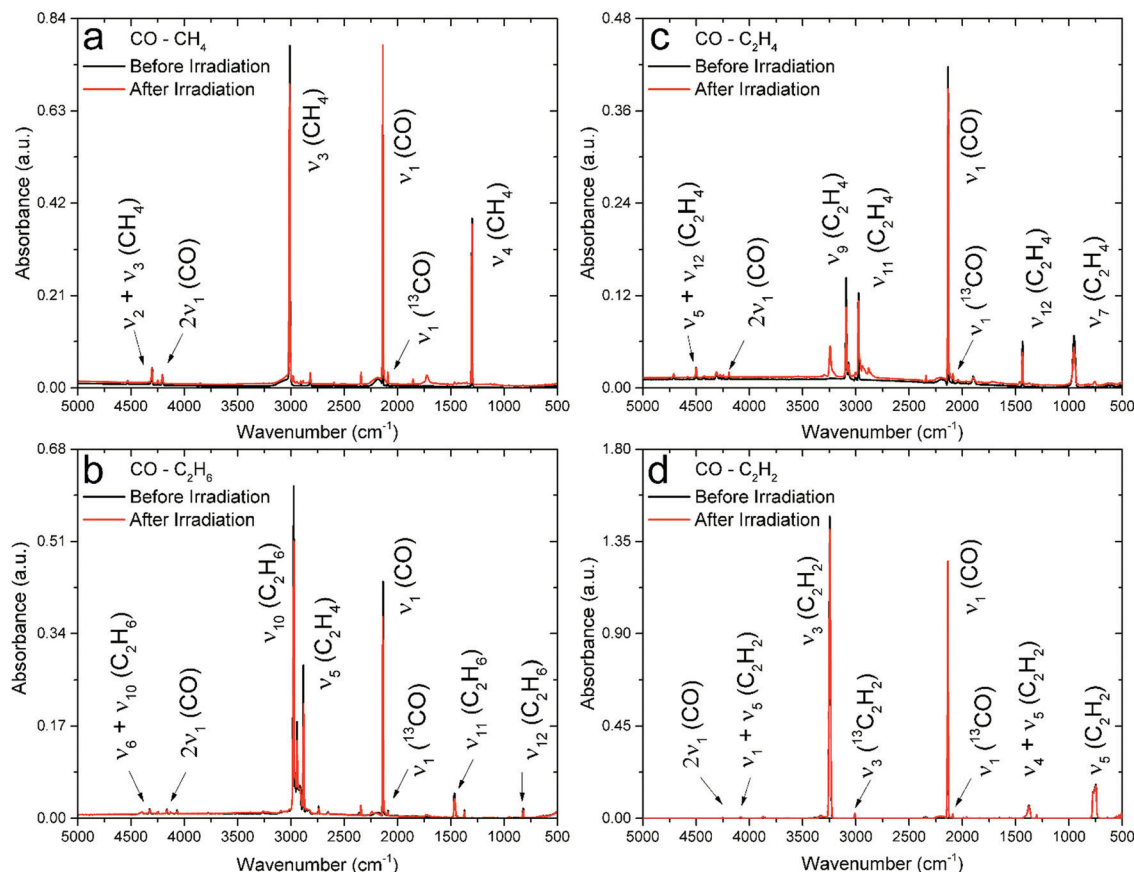


Fig. 2 Infrared spectra from 500 to 5000 cm<sup>-1</sup> before (black) and after (red) irradiation of (a) carbon monoxide–methane (CO–CH<sub>4</sub>), (b) carbon monoxide–ethane (CO–C<sub>2</sub>H<sub>6</sub>), (c) carbon monoxide–ethylene (CO–C<sub>2</sub>H<sub>4</sub>), and (d) carbon monoxide–acetylene (CO–C<sub>2</sub>H<sub>2</sub>). Assignments of reactants and products are compiled in Table 2.

ISM, but the other less stable isomers have not been detected to date.<sup>1</sup> Interestingly the sublimation profile of C<sub>2</sub>H<sub>2</sub>O at PI = 10.82 eV shows two peaks in the carbon monoxide–acetylene system (Fig. S7, ESI†). The first peak observed in the sublimation spectrum corresponds to ketene as tuning the PI energy below ethynol's ionization energy (9.75 eV) still shows a signal, and this can only be due to ketene. This second peak is due to another isomer that could be ionized by the higher photon energy since this second peak does not appear in any lower PI energies utilized. Here, this second peak may be due to ethynol and/or oxirene, but is more likely to be due to ethynol, and the calculated photoionization cross section is very low at 10.49 eV. This assignment is further supported by analysis of the C<sub>2</sub>H<sub>4</sub>O and C<sub>3</sub>H<sub>6</sub>O systems, where isomers incorporating an oxygen atom into the ringed molecule did not occur. Furthermore, the higher sublimation temperature also supports the formation of ethynol as the ethenol (CH<sub>2</sub>CHOH) and 1-propenol (CH<sub>3</sub>CHCHOH) isomers sublime at higher temperatures than their aldehyde isomers acetaldehyde (CH<sub>3</sub>CHO) and propanal (CH<sub>3</sub>CH<sub>2</sub>CHO), respectively. For the carbon monoxide–methane and –ethane systems this ion signal decreases corresponding to the PI cross section of ketene. Alternatively, the carbon monoxide–ethylene experiments showed a large decrease in the signal when tuning the PI energy from 10.49 eV to 9.60 eV.

Similarly to the C<sub>2</sub>H<sub>2</sub>O ion signal observed at 10.82 eV, a bimodal structure was observed at PI = 10.49 eV for C<sub>2</sub>H<sub>4</sub>O in the carbon monoxide–methane system, and tentatively in the carbon monoxide–ethane and –ethylene ices, but no signal was detected in the acetylene containing ice. Again the doublet structure suggests that multiple isomers contribute to the C<sub>2</sub>H<sub>4</sub>O ion signal. The three isomers possible for this signal include ethenol (CH<sub>2</sub>CHOH, IE = 9.33 ± 0.05 eV),<sup>100</sup> acetaldehyde (CH<sub>3</sub>CHO, IE = 10.23 ± 0.01 eV),<sup>100</sup> and oxirane (c-C<sub>2</sub>H<sub>4</sub>O, IE = 10.56 ± 0.01 eV).<sup>101</sup> Interestingly, all of these isomers have been detected in the ISM.<sup>1</sup> First, at a PI energy of 10.49 eV the cyclic oxirane isomer cannot be ionized and therefore cannot be detected. However, the bimodal structure of the C<sub>2</sub>H<sub>4</sub>O sublimation peak suggests that it is due to more than a single isomer, which would indicate that both the remaining isomers were formed. By tuning the PI energy below the ionization energy of acetaldehyde (IE = 10.23 ± 0.01 eV), it is shown that both acetaldehyde and ethenol are formed as the first peak is no longer observed, but the second peak is still detectable in the carbon monoxide–methane and –ethane mixtures. Therefore, the initial peak belongs to acetaldehyde, while the latter peak is due to ethenol. Ethenol can only be tentatively identified in the carbon monoxide–ethylene ice, but acetaldehyde can be confirmed.



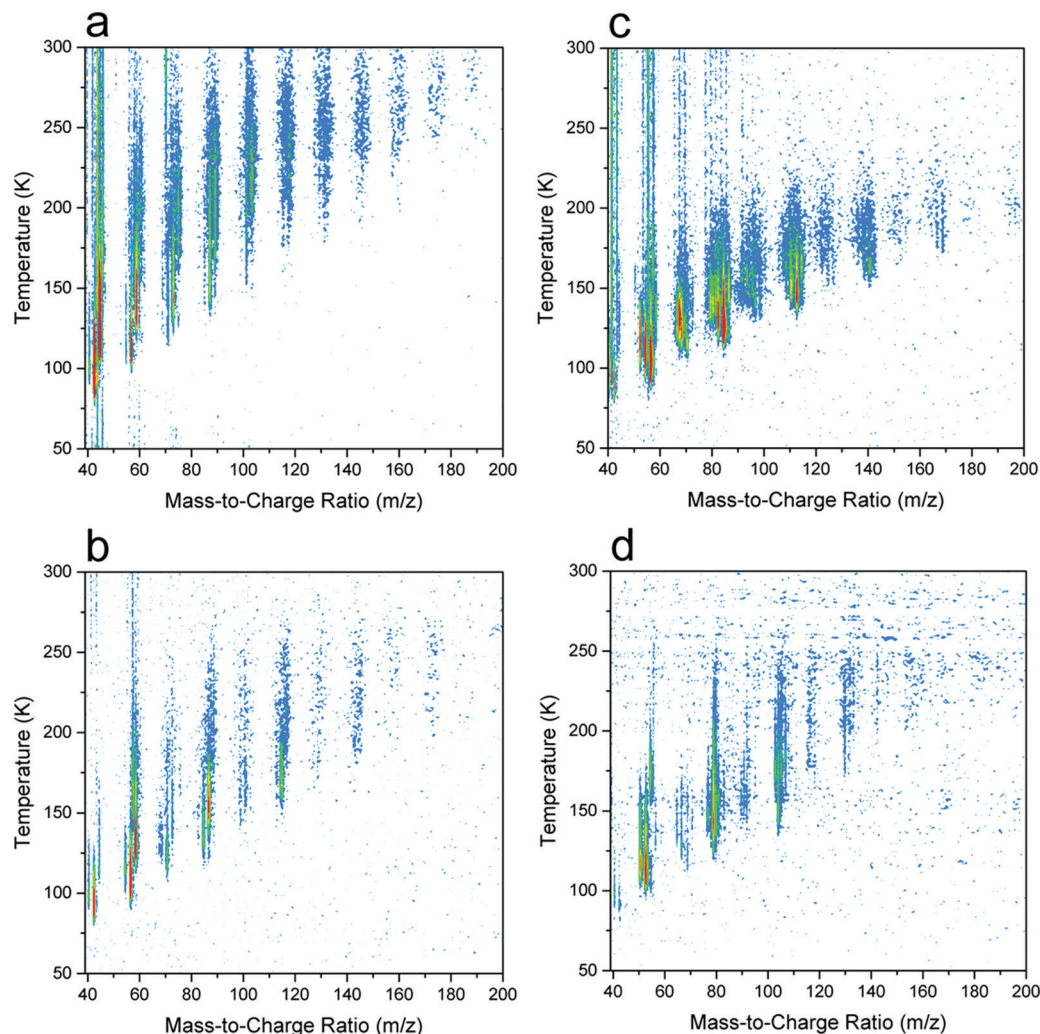


Fig. 3 PI-ReTOF-MS data recorded at a photon energy of 10.49 eV as a function of temperature of the newly formed products subliming into the gas phase from the irradiated (a) carbon monoxide–methane (CO–CH<sub>4</sub>), (b) carbon monoxide–ethane (CO–C<sub>2</sub>H<sub>6</sub>), (c) carbon monoxide–ethylene (CO–C<sub>2</sub>H<sub>4</sub>), and (d) carbon monoxide–acetylene (CO–C<sub>2</sub>H<sub>2</sub>) ices.

Finally, the most highly saturated form of this group is the C<sub>2</sub>H<sub>6</sub>O ion signal corresponding to ethanol (CH<sub>3</sub>CH<sub>2</sub>OH, IE = 10.48 ± 0.07 eV) and/or dimethyl ether (CH<sub>3</sub>OCH<sub>3</sub>, IE = 10.03 ± 0.03 eV).<sup>102</sup> Like the C<sub>2</sub>H<sub>4</sub>O isomers, both C<sub>2</sub>H<sub>6</sub>O isomers have been detected in the ISM.<sup>1</sup> A very small signal corresponding to C<sub>2</sub>H<sub>6</sub>O ions was only detected in the carbon monoxide–methane system. While the tunable energies utilized in that study were not designed to separate the C<sub>2</sub>H<sub>6</sub>O isomers, there were two observable peaks at 103–120 K and 147–202 K that corresponded well to the sublimation events for dimethyl ether (98–115 K) and ethanol (140–153 K). These ranges were determined from calibration ices of dimethyl ether and ethanol that were deposited and sublimed in the same way as the carbon monoxide–hydrocarbon ices while monitoring with PI-ReTOF-MS at 10.49 eV.<sup>40,83</sup>

**3.2.2. C<sub>3</sub>H<sub>n</sub>O (*n* = 2, 4, 6, 8).** Ions corresponding to the general formula C<sub>3</sub>H<sub>n</sub>O (*n* = 2, 4, 6, 8) were also detected using PI-ReTOF-MS (Fig. 5 and Fig. S8–S10, ESI<sup>†</sup>). The assignment of molecules to C<sub>3</sub>H<sub>2</sub>O (*m/z* = 54), C<sub>3</sub>H<sub>4</sub>O (*m/z* = 56), C<sub>3</sub>H<sub>6</sub>O (*m/z* = 58),

and C<sub>3</sub>H<sub>8</sub>O (*m/z* = 60) in this group was also confirmed *via* their isotopic shifts (Table 3). Here, the C<sub>3</sub>H<sub>2</sub>O (*m/z* = 54), C<sub>3</sub>H<sub>4</sub>O (*m/z* = 56), and C<sub>3</sub>H<sub>6</sub>O (*m/z* = 58) ion signals were observed in all the carbon monoxide–hydrocarbon ices, and the C<sub>3</sub>H<sub>8</sub>O (*m/z* = 60) ion signal was detected only in the carbon monoxide–methane system and tentatively in the carbon monoxide–ethane ice at PI = 10.49 eV. The sublimation event for the C<sub>3</sub>H<sub>n</sub>O ions, as well as the isotopologues studied, began at 98 K, 91 K, 117 K and 112 K in the ices in which they were observed for increasing *n*. Similarly to the C<sub>2</sub>H<sub>n</sub>O system, most of the sublimation profiles of this group display multiple peaks in several of the spectra again, or very broad peaks, suggesting that more than a single isomer was formed.

Surprisingly, the ions corresponding to C<sub>3</sub>H<sub>2</sub>O show different sublimation profiles across the different ice mixtures, which are all non-polar. Here, the C<sub>3</sub>H<sub>2</sub>O group consists of three isomers, methyleneketene (CH<sub>2</sub>CCO, IE = 8.90 ± 0.05 eV), cyclopropenone (c-C<sub>3</sub>H<sub>2</sub>O, IE = 9.26 ± 0.05 eV), and propynal (HCCCHO, IE = 10.62 ± 0.15 eV).<sup>38</sup> Both the propynal and

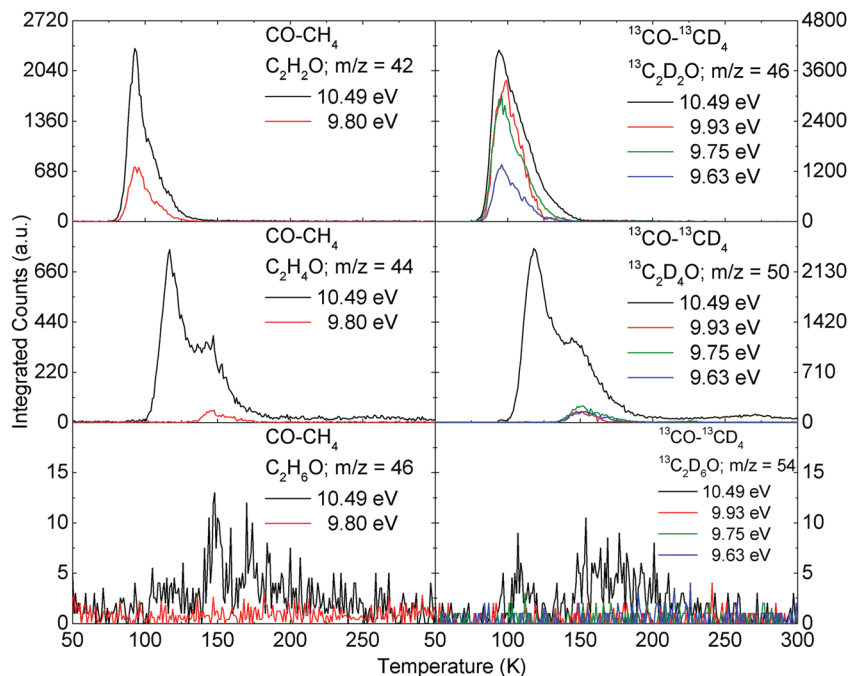


Fig. 4 PI-ReTOF-MS ion signals for  $C_2H_nO$  ( $n = 2, 4, 6$ ) versus temperature subliming from carbon monoxide–methane ice ( $CO-CH_4$ ;  $^{13}CO-^{13}CD_4$ ).

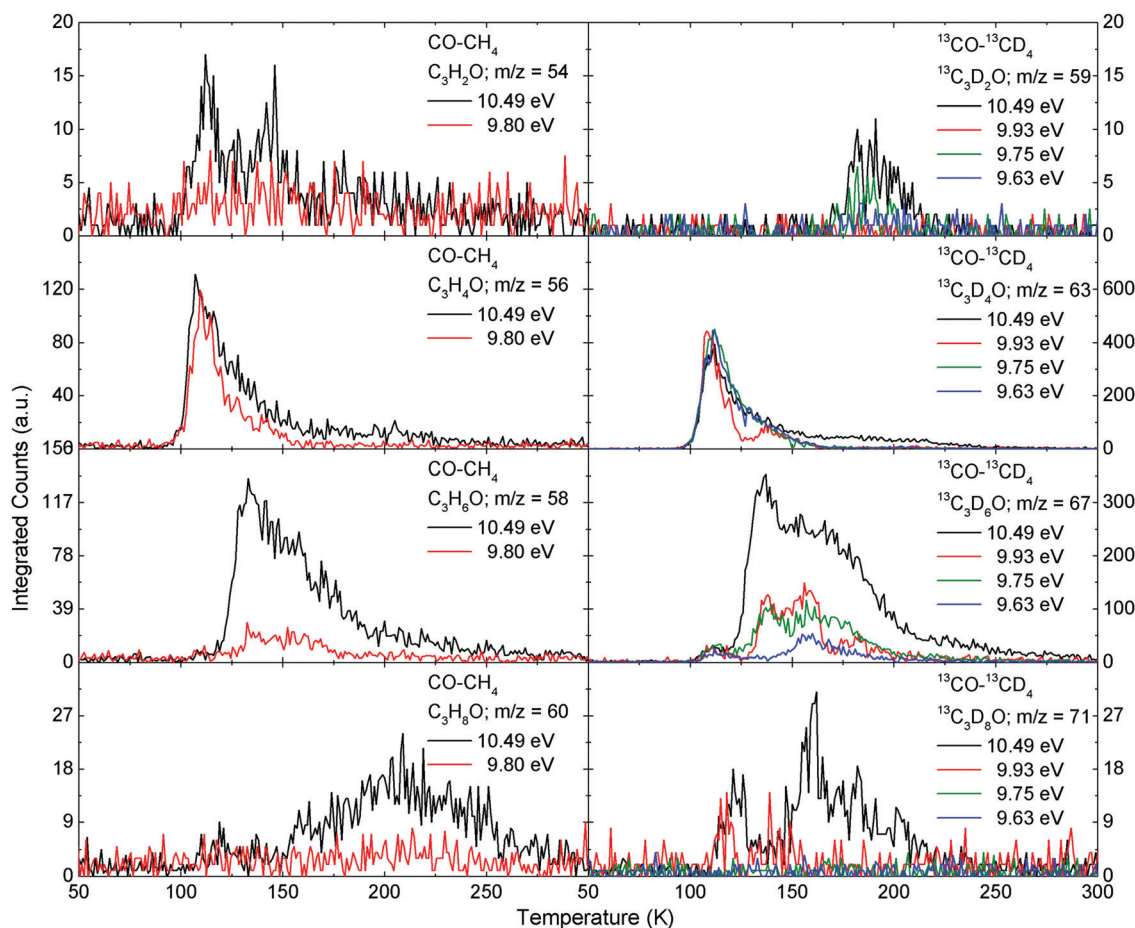


Fig. 5 PI-ReTOF-MS ion signals for  $C_3H_nO$  ( $n = 2, 4, 6, 8$ ) versus temperature subliming from carbon monoxide–methane ice ( $CO-CH_4$ ;  $^{13}CO-^{13}CD_4$ ).

cyclopropenone isomers have been detected in the ISM, but the methyleneketene isomer remains elusive.<sup>1</sup> Utilizing a PI energy of 10.82 eV, the propynal isomer was confirmed to form in the carbon monoxide–acetylene system and was found to sublime at 125–155 K. The cyclopropenone isomer was also confirmed by tuning the PI energy below its IE of  $9.26 \pm 0.15$  eV, and this resulted in no detectable signal, indicating that the second observed peak, subliming at 150–230 K, was due to cyclopropenone. The carbon monoxide–methane ice produced a very weak ion signal corresponding to cyclopropenone at 10.49 eV as well as at 9.75 eV subliming from 168 to 220 K. The carbon monoxide–ethane system can only tentatively identify the formation of the propynal isomer because of the possible signal overlap from the molecules corresponding to the molecular formula  $C_4H_8$ . This hydrocarbon was shown to sublime at 80–120 K, but the observed sublimation profile persisted until 148 K, suggesting that the propynal isomer may also contribute to the signal. Investigating the carbon monoxide–ethylene system shows that a peak subliming from about 120–165 K was observed at PI = 10.49 eV, and tuning to a lower PI energy of 9.60 eV resulted in a disappearance of the signal. This lack of signal shows that the carbon monoxide–ethylene ice produces only propynal.

Next, the  $C_3H_4O$  group consists of several possible isomers including methylketene ( $CH_3CHCO$ , IE =  $8.90 \pm 0.05$  eV), cyclopropanone ( $c-C_3H_4O$ , IE =  $9.10 \pm 0.10$  eV), and propenal ( $C_2H_3CHO$ , IE =  $9.95 \pm 0.05$  eV).<sup>103</sup> The propenal isomer has been the only isomer detected in the ISM.<sup>1</sup> The carbon monoxide–ethylene system has been previously discussed with respect to the  $C_3H_4O$  isomers.<sup>24,66</sup> Briefly, the isotopically labeled system displayed a bimodal structure at PI = 10.49 eV. Here, the tuning of the PI energy to 9.60 eV resulted in the second peak no longer being detected. This result along with the analysis of the formation mechanisms of the different isomers allowed for the latter peak to be identified as propenal and the first peak to be assigned to cyclopropenone. For the carbon monoxide–methane and ethane isotopic ices a broad peak was observed to sublime at 95–200 K at PI = 10.49 eV. Tuning the PI energy to 9.93 eV, 9.75 eV, and 9.63 eV for the carbon monoxide–methane system and to 9.80 eV and 9.60 eV for the monoxide–ethane system causes the sublimation profile to only be detectable at 95–155 K and 95–135 K, respectively. This change in the signal shows that the propenal isomer was likely formed and corresponded to the higher temperature portion of the sublimation profile at 10.49 eV. The PI energies utilized for these systems do not allow for any further isomers to be definitively identified, but the remaining sublimation profile measured below 10.49 eV matches very well with the spectrum assigned to cyclopropenone in the carbon monoxide–ethylene system. Although the ion signal corresponding to  $C_3H_4O$  also overlaps with *n*-butane ( $C_4H_{10}$ ), in the carbon monoxide–ethane isotopic ice, this hydrocarbon has been shown to have a relatively weak signal and therefore is only a partial contributor to the recorded signal. The signal detected in the carbon monoxide–acetylene ice cannot be due to methylketene, and is unlikely to be due to cyclopropanone, since no signal is detected at PI = 9.15 eV. The sublimation temperature range of this peak (120–155 K)

matches very well with that of the propenal peak observed in the carbon monoxide–ethylene ice.

The ion signal corresponding to  $C_3H_6O$  was detected across all the ice mixtures and could correspond to multiple isomers such as (*E/Z*)-1-propanol ( $CH_3CHCHOH$ , IE =  $8.70 \pm 0.03$  eV), acetone ( $CH_3C(O)CH_3$ , IE =  $9.70 \pm 0.01$  eV), propanal ( $CH_3CH_2CHO$ , IE =  $9.96 \pm 0.01$  eV), and propylene oxide ( $c-C_3H_6O$ , IE =  $10.22 \pm 0.02$  eV). Remarkably, propanal, acetone, and propylene oxide have all been detected in the ISM, with the latter isomer representing the first chiral molecule detected in the ISM – albeit present as a racemic mixture.<sup>1</sup> In the carbon monoxide–methane system the sublimation profile shows an initial peak followed by a second broad peak, and a similar structure was observed in the carbon monoxide–ethane system as well at PI = 10.49 eV. The carbon monoxide–ethane system has previously been explored.<sup>10</sup> To summarize, by tuning the ionization energy to 9.80 eV, a large decrease in the signal between 110 and 150 K was observed, but upon decreasing the PI to 9.60 eV no change in the spectrum was observed. These results proved that only propanal and not acetone was formed in this system, and that the remaining peak, subliming from 150 to 190 K, was due to (*E/Z*)-1-propanol. Similarly, for the carbon monoxide–methane system, by adjusting the PI energy below propanal's IE but above acetone's IE, between PI = 9.93 eV and 9.75 eV, the signal showed a large decrease in intensity that was not directly associated with the change in the photoionization cross section of acetone from 110 to 150 K. Therefore, a small portion of this ion signal is likely due to propanal, and by tuning the PI energy to 9.63 eV, acetone could also be confirmed as the portion of the signal at 110–150 K was no longer detected. However, a small peak still remained in the 150–180 K region, which matches nicely with the assignment in the carbon monoxide–ethane system of (*E/Z*)-1-propanol. Alternatively, the carbon monoxide–ethylene and –acetylene systems' ion signals for  $C_3H_6O$  were relatively less intense and followed a similar sublimation range to each other from 117 to 155 K. The PI energies utilized for these systems do not allow the discrimination of acetone and propanal, but the non-detection of signals at 9.60 eV and 9.15 eV in the carbon monoxide–ethylene and –acetylene systems, respectively, shows that either of these two possible isomers could be formed.

Finally, there are only three possible isomers with respect to  $C_3H_8O$ : 1-propanol ( $CH_3CH_2CH_2OH$ ;  $10.22 \pm 0.06$  eV), 2-propanol ( $CH_3CH(OH)CH_3$ ;  $10.12 \pm 0.07$  eV), and methylethyl ether ( $CH_3OC_2H_5$ ;  $9.72 \pm 0.07$  eV).<sup>41</sup> To date, only the methylethyl ether isomer has been detected in the ISM.<sup>1</sup> An ion signal corresponding to the molecular formula  $C_3H_8O$  was only detectable in the carbon monoxide–methane system and tentatively in the carbon monoxide–ethane system with an initial peak subliming at 111–130 K, in the carbon monoxide–methane system, and a second peak detected at 147–215 K in both the methane and ethane containing ices. By tuning the PI energy to 9.93 eV, it was revealed that only the first peak was still detectable, which confirmed that it is due to methylethyl ether, while the second peak is due to 1-propanol and/or 2-propanol in the carbon monoxide–methane system. However, tuning



the PI energy for the carbon monoxide–ethane system below 10.49 eV to 9.80 eV results in no detectable signal, thus confirming that only 1-propanol and/or 2-propanol are formed. Furthermore, sublimation onset temperatures of 135 K, corresponding to the second sublimation peak, have been measured for the 1-propanol and 2-propanol isomers.<sup>41</sup>

**3.2.3.  $C_4H_nO$  ( $n = 4, 6, 8, 10$ ).** Also, ions corresponding to  $C_4H_4O$  ( $m/z = 68$ ),  $C_4H_6O$  ( $m/z = 70$ ),  $C_4H_8O$  ( $m/z = 72$ ), and  $C_4H_{10}O$  ( $m/z = 74$ ) were detected using PI-ReTOF-MS (Fig. 6 and Fig. S11–S13, ESI†). The ion signal for  $C_4H_4O$  ( $m/z = 68$ ) was detected in each system. Meanwhile, the  $C_4H_6O$  ( $m/z = 70$ ) and  $C_4H_8O$  ( $m/z = 72$ ) ion signals were observed in all the systems except for the carbon monoxide–acetylene ice. Finally, the signal corresponding to  $C_4H_{10}O$  ( $m/z = 74$ ) was only produced in the carbon monoxide–methane and –acetylene ices. The sublimation onset temperatures for the  $C_4H_nO$  ions, as well as the isotopologues studied, began at 115 K, 112 K, 125 K and 148 K with respect to increasing  $n$ . Due to the increased complexity of these groups, reflected in the number of structural isomers and their similar IEs, conclusive assignments are not possible.<sup>38</sup> The  $C_4H_4O$  group was detected in each carbon monoxide–hydrocarbon system, and throughout the carbon monoxide–methane, –ethylene, and –acetylene systems tuning below a PI energy of 10.49 eV results in no signal being detected.

Similarly, the carbon monoxide–ethane system follows this trend as no signal is detected beyond 150 K at a PI less than 10.49 eV, and the remaining signal is due to the hydrocarbon group  $C_5H_{10}$ .<sup>54</sup> The only isomer with a known IE above 10.00 eV that may contribute to this signal is methylethynyl ketone ( $CH_3C(O)CCH$ , IE =  $10.23 \pm 0.05$  eV).<sup>38</sup>

Again, the complexity of the  $C_4H_6O$  group makes definitive assignments currently impossible. Interestingly though, almost all of the known isomers have ionization energies below 10.00 eV.<sup>38</sup> Although this group was detected in all the systems, except for carbon monoxide–acetylene, each system in which  $C_4H_6O$  was detected had a unique sublimation profile. First, the carbon monoxide–methane ice showed a very broad peak from 110 to 260 K at PI = 10.49 eV, and decreasing the PI energy to 9.93 eV, 9.75 eV, and 9.63 eV resulted in a signal from 110 to 215 K and peaking at 125 K to be observed. In the carbon monoxide–ethane ice a much sharper peak was detected from 110 to 155 K, with a maximum at 125 K that matched that of the carbon monoxide–methane ice closely. This similarity suggests that common isomers are formed from the carbon monoxide–methane and –ethane systems. Finally, in the carbon monoxide–ethylene ice this ion signal produced an initial peak, subliming from 110 to 130 K, with a maximum at 125 K and the second peak at 135–175 K. Here, the first peak observed matches the

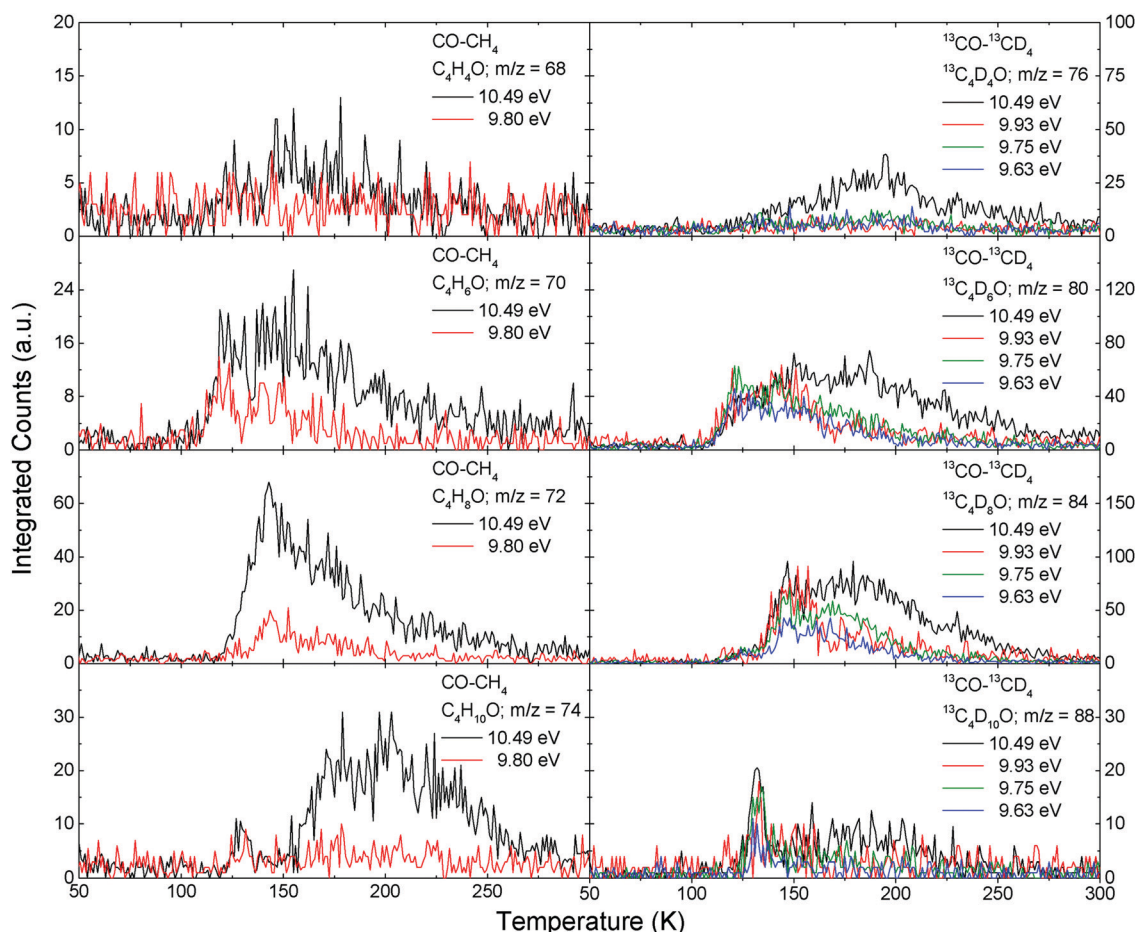


Fig. 6 PI-ReTOF-MS ion signals for  $C_4H_nO$  ( $n = 4, 6, 8, 10$ ) versus temperature subliming from carbon monoxide–methane ice ( $CO-CH_4$ ;  $^{13}CO-^{13}CD_4$ ).

peak detected from carbon monoxide–methane and –ethane. Interestingly, the second peak is no longer detectable when utilizing a PI energy of 9.60 eV, which suggests that it could be due to 2-methyl-propenal ( $\text{CH}_2\text{C}(\text{CH}_3)\text{CHO}$ , IE =  $9.92 \pm 0.05$  eV), 2-butenal ( $\text{CH}_3\text{CHCHCHO}$ , IE =  $9.73 \pm 0.05$  eV), and/or 1-methyl-propenal ( $\text{CH}_2\text{CH}_2\text{C}(\text{CH}_3)\text{O}$ , IE =  $9.65 \pm 0.02$  eV). Although there are several other isomers with IEs in this range, these isomers are noted as their close relative, propenal, was observed to sublime from 120 to 155 K in the carbon monoxide–ethylene ice, and it is likely that this larger aldehyde will sublime at relatively higher temperatures.

Although the  $\text{C}_4\text{H}_8\text{O}$  group is very complex, with over 30 isomers having overlapping IEs, the 1-butanal ( $\text{CH}_3\text{CH}_2\text{CH}_2\text{CHO}$ , IE =  $9.82 \pm 0.04$  eV) and 2-methyl-propanal ( $\text{CH}_3\text{CH}(\text{CH}_3)\text{CHO}$ , IE =  $9.71 \pm 0.02$  eV) isomers have unique IEs. Therefore, experiments were designed for the carbon monoxide–methane system to determine if either of these isomers was formed.<sup>41</sup> Here, tuning the PI energy to 9.93 eV and then 9.75 eV resulted in a measurable change in the related ion signal, which was detected to sublime from 125 to 275 K at PI = 10.49 eV, and this change can be related to the 1-butanal (IE =  $9.82 \pm 0.04$  eV) isomer. Furthermore, by tuning the energy to 9.63 eV the signal again differed, and this observed change can be related to the 2-methyl-propanal (IE =  $9.71 \pm 0.02$  eV) isomer. Even at the low PI energy of 9.63 eV a signal remained though, showing that other isomers are formed. The carbon monoxide–ethane system also exhibited a corresponding ion signal for this group that matched the sublimation profile detected for monoxide–methane, but no conclusive information about the isomers formed in this system can be extracted. The signal detected in the monoxide–ethylene system has a narrower peak than the previous two systems from 125 to 175 K, and is no longer detectable at PI = 9.60 eV, which suggests that it could be related to one of the isomers above.

The  $\text{C}_4\text{H}_{10}\text{O}$  group was only detectable in the carbon monoxide–methane and –acetylene systems, and each system showed a sublimation onset temperature of 127 K. Again the large number of isomers with overlapping IEs does not permit definitive assignments, but an observed change in the sublimation profile between 10.49 eV and 9.75 eV shows that the 1-butanol ( $\text{CH}_3\text{CH}_2\text{CH}_2\text{CH}_2\text{OH}$ , IE =  $9.99 \pm 0.05$  eV), 2-butanol ( $\text{CH}_3\text{CH}_2\text{CH}(\text{OH})\text{CH}_3$ , IE =  $9.88 \pm 0.03$  eV), 2-methyl-1-propanol ( $\text{CH}_3\text{CH}(\text{CH}_3)\text{CH}_2\text{OH}$ , IE =  $10.02 \pm 0.02$  eV), and/or 2-methyl-2-propanol ( $\text{CH}_3\text{C}(\text{OH})(\text{CH}_3)_2$ , IE =  $9.90 \pm 0.03$  eV) may be formed. However, the remaining signal at 9.75 eV shows that the other isomers with known IEs, including 2-methoxypropane ( $\text{CH}_3\text{CH}(\text{OCH}_3)_2$ , IE =  $9.45 \pm 0.04$  eV), methylpropyl ether ( $\text{C}_3\text{H}_7\text{OCH}_3$ , IE =  $9.41 \pm 0.07$  eV), and/or ethyl ether ( $\text{C}_2\text{H}_5\text{OC}_2\text{H}_5$ , IE =  $9.51 \pm 0.03$  eV), may also be formed. The ion signal detected in the carbon monoxide–acetylene ice is observed even at a PI energy of 9.15 eV, suggesting that it could be due to another isomer with an unknown IE, or possibly due to  $\text{C}_5\text{H}_4\text{O}$  ions.

**3.2.4.  $\text{C}_5\text{H}_n\text{O}$  ( $n = 4, 6, 8, 10$ ).** The next largest group detected *via* PI-ReTOF-MS, containing a single oxygen atom, corresponds to  $\text{C}_5\text{H}_n\text{O}$  ( $n = 4, 6, 8, 10$ ) ions (Fig. 7 and Fig. S14–S16, ESI†). The signal for  $\text{C}_5\text{H}_4\text{O}$  ( $m/z = 80$ ) ions was detected only in the carbon monoxide–ethylene mixture and tentatively in the carbon

monoxide–acetylene mixture. Interestingly, the  $\text{C}_5\text{H}_6\text{O}$  ( $m/z = 82$ ) and  $\text{C}_5\text{H}_8\text{O}$  ( $m/z = 84$ ) ions were observed in all the systems, but  $\text{C}_5\text{H}_{10}\text{O}$  ( $m/z = 86$ ) signal was only detected in the carbon monoxide–methane, –ethane, and –ethylene ices. The sublimation temperatures for the  $\text{C}_5\text{H}_n\text{O}$  molecules started at 135 K, 128 K, 124 K, 120 K and 134 K with respect to an increase in  $n$ . The  $\text{C}_5\text{H}_4\text{O}$  ions for this group were observed in both the carbon monoxide–ethylene and –acetylene mixtures with unique sublimation profiles at PI = 10.49 eV. Tuning the PI energy to 9.60 eV results in no detectable signal, and this – of the isomers with known ionization energies – suggests that 2,4-cyclopentadiene-1-one ( $\text{c}-(\text{C}_5\text{H}_4)\text{O}$ ), which has a vertical IE of 9.49 eV, is not formed. Alternatively, in the carbon monoxide–acetylene ice this ion signal is still observable at a PI energy of 9.15 eV, showing that alternative isomers are formed from the previous system.

$\text{C}_5\text{H}_6\text{O}$  ions were observed in all the systems with sublimation onset temperatures of 115 K observed in the carbon monoxide–ethane and –ethylene systems, while the onset temperature was detected at 140 K in the carbon monoxide–methane and –acetylene systems. Tuning the PI energy below 10.49 eV resulted in no signal being detected from either the carbon monoxide–methane or –acetylene system. However, a signal was still detectable even at PI = 9.60 eV in both the carbon monoxide–ethane and –ethylene systems. Note that the carbon monoxide–ethane isotopic ion signal also is overlapped by that of the  $\text{C}_6\text{H}_{12}$  hydrocarbon ion, which has been detected as a product from pure ethane ices.<sup>54</sup> These unique sublimation profiles suggest that a variety of isomers are formed *via* mechanisms specific to each hydrocarbon reactant.

Similarly,  $\text{C}_5\text{H}_8\text{O}$  ions were detected in each system studied, and in the carbon monoxide–ethane and –ethylene ices the sublimation onset temperature was 118 K, while the onset temperature was detected at 140 K in the carbon monoxide–methane and –acetylene systems. Interestingly, the ion signals for the carbon monoxide–methane and –acetylene systems are unique with no overlap from other possible products, but the carbon monoxide–ethane ion signal may also have contributions from  $\text{C}_6\text{H}_{14}$  as well as  $\text{C}_4\text{H}_2\text{O}_2$  and the carbon monoxide–ethylene signal may also be due to  $\text{C}_6\text{H}_4\text{O}$  with respect to the isotopic studies. This signal was detectable in all the systems below 10.49 eV, showing that many different isomers are likely formed.<sup>38</sup>

All the systems detected a signal corresponding to  $\text{C}_5\text{H}_{10}\text{O}$  ions. The signal from the carbon monoxide–methane sample was observed to be very broad and sublimed from 125 to 275 K. However, the sublimation profiles observed for the carbon monoxide–ethane and –ethylene systems span 135–200 K, showing that there are likely different isomers formed. Also, the carbon monoxide–ethane and –ethylene ions could be overlapped by signals due to  $\text{C}_4\text{H}_4\text{O}_2$  and  $\text{C}_6\text{H}_4\text{O}$ , respectively, in the isotopic experiments. Interestingly, there is still a small signal recorded at PI = 8.40 eV in the carbon monoxide–ethane system, and out of 77 reported  $\text{C}_5\text{H}_{10}\text{O}$  isomers only propen-1,2-dimethylol ( $\text{CH}_3\text{C}(\text{CH}_3)\text{C}(\text{CH}_3)\text{OH}$ , IE =  $8.15 \pm 0.15$  eV) had an IE below 8.40 eV.<sup>38</sup> However, this is not conclusive that this isomer is the only one responsible for the remaining signal as

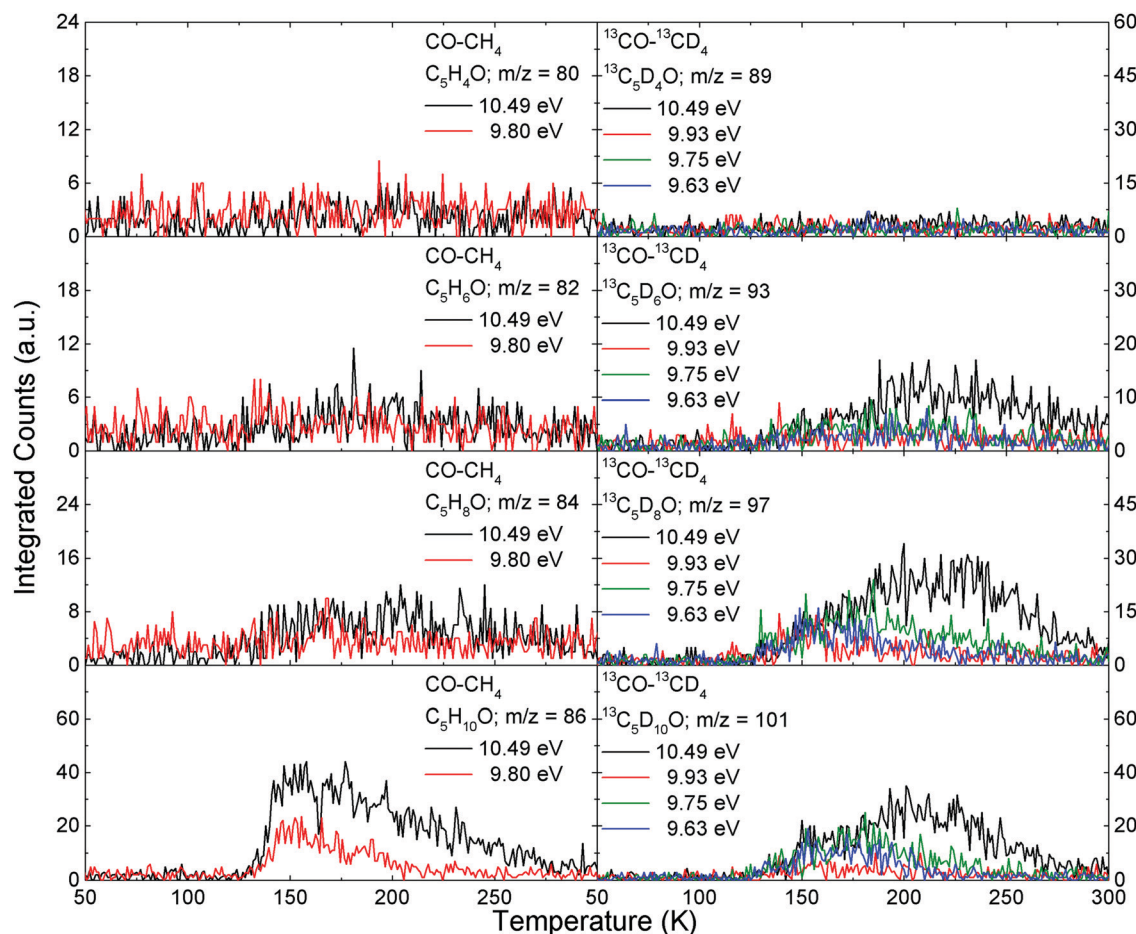


Fig. 7 PI-ReTOF-MS ion signals for  $C_5H_nO$  ( $n = 4, 6, 8, 10$ ) versus temperature subliming from carbon monoxide–methane ice ( $CO-CH_4$ ;  $^{13}CO-^{13}CD_4$ ).

several isomers had no IE reported. The carbon monoxide–acetylene ion signal produced can only be tentatively assigned as it is very weak.

**3.2.5.  $C_6H_nO$  ( $n = 4, 6, 8, 10, 12, 14$ ).** Also, ions corresponding to  $C_6H_nO$  ( $n = 4, 6, 8, 10, 12, 14$ ) were detected using PI-ReTOF-MS (Fig. 8 and Fig. S17–S19, ESI†). The signals for  $C_6H_4O$  ( $m/z = 92$ ) and  $C_6H_6O$  ( $m/z = 94$ ) were only detected as products from the carbon monoxide–ethylene and –acetylene mixtures. The  $C_6H_8O$  ( $m/z = 96$ ) signal was tentatively observed in both the carbon monoxide–methane and –ethylene systems. Next,  $C_6H_{10}O$  ( $m/z = 98$ ) ions were found to sublime from all of the ice mixtures except for carbon monoxide–acetylene. Only the carbon monoxide–methane and –ethane ices produced signals corresponding to  $C_6H_{12}O$  ( $m/z = 100$ ), and  $C_6H_{14}O$  ( $m/z = 102$ ) was only observed in the monoxide–methane and –ethylene mixtures. The sublimation temperatures of  $C_6H_nO$  ions were 135 K, 140 K, 137 K, 140 K, 150 K and 148 K for  $n = 4, 6, 8, 10, 12$ , and 14, respectively.

Ions corresponding to the molecular formula  $C_6H_4O$  were only detected, tentatively, in the carbon monoxide–ethylene and –acetylene systems. For the ethylene containing ice the isotopically shifted sublimation profile overlaps with that of  $C_5H_{10}O$ , which can explain the increased intensity of the signal. Tuning the PI energy to 9.60 eV still allows for a signal

to be detected, showing that isomers with lower IEs, such as 2,4-cyclopentadien-1-ylidene methanone ( $c-(C_5H_4)CO$ , IE = 8.05 eV), were also formed.<sup>38</sup> The non-isotopically labeled system only detected a tentative signal less than 15 counts subliming from 140 to 200 K. This ion signal, although weak, is also observed in the acetylene mixture, and the sublimation profile extends from 140 to 280 K.

Like the previous system,  $C_6H_6O$  ions were only detected in the unsaturated hydrocarbon containing systems. The carbon monoxide–ethylene produced signal sublimes from 130 to 200 K and is not detectable at a PI energy of 9.60 eV. Also, only a very weak signal is observed in the acetylene mixture, making this a tentative detection, and the sublimation profile extends from 150 to 275 K. An interesting isomer that can be photo-ionized, and possibly formed, at these energies is phenol ( $c-(C_6H_5)OH$ , IE =  $8.49 \pm 0.02$  eV),<sup>38</sup> which has been tentatively detected in the ISM.<sup>1</sup>

Next,  $C_6H_8O$  ions were only tentatively observed in methane and ethylene containing ices, and the signal in the isotopic carbon monoxide–ethane ice is due to  $C_7H_{14}$ .<sup>54</sup> By decreasing the PI energy below 10.49 eV, the weak signal observed in both systems is considerably decreased, but still detectable. Possible isomers related to these signals could be 2,4-hexadienal ( $CH_3(CH)_4CHO$ , IE =  $9.22 \pm 0.03$  eV), 2-cyclohexenone



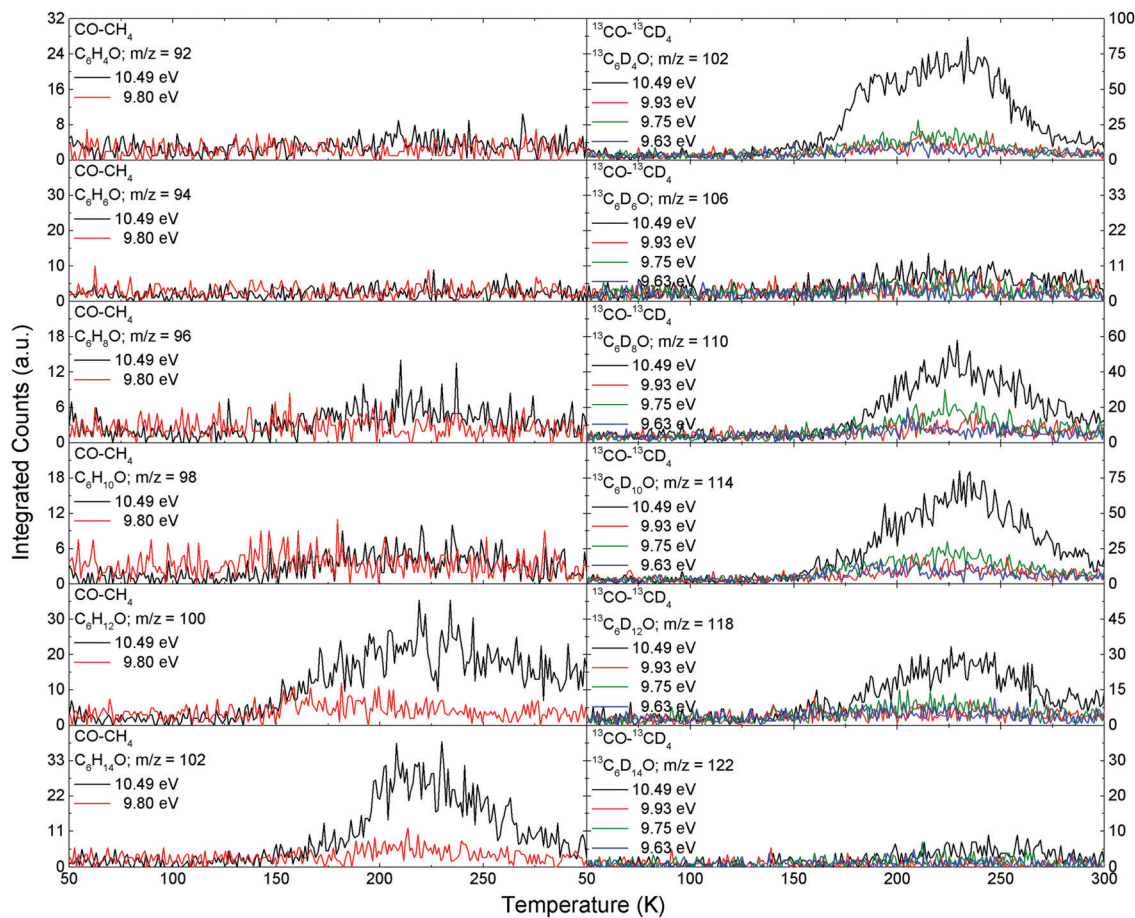


Fig. 8 PI-ReTOF-MS ion signals for  $C_6H_nO$  ( $n = 4, 6, 8, 10, 12, 14$ ) versus temperature subliming from carbon monoxide-methane ice ( $CO-CH_4$ ;  $^{13}CO-^{13}CD_4$ ).

( $c\text{-}(C_6H_8)O$ ,  $IE = 9.23 \pm 0.05$  eV), and 4-methylpentyn-3-one ( $CH_3(CH_3)CHC(O)CCH$ ,  $IE = 9.89$  eV) as these ionization energies are reported as vertical values.<sup>38</sup> The carbon monoxide-methane signal was recorded from 175 to 290 K, but the carbon monoxide-ethylene ion only sublimed from 130 to 210 K.

Also,  $C_6H_{10}O$ ,  $C_6H_{12}O$ , and  $C_6H_{14}O$  ions were tentatively detected in the carbon monoxide-ethane and -ethylene ices, and the  $C_6H_{12}O$  signal was also observed as the product in the carbon monoxide-methane system. Decreasing the PI energy below 10.49 eV results in no signal detected from the carbon monoxide-methane and -ethylene ices for all of these possible ions, but even at 9.60 eV a signal is observed in the carbon monoxide-ethane system for  $C_6H_{10}O$ ,  $C_6H_{12}O$ , and  $C_6H_{14}O$  ions. Possible  $C_6H_{10}O$  isomers for these signals include cyclohexanone ( $c\text{-}(C_6H_{10})O$ ,  $IE = 9.16 \pm 0.02$  eV), 2-methyl-2-pentenal ( $CH_3CH_2CHC(CH_3)CHO$ ,  $IE = 9.54$  eV), and 2-hexenal ( $CH_3(CH_2)_2(CH_2)CHO$ ,  $IE = 9.65$  eV).<sup>38</sup> Feasible  $C_6H_{12}O$  isomers are 2-hexanone ( $CH_3(CH_2)_3C(O)CH_3$ ,  $IE = 9.35 \pm 0.06$  eV), hexanal ( $CH_3(CH_2)_4CHO$ ,  $IE = 9.72 \pm 0.05$  eV), and cyclohexanol ( $c\text{-}(C_6H_{11})OH$ ,  $IE = 10.0 \pm 0.2$  eV).<sup>38</sup> The most saturated system in this group,  $C_6H_{14}O$ , has many different possible isomers including 2-hexanol ( $CH_3(CH_2)_3CH(OH)CH_3$ ,  $IE = 9.80 \pm 0.03$  eV) and 1-hexanol ( $CH_3(CH_2)_5OH$ ,  $IE = 9.89$  eV).<sup>38</sup>

**3.2.6.  $C_2H_nO_2$  ( $n = 2, 4$ ).** Also detected were ions corresponding to  $C_2H_nO_2$  ( $n = 2, 4$ ), which is the smallest group to contain two oxygen atoms (Fig. 9 and Fig. S20–S22, ESI†). This group consists of  $C_2H_2O_2$  ( $m/z = 58$ ), which was tentatively observed in all the systems, but the isotopic shift in the carbon monoxide-ethylene and acetylene ices still allows for an overlap with the  $C_4H_8$  hydrocarbon and cannot be confirmed. The  $C_2H_4O_2$  ( $m/z = 60$ ) signal was only detected in the carbon monoxide-methane ice. The sublimation temperatures for the  $C_2H_nO_2$  ions, as well as the isotopologues studied, began at 104 K and 148 K for  $C_2H_2O_2$  and  $C_2H_4O_2$ , respectively.

Here,  $C_2H_2O_2$  can belong to several isomers including ethyne-1,2-diol ( $HOCCOH$ ,  $9.42 \pm 0.1$  eV), glyoxal ( $HC(O)CHO$ ,  $10.2 \pm 0.1$  eV),<sup>104</sup> and 2-oxiranone ( $c\text{-}(C_2H_2O)_2O$ ,  $10.96 \pm 0.1$  eV). The ion signal detected in the carbon monoxide-methane isotopic system is a unique signal with no overlap from other ions, and the carbon monoxide-ethane isotopic system has an overlap from  $C_3H_8O$  ions, which only contributes a small portion to the overall signal at 160 K. The ion signal detected from carbon monoxide-methane showed two peaks, with the first being very small and subliming from 104 to 124 K, and the second sublimation event occurring at 125–180 K. Decreasing the PI energy below 10.00 eV resulted in the second peak no

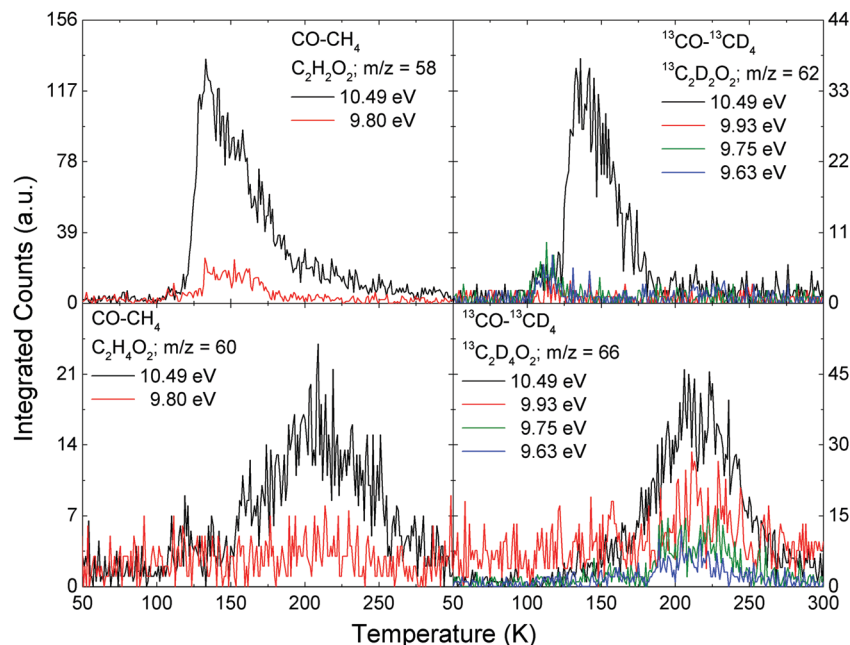


Fig. 9 PI-ReTOF-MS ion signals for  $C_2H_nO_2$  ( $n = 2, 4$ ) versus temperature subliming from carbon monoxide–methane ice ( $CO-CH_4$ ;  $^{13}CO-^{13}CD_4$ ).

longer being detected, therefore confirming that it belonged to glyoxal. This assignment is also in agreement with sublimation profiles from previous studies tentatively identifying glyoxal,<sup>31,105</sup> and these tunable experiments definitively confirm its presence in carbon monoxide–methane ices. However, the initial peak remained even at lower PI energies of 9.93 eV, 9.75 eV, and 9.63 eV, which suggests that it may belong to the ethyne-1,2-diol ( $9.42 \pm 0.1$  eV) isomer, but due to the very low intensity of this signal it can only be tentatively assigned. The 2-oxiranone isomer will not be detected in any of the experiments due to its higher IE of 10.96 eV. The tentative detection of the glyoxal isomer in the carbon monoxide–ethane system is due to the low intensity of the signal, but the disappearance of any notable signal at 9.80 eV suggests that it was formed. In both the carbon monoxide–ethylene and –acetylene ices this ion signal is overlapped by a major hydrocarbon product,  $C_4H_8$ , making a definitive identification impossible. However, in both systems this ion signal shows a broad peak that spans a sublimation temperature range much larger than that corresponding to  $C_4H_8$  alone.<sup>53</sup> In both systems the sublimation event ends at 190 K, which matches very closely to the confirmed glyoxal sublimation profile.

Next, the  $C_2H_4O_2$  signal was only detectable in the carbon monoxide–methane system, and this could be due to ethene-1,2-diol ( $CH(OH)CHOH$ , IE =  $9.62 \pm 0.04$  eV)<sup>38</sup> or glycolaldehyde ( $CH_2(OH)CHO$ , IE =  $9.95 \pm 0.05$  eV),<sup>106</sup> but not methyl formate ( $HC(O)OCH_3$ , IE =  $10.85 \pm 0.05$  eV) or acetic acid ( $CH_3C(O)OH$ , IE =  $10.65 \pm 0.02$  eV) due to their IEs being greater than 10.49 eV.<sup>38</sup> Three of these isomers, glycolaldehyde, methyl formate, and acetic acid, have already been detected in the ISM.<sup>1</sup> The sublimation profile recorded at PI = 10.49 eV ranges from 145 to 270 K, but changing the PI energy to 9.93 eV, 9.75 eV, or 9.63 eV results in an altered signal from 178 to 260 K.

By tuning the PI energy below 9.95 eV, the glycolaldehyde isomer can no longer be efficiently photoionized and therefore no longer be detected, thus confirming its contribution to the ion signal from 145 to 178 K. This assignment agrees very well with previous sublimation profiles assigned to glycolaldehyde.<sup>32,105</sup> Furthermore, the remaining sublimation event can only be due to the ethene-1,2-diol isomer at PI = 9.75 eV and 9.63 eV, and this signal also matches very well with previously recorded sublimation profiles.<sup>32</sup>

**3.2.7.  $C_3H_nO_2$  ( $n = 4, 6, 8$ ).** Products corresponding to  $C_3H_nO_2$  ( $n = 4, 6, 8$ ) ions were detected using PI-ReTOF-MS (Fig. 10 and Fig. S23–S25, ESI†). Ions consistent with  $C_3H_4O_2$  ( $m/z = 72$ ) ions were observed from the carbon monoxide–methane and –ethylene ices. Signals corresponding to  $C_3H_6O_2$  ( $m/z = 74$ ) ions were observed in the carbon monoxide–methane and –acetylene ices, and  $C_3H_8O_2$  ( $m/z = 76$ ) signals were observed only in the carbon monoxide–acetylene ices. It should be noted for this group that in each case these ion signals still have overlap from other molecules detected, such as hydrocarbons, even in several of the isotopic systems. These ion signals were observed to sublime at 123 K, 140 K and 135 K with respect to increasing  $n$ .

The  $C_3H_4O_2$  signal was observed only in the carbon monoxide–methane system, and the signal detected from the ethylene system corresponds to the hydrocarbon  $C_6H_8$ .<sup>53</sup> At PI = 10.49 eV the carbon monoxide–methane signal suggests that there are three sublimation events with maxima at 146 K, 178 K, and 230 K. Decreasing the PI energy to 9.93 eV showed that two peaks are still present, with the first subliming from 125 to 162 K and the latter from 165 to 210 K. Tuning the PI energy to 9.75 eV results in a decrease in the intensity of the initial peak with little change to the second peak. Finally, by altering the PI energy to 9.63 eV only the second peak was detectable. Although not many

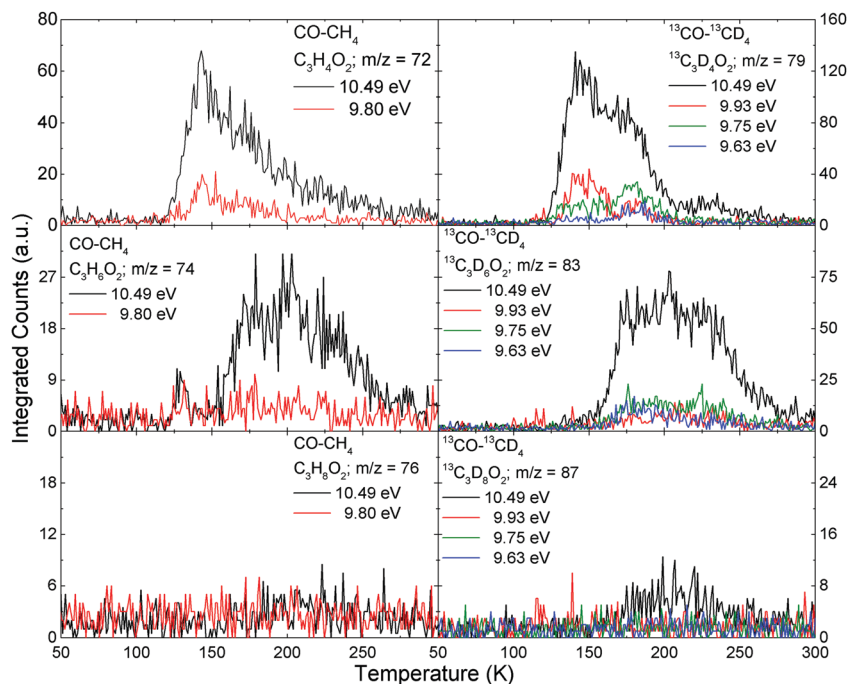


Fig. 10 PI-ReTOF-MS ion signals for  $C_3H_nO_2$  ( $n = 4, 6, 8$ ) versus temperature subliming from carbon monoxide–methane ice ( $CO-CH_4$ ;  $^{13}CO-^{13}CD_4$ ).

of the isomers for this system have known IEs, the methylglyoxal ( $CH_3C(O)CHO$ , IE =  $9.60 \pm 0.06$  eV)<sup>38</sup> isomer could be responsible for the second sublimation event since a similar molecule, glyoxal, was confirmed to form in this system.

Similarly, the  $C_3H_6O_2$  signal was only observed in the carbon monoxide–methane system, and the signal detected from the acetylene system corresponds to the hydrocarbon  $C_6H_2$  in the unlabeled signal and the isotopically shifted signal corresponds to  $C_6H_6$  ions.<sup>53</sup> Utilizing a PI energy below 10.49 eV resulted in a substantial decrease in signal, but the profile remained broad, suggesting that the isomer(s) responsible for this signal is still ionized. Therefore, several of the isomers with known IEs can be assumed to be minor products or have not formed, including 1-hydroxyacetone ( $CH_3C(O)CH_2OH$ , IE = 10.0 eV), methyl acetate ( $CH_3C(O)OCH_3$ , IE = 10.25 eV), and propanoic acid ( $C_2H_5C(O)OH$ , IE = 10.44 eV). The ethyl formate ( $HC(O)OC_2H_5$ , IE = 10.61 eV) and methyl acetate isomers of this group have been detected in the ISM.<sup>1</sup>

Finally, the  $C_3H_8O_2$  ion signal was tentatively observed in the carbon monoxide–acetylene system. The signal detected from the acetylene system can correspond to the hydrocarbon  $C_6H_4$  in the unlabeled signal and the isotopically shifted signal overlaps with that of  $C_6H_8$  ions. However, the sublimation profiles recorded at 10.82 eV and 10.49 eV display two sublimation events, with the first reaching a maximum at 149 K and the second peak ranging from about 150 to 275 K. Here, the first sublimation event matches very well with the unlabeled signal, suggesting that it is from the same ion, but more information about the ionization energies of the possible isomers is needed to constrain if this signal is only due to  $C_3H_8O_2$  ions.

**3.2.8.  $C_4H_nO_2$  ( $n = 4, 6, 8, 10$ ).** The next largest group detected containing two oxygen atoms corresponds to  $C_4H_nO_2$

( $n = 2, 4, 6, 8, 10$ ) ions *via* PI-ReTOF-MS (Fig. 11 and Fig. S26–S28, ESI†). This complex group of molecules  $C_4H_4O_2$  ( $m/z = 84$ ),  $C_4H_6O_2$  ( $m/z = 86$ ),  $C_4H_8O_2$  ( $m/z = 88$ ), and  $C_4H_{10}O_2$  ( $m/z = 90$ ) have multiple overlapping ion signals from other products even in the isotopically shifted systems. These sublimation signals were recorded at various onset temperatures between the different systems and this is due to the contribution of other confirmed molecules that overlap with these mass-to-charge ratios.

The  $C_4H_4O_2$  ion signal was only confirmed *via* the carbon monoxide–methane isotopic system, and only tentatively from carbon monoxide–ethane and –ethylene ices due to the overlap from  $C_5H_{10}O$ , and  $C_6H_{10}$ , respectively, in the isotopic systems. The sublimation profile detected from the carbon monoxide–methane ice was recorded from 145 to 295 K at PI = 10.49 eV. After changing the PI energy to less than 10.49 eV the profile was observed to sublime only from 145 to 150 K. Thus, multiple isomers can be confirmed to form from the methane containing ice mixture. Isomers possibly formed that correspond to this group include 1,4-dioxin ( $c-C_4H_4O_2$ , IE =  $7.75 \pm 0.02$  eV) and propiolic acid ( $CHCC(O)OCH_3$ , IE = 10.3 eV).

Also, an ion signal corresponding to the molecular formula  $C_4H_6O_2$  was confirmed in the monoxide–methane and –ethane isotopic systems, but only tentatively in ethylene ices because of the overlap from  $C_6H_{12}$ . Here, the sublimation event was detected from 142 to 275 K and 130 to 210 K in the methane and ethane ices at PI = 10.49 eV. Decreasing the PI energy to 9.93 eV, 9.75 eV, and 9.63 eV produces a sublimation profile with two maxima at 150 K and 180 K from the methane ice. Interestingly, both the methane and ethane  $C_4H_6O_2$  ion signals were still detectable at PI energies of 9.63 eV and 9.60 eV, respectively. Furthermore, the shapes of the signals remain similar between the different PI energies utilized. There are



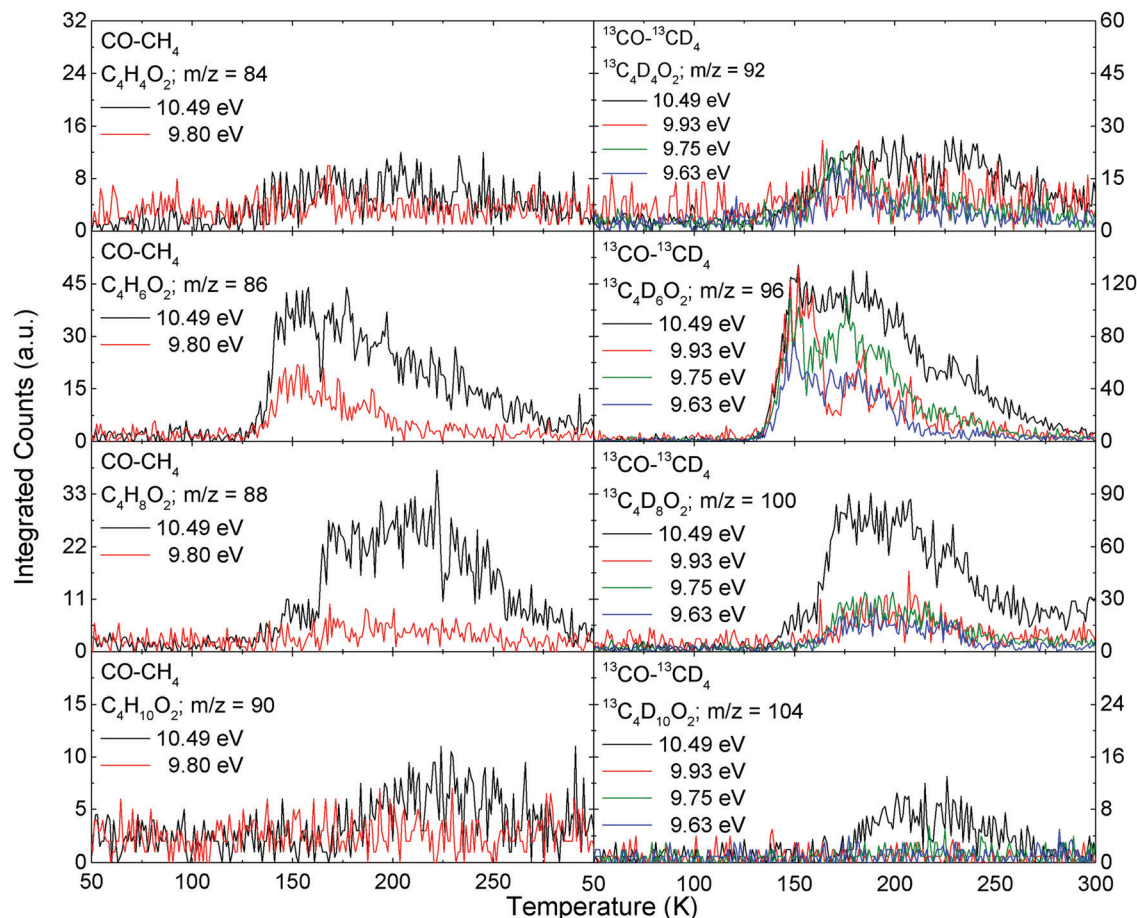


Fig. 11 PI-ReTOF-MS ion signals for  $C_4H_nO_2$  ( $n = 4, 6, 8, 10$ ) versus temperature subliming from carbon monoxide–methane ice ( $CO-CH_4$ ;  $^{13}CO-^{13}CD_4$ ).

multiple isomers of this group that have IEs below 9.60 eV and therefore could contribute to this signal. One of these isomers 2,3-butadione ( $CH_3(CO)_2CH_3$ ,  $IE = 9.23 \pm 0.03$  eV)<sup>38</sup> is a possibility and is pointed out here due to its similarity of structure to the acetaldehyde molecule, which was verified to form in each of these three systems.

Next, the signal due to ions of the molecular formula  $C_4H_8O_2$  was confirmed *via* the carbon monoxide–methane system, and tentatively in the carbon monoxide–ethane ice. The sublimation profile detected from the carbon monoxide–methane ice ranged from 135 to 300 K at a PI of 10.49 eV. This signal had a small shoulder from 135 to 160 K that disappeared when the PI energy was decreased below 10.49 eV, but a signal from 160 to 250 K was still present. The ion signal detected from the carbon monoxide–ethane system sublimed from 160 to 250 K utilizing a PI of 10.49 eV, but was no longer detectable at lower PI energies. This sublimation event from 160 to 250 K suggests that similar isomers were formed in both systems, but that additional isomers were also formed from the methane containing ice. Two isomers with IEs related to these changes in the ion signals are butanoic acid ( $CH_3(CH_2)_2C(O)OH$ ,  $IE = 10.17 \pm 0.05$  eV) and 2-methylpropanoic acid ( $[(CH_3)_2CHC(O)OH]$ ,  $IE = 10.24 \pm 0.12$  eV).<sup>38</sup>

Lastly,  $C_4H_{10}O_2$  ions were detected tentatively in the carbon monoxide–methane, –ethylene, and –acetylene ices. However, the ion signals corresponding to ethylene and acetylene can be accounted for *via* the hydrocarbons  $C_7H_{10}$  and  $C_8H_4$  in both of these isotopic systems.<sup>53</sup> Although the methane ion signal also overlaps with that of  $C_4H_{10}O_2$ , its similarity in signal between the natural and isotopically labeled systems suggests that it may be due to  $C_4H_{10}O_2$  ions. This ion signal was only detectable at PI = 10.49 eV subliming from 175 to 275 K. Unfortunately, most isomers for this group do not have reported IEs, but this information allows for methoxypropanol ( $CH_3CH_2CH(OH)OCH_3$ ,  $IE = 9.3$  eV) to be ruled out as a possible product.<sup>38</sup>

**3.2.9.  $C_5H_nO_2$  ( $n = 6, 8$ ).** A signal corresponding to  $C_5H_nO_2$  ( $n = 6, 8$ ) ions was also detected using PI-ReTOF-MS (Fig. 12 and Fig. S29–S31, ESI†). Both of these molecules,  $C_5H_6O_2$  ( $m/z = 98$ ) and  $C_5H_8O_2$  ( $m/z = 100$ ), were detected as products in the carbon monoxide–methane ice and tentatively from the carbon monoxide–ethane ice. With respect to  $C_5H_6O_2$  ions, the carbon monoxide–methane sublimation profile at PI = 10.49 eV displays a possible bimodal structure with maxima at 185 K and 245 K. Changing the PI energy to 9.93 eV, 9.75 eV, or 9.63 eV results in the first peak being still detected, but the second peak is no longer present. Like several of the previous ions detected this is

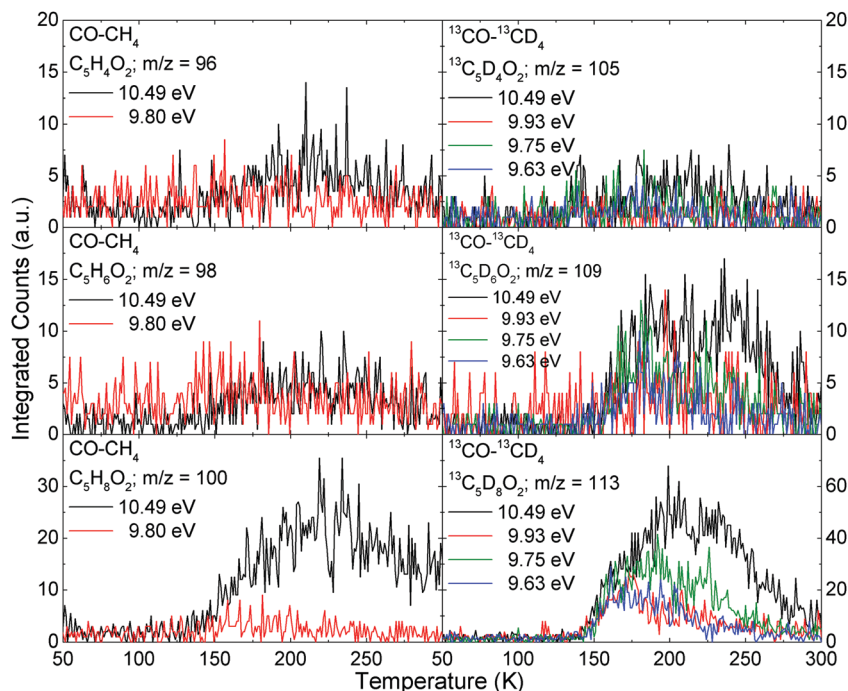


Fig. 12 PI-ReTOF-MS ion signals for  $C_5H_nO_2$  ( $n = 4, 6, 8$ ) versus temperature subliming from carbon monoxide–methane ice ( $CO-CH_4$ ;  $^{13}CO-^{13}CD_4$ ).

likely due to different isomers being produced. The ethane containing ice displays a sublimation profile from 145 to 210 K, and this signal was detected for each PI energy used. However, this ion signal could overlap with that of  $C_6H_{12}O$  ions. Possible isomers formed for this group include 3-hydroxy-2-cyclopenten-1-one ( $c-(C_5H_5)OOH$ , IE =  $9.22 \pm 0.05$  eV) and 1,3-cyclopentanedione ( $c-(C_5H_6)(1-O)(3-O)$ , IE =  $9.46 \pm 0.05$  eV).<sup>38</sup>

The  $C_5H_8O_2$  signal was observable in both the carbon monoxide–methane and –ethane systems. The methane ice produced a broad sublimation profile spanning 140–295 K, while the ethane ice displayed a peak subliming from 140 to 200 K. Altering the PI energy to 9.93 eV, 9.75 eV, or 9.63 eV still results in a sublimation profile from 140 to 275 K in the carbon monoxide–methane system. Here, the later portion of the 10.49 eV signal is no longer detected and must be due to another isomer. Likewise, the ion signal from the ethane experiment is observed at PI energies of 9.80 eV and 9.60 eV, but no longer detected at a low PI energy of 8.40 eV. Two possible isomers possibly formed following these constraints are 2,4-pentanedione ( $CH_3C(O)CH_2C(O)CH_3$ , IE =  $8.85 \pm 0.02$  eV) and 1,3-cyclopentanedione ( $CH_3C(CH_3)CHC(O)OH$ , IE = 9.63 eV).<sup>38</sup>

**3.2.10.  $C_6H_nO_2$  ( $n = 8, 10, 12$ ).** The ions corresponding to  $C_6H_nO_2$  ( $n = 8, 10, 12$ ) were detected using PI-ReTOF-MS (Fig. 13 and Fig. S32–S34, ESI†). The  $C_6H_8O_2$  ( $m/z = 112$ ),  $C_6H_{10}O_2$  ( $m/z = 114$ ), and  $C_6H_{12}O_2$  ( $m/z = 116$ ) ions could only be observed in the carbon monoxide–methane and –ethane systems. The  $C_6H_8O_2$  signal sublimed from 175 to 300 K in the methane ice at PI = 10.49 eV and this signal was significantly reduced when a lower PI energy was utilized. Alternatively, the signal for  $C_6H_8O_2$  from the ethane system was observed from 150 to 275 K, and was detected for PI energies of 10.49 eV, 9.80 eV, 9.60 eV, and 8.40 eV.

These differences show that unique isomers are formed between the two ice mixtures. Possible isomers include 2,5-dimethyl-3-furanone ( $c-(C_4H_2O)(2-CH_3)(3-O)(5-CH_3)$ , IE =  $8.23 \pm 0.05$  eV), 1,3-cyclohexanedione ( $c-(C_6H_8)(1-O)(3-O)$ , IE =  $9.52 \pm 0.05$  eV), and 1,4-cyclohexanedione ( $c-(C_6H_8)(1-O)(4-O)$ , IE = 9.85 eV).<sup>38</sup>

Next, the  $C_6H_{10}O_2$  signal was detected in the methane ice at 150–295 K at 10.49 eV and also *via* lower PI energies of 9.93 eV, 9.75 eV, and 9.63 eV with only a decrease in intensity observed. The  $C_6H_{10}O_2$  ion was also confirmed to be a product from the ethane ice, and sublime at 145–225 K for several PIs utilized (10.49 eV, 9.80 eV, and 9.60 eV). However, no signal was detected for this ion at a PI energy of 8.40 eV. Several conceivable isomers include 3-methyl-2,4-pentanedione ( $CH_3C(O)CH(CH_3)C(O)CH_3$ , IE = 8.55 eV), 2-hydroxycyclohexanone ( $c-(C_6H_9)(1-O)(2-OH)$ , IE = 9.70 eV), and 2-butenic acid ethyl ester ( $CH_3CH_2OC(O)(CH_2)_2CH_3$ , IE = 10.11 eV).<sup>38</sup>

Finally, the  $C_6H_{12}O_2$  signal was also detected in the methane ice subliming at 175–295 K with PI = 10.49 eV, and tuning the PI energy to a lower value results in only a weak tentative signal. The ethane system produced a sublimation profile from 175 to 250 K and the  $C_6H_{12}O_2$  signal was detectable at 9.80 eV and 9.60 eV, but not at 8.40 eV. Isomers possibly contributing to this signal therefore include butyl acetate ( $CH_3(CH_2)_3OC(O)CH_3$ , IE =  $9.92 \pm 0.05$  eV), isobutyl acetate ( $CH_3(CH_3)CHCH_2OC(O)CH_3$ , IE = 9.97 eV), and pentanoic acid ( $CH_3(CH_2)_3C(O)OH$ , IE =  $10.4 \pm 0.2$  eV).<sup>38</sup>

**3.2.11.  $C_4H_nO_3$  ( $n = 4, 6, 8$ ).** The ions corresponding to  $C_4H_nO_3$  ( $n = 4, 6, 8$ ) were also detected using PI-ReTOF-MS (Fig. 14 and Fig. S35–S37, ESI†). Each of the corresponding ions,  $C_4H_4O_3$  ( $m/z = 84$ ),  $C_4H_6O_3$  ( $m/z = 86$ ), and  $C_4H_8O_3$  ( $m/z = 88$ ), could only be detected in the carbon monoxide–methane system. The  $C_4H_4O_3$  signal was detected from 150 to 280 K at

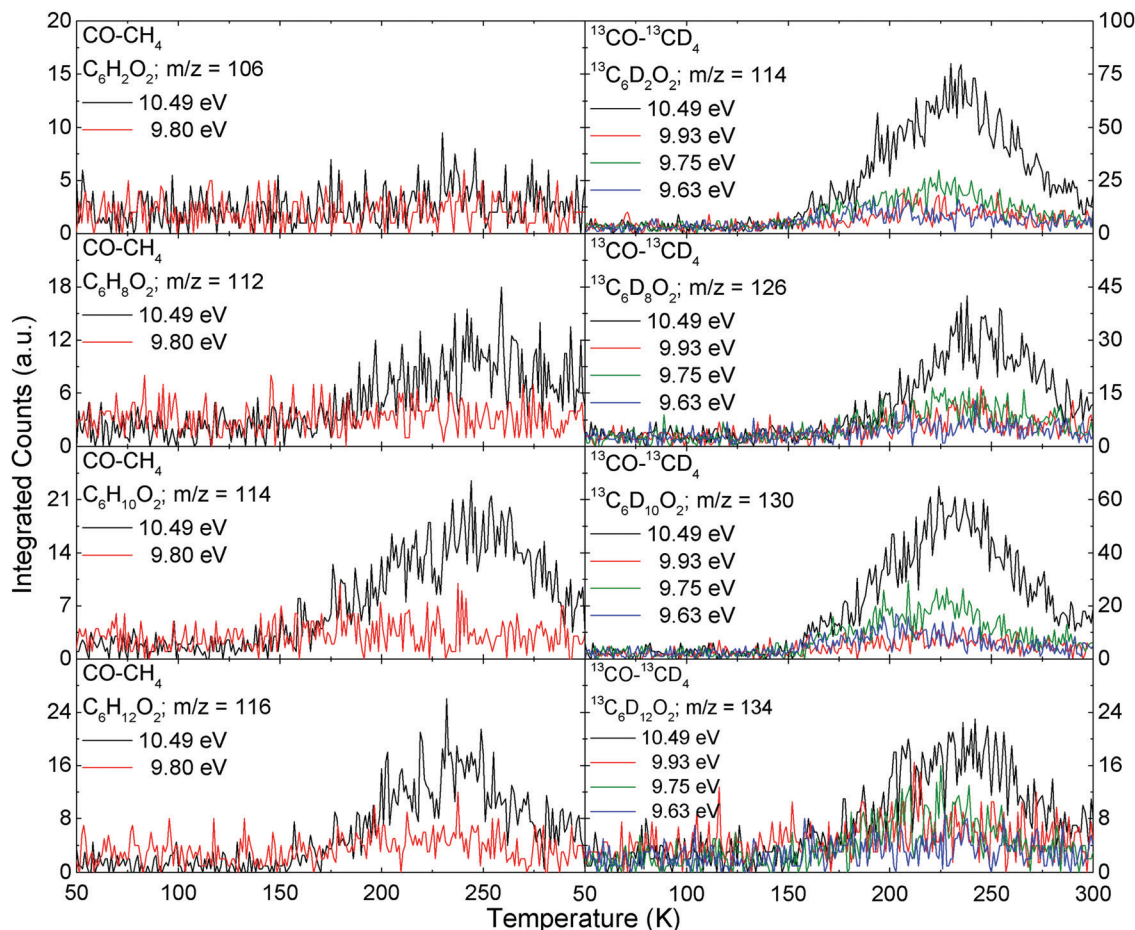


Fig. 13 PI-ReTOF-MS ion signals for  $C_6H_nO_2$  ( $n = 2, 8, 10, 12$ ) versus temperature subliming from carbon monoxide-methane ice ( $CO-CH_4$ ;  $^{13}CO-^{13}CD_4$ ).

PI energies of 10.49 eV, 9.93 eV, 9.75 eV, and 9.63 eV. Similarly, the  $C_4H_6O_3$  ion signal was recorded from 145 to 285 K at PI energies of 10.49 eV, 9.93 eV, 9.75 eV, and 9.63 eV. Finally,  $C_4H_8O_3$  ions were detected from 150 to 280 K at PI energies of 10.49 eV, 9.93 eV, and 9.75 eV. However, when utilizing a PI energy of 9.63 eV, a sublimation profile is revealed from 155 to 220 K. Isomers corresponding to  $C_4H_4O_3$ ,  $C_4H_6O_3$ , and  $C_4H_8O_3$  include succinic anhydride ( $c-(C_4H_4O)(2-O)(5-O)$ , IE = 10.84 eV), isobutyl acetate ( $CH_3OC(O)C(O)CH_3$ , IE = 9.88 eV), and 2-hydroxyisobutyric acid ( $CH_3C(CH_3)(OH)C(O)OH$ , IE =  $10.9 \pm 0.1$  eV), respectively.<sup>38</sup>

**3.2.12.  $C_5H_nO_3$  ( $n = 6, 8$ ).** The final group containing three oxygen atoms corresponded to  $C_5H_nO_3$  ( $n = 6, 8$ ) ions, and was detected using PI-ReTOF-MS (Fig. 15 and Fig. S38–S40, ESI†). The ions related to  $C_5H_6O_3$  ( $m/z = 114$ ) and  $C_5H_8O_3$  ( $m/z = 116$ ) were observed in the carbon monoxide-methane system and tentatively in the ethane containing ice. In the methane studies a sublimation profile from 150 to 290 K was recorded for both the  $C_5H_6O_3$  and  $C_5H_8O_3$  ions, and both of these ions were observed for all PI energies utilized. The ethane mixture produced tentative ion signals from 175 to 250 K for both the  $C_5H_6O_3$  and  $C_5H_8O_3$  related signals. Again these signals persisted at lower PI energies of 9.80 eV and 9.60 eV, but were no

longer detectable at PI = 8.40 eV. Isomers belonging to these groups are 2,3,4-pentanetrione ( $CH_3(CO)_3CH_3$ , IE = 9.52 eV) and methylacetoacetate ( $CH_3OC(O)CH_2C(O)CH_3$ , IE = 9.82 eV), respectively.<sup>38</sup>

### 3.3. Specific isomer yields

Since several specific molecules could be uniquely identified, their yields can be calculated if their photoionization cross sections are known. The methodology for determining the yields of the definitively identified products has been described previously.<sup>41</sup> Briefly, calibration ices were deposited onto the substrate, quantified *via* infrared absorption coefficients, and sublimed while monitoring with PI-ReTOF-MS. Next, by integrating each calibration compound's ion signal *versus* temperature, and accounting for the respective photoionization cross section, the signal intensity detected *via* PI-ReTOF-MS can be correlated with the number of molecules in the ice. By utilizing this calibration factor and the calculated dose deposited into the ice from the CASINO simulations the yield in molecules per energy deposited can be calculated for individual molecules from PI-ReTOF-MS counts and that molecule's PI cross section (Table 4). For instances where certain molecules were tentatively assigned due to the possible overlap of other isomers the yield calculations have



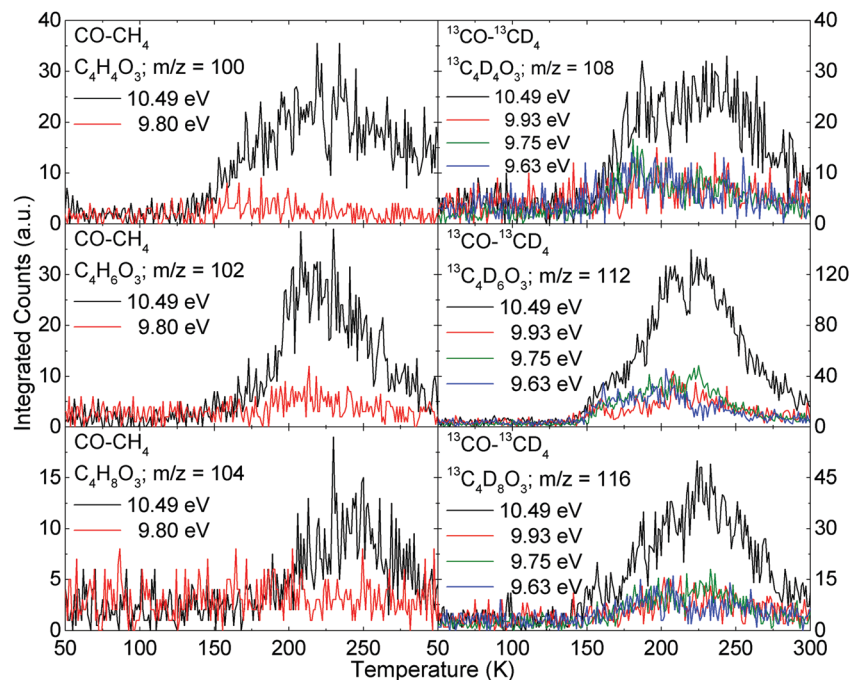


Fig. 14 PI-ReTOF-MS ion signals for  $C_4H_nO_3$  ( $n = 4, 6, 8$ ) versus temperature subliming from carbon monoxide–methane ice ( $CO-CH_4$ ;  $^{13}CO-^{13}CD_4$ ).

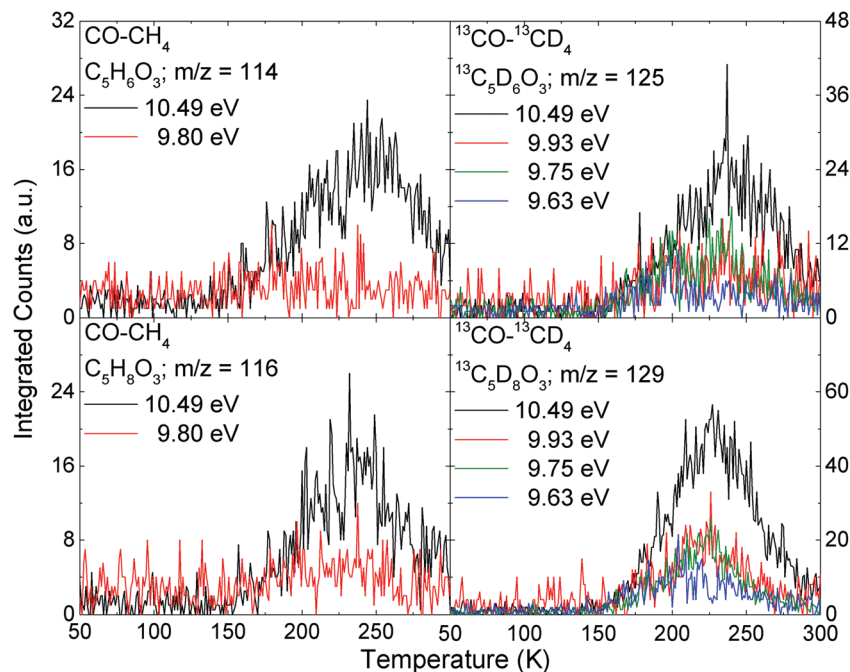


Fig. 15 PI-ReTOF-MS ion signals for  $C_5H_nO_3$  ( $n = 6, 8$ ) versus temperature subliming from carbon monoxide–methane ice ( $CO-CH_4$ ;  $^{13}CO-^{13}CD_4$ ).

been carried out assuming that only a single isomer is present and therefore yields an upper limit.

Four isomers were detected, at least tentatively, across all of the mixtures studied. The ketene isomer was produced at yields of  $1.24 \pm 0.37 \times 10^{-2}$  molecules  $eV^{-1}$ ,  $3.83 \pm 1.15 \times 10^{-4}$  molecules  $eV^{-1}$ ,  $4.13 \pm 1.24 \times 10^{-5}$  molecules  $eV^{-1}$ , and  $7.62 \pm 2.29 \times 10^{-5}$  molecules  $eV^{-1}$  in the carbon monoxide–methane and –ethane systems, and tentatively in the ethylene

and acetylene systems, respectively. Propenal was produced in the carbon monoxide–ethylene system and tentatively in the methane, ethane, and acetylene systems at yields of  $2.14 \pm 0.64 \times 10^{-4}$  molecules  $eV^{-1}$ ,  $8.67 \pm 2.60 \times 10^{-4}$  molecules  $eV^{-1}$ ,  $3.34 \pm 1.00 \times 10^{-4}$  molecules  $eV^{-1}$ , and  $1.33 \pm 0.40 \times 10^{-4}$  molecules  $eV^{-1}$ , respectively. Also, the propanal isomer was formed *via* the carbon monoxide–ethane ice and tentatively in the carbon monoxide–methane, –ethylene, and –acetylene systems

Table 4 Specific molecules detected in the carbon monoxide–hydrocarbon studies

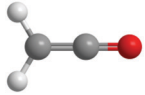
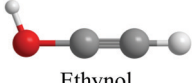
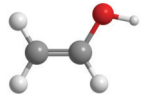
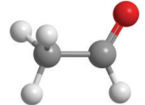
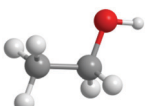
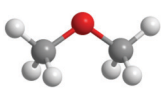
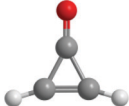
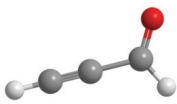
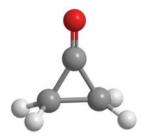
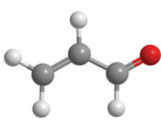
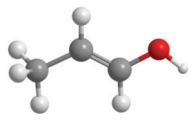

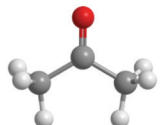
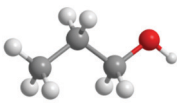

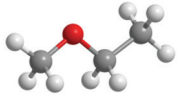
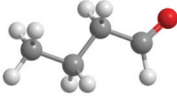
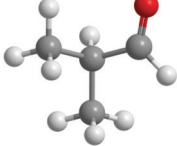
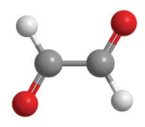
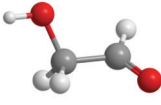
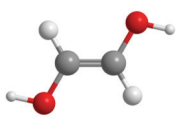
Formula	Detected isomer	ISM detection <sup>a</sup>	Yield (molecules eV <sup>-1</sup> )				Important functional group
			CO–CH <sub>4</sub>	CO–C <sub>2</sub> H <sub>6</sub>	CO–C <sub>2</sub> H <sub>4</sub>	CO–C <sub>2</sub> H <sub>2</sub>	
C <sub>2</sub> H <sub>2</sub> O	 Ketene	Yes	$1.24 \pm 0.37 \times 10^{-2}$	$3.83 \pm 1.15 \times 10^{-4}$	$4.13 \pm 1.24 \times 10^{-5c}$	$7.62 \pm 2.29 \times 10^{-5c}$	Carbonyl (C=O)
	 Ethynol	Not detected	Not detected	Not detected	Not detected	Tentative detection <sup>d</sup>	Alcohol (O–H)
C <sub>2</sub> H <sub>4</sub> O	 Ethenol	Yes	$1.48 \pm 0.44 \times 10^{-3}$	$1.51 \pm 0.45 \times 10^{-4}$	$5.96 \pm 1.79 \times 10^{-5c}$	Not detected	Alcohol (O–H)
	 Acetaldehyde	Yes	$1.01 \pm 0.30 \times 10^{-2}$	$1.30 \pm 0.39 \times 10^{-4}$	$3.01 \pm 0.90 \times 10^{-5c}$	Not detected	Carbonyl (C=O)
C <sub>2</sub> H <sub>6</sub> O	 Ethanol	Yes	$5.34 \pm 1.60 \times 10^{-4c}$	Not detected	Not detected	Not detected	Alcohol (O–H)
	 Dimethyl Ether	Yes	$1.28 \pm 0.38 \times 10^{-5c}$	Not detected	Not detected	Not detected	Ether (C–O–C)
C <sub>3</sub> H <sub>2</sub> O	 Cyclopropenone	Yes	Tentative detection <sup>d</sup>	Not detected	Not detected	Yes <sup>d</sup>	Carbonyl (C=O)
	 Propynal	Yes	Not detected	Tentative detection <sup>d</sup>	Yes <sup>d</sup>	Yes <sup>d</sup>	Carbonyl (C=O)
C <sub>3</sub> H <sub>4</sub> O	 Cyclopropanone	Not detected	Tentative detection <sup>d</sup>	Tentative detection <sup>d</sup>	Yes <sup>d</sup>	Not detected	Carbonyl (C=O)
	 Propenal	Yes	$8.67 \pm 2.60 \times 10^{-4c}$	$3.34 \pm 1.00 \times 10^{-4c}$	$2.14 \pm 0.64 \times 10^{-4}$	$1.33 \pm 0.40 \times 10^{-4c}$	Carbonyl (C=O)
C <sub>3</sub> H <sub>6</sub> O	 1-Propenol	Not detected	$1.52 \pm 0.61 \times 10^{-4c}$	$2.36 \pm 0.94 \times 10^{-4}$	Not detected	Not detected	Alcohol (O–H)

Table 4 (continued)

Formula	Detected isomer	ISM detection <sup>a</sup>	Yield (molecules eV <sup>-1</sup> )				Important functional group
			CO-CH <sub>4</sub>	CO-C <sub>2</sub> H <sub>6</sub>	CO-C <sub>2</sub> H <sub>4</sub>	CO-C <sub>2</sub> H <sub>2</sub>	
	 Propanal	Yes	$1.11 \pm 0.33 \times 10^{-3c}$	$8.84 \pm 2.65 \times 10^{-4}$	$1.25 \pm 0.38 \times 10^{-4c}$	$3.18 \pm 0.95 \times 10^{-5c}$	Carbonyl (C=O)
	 Acetone	Yes	$5.44 \pm 1.63 \times 10^{-4}$	Not detected	$1.06 \pm 0.32 \times 10^{-4c}$	$2.69 \pm 0.81 \times 10^{-5c}$	Carbonyl (C=O)
	 1-propanol	Not detected	$2.20 \pm 0.90 \times 10^{-4b,c}$	$1.57 \pm 0.63 \times 10^{-4b}$	Not detected	Not detected	Alcohol (O-H)
C <sub>3</sub> H <sub>8</sub> O	 2-propanol	Not detected	$1.20 \pm 0.50 \times 10^{-3b,c}$	$8.69 \pm 3.48 \times 10^{-4b}$	Not detected	Not detected	Alcohol (O-H)
	 Methylethyl Ether	Yes	$2.10 \pm 0.90 \times 10^{-5}$	Not detected	Not detected	Not detected	Ether (C-O-C)
	 1-butanal	Not detected	$2.00 \pm 0.80 \times 10^{-4}$	$1.00 \pm 0.04 \times 10^{-4c}$	$5.93 \pm 2.37 \times 10^{-5c}$	Not detected	Carbonyl (C=O)
C <sub>4</sub> H <sub>8</sub> O	 2-methyl propanal	Not detected	$1.32 \pm 0.53 \times 10^{-4}$	$1.00 \pm 0.40 \times 10^{-4c}$	$4.45 \pm 1.78 \times 10^{-5c}$	Not detected	Carbonyl (C=O)
C <sub>2</sub> H <sub>2</sub> O <sub>2</sub>	 Glyoxal	Not detected	Yes <sup>d</sup>	Tentative detection <sup>d</sup>	Tentative detection <sup>d</sup>	Tentative detection <sup>d</sup>	Carbonyl (C=O)
	 Glycolaldehyde	Yes	Yes <sup>d</sup>	Not detected	Not detected	Not detected	Carbonyl (C=O) Alcohol (O-H)
C <sub>2</sub> H <sub>4</sub> O <sub>2</sub>	 Ethene-1,2-diol	Not detected	Yes <sup>d</sup>	Not detected	Not detected	Not detected	Alcohol (O-H)

<sup>a</sup> See text for ISM detection references. <sup>b</sup> These isomers have IEs too similar to differentiate which was produced. <sup>c</sup> A tentative detection with yields calculated assuming only this isomer was produced. <sup>d</sup> No photoionization cross section data available.

with yields of  $8.84 \pm 2.65 \times 10^{-4}$  molecules  $\text{eV}^{-1}$ ,  $1.11 \pm 0.33 \times 10^{-3}$  molecules  $\text{eV}^{-1}$ ,  $1.25 \pm 0.38 \times 10^{-4}$  molecules  $\text{eV}^{-1}$ , and  $3.18 \pm 0.95 \times 10^{-5}$  molecules  $\text{eV}^{-1}$ , respectively. Finally, glyoxal was also detected in the carbon monoxide–methane system and tentatively in the ethane, ethylene, and acetylene systems, but no PI cross section data are currently available to allow for the calculation of its yield. Inspecting these yields shows that the ketene, propenal, and propanal isomers were all produced with the highest abundance in the carbon monoxide–methane system.

It is also interesting to compare the yields of the structural isomers detected between the systems. For the  $\text{C}_2\text{H}_4\text{O}$  isomers, ethenol was produced at yields of  $1.48 \pm 0.44 \times 10^{-3}$  molecules  $\text{eV}^{-1}$ ,  $1.51 \pm 0.45 \times 10^{-4}$  molecules  $\text{eV}^{-1}$ , and  $5.96 \pm 1.79 \times 10^{-5}$  molecules  $\text{eV}^{-1}$ , and acetaldehyde was formed in yields of  $1.01 \pm 0.30 \times 10^{-2}$  molecules  $\text{eV}^{-1}$ ,  $1.30 \pm 0.39 \times 10^{-4}$  molecules  $\text{eV}^{-1}$ , and  $3.01 \pm 0.90 \times 10^{-5}$  molecules  $\text{eV}^{-1}$  in the carbon monoxide–methane and –ethane systems, and tentatively in the ethylene ice, respectively. The  $\text{C}_2\text{H}_6\text{O}$  isomers ethanol and dimethyl ether were only tentatively observed in the carbon monoxide–methane system in yields of  $5.34 \pm 1.60 \times 10^{-4}$  molecules  $\text{eV}^{-1}$  and  $1.28 \pm 0.38 \times 10^{-5}$  molecules  $\text{eV}^{-1}$ , respectively. The  $\text{C}_3\text{H}_6\text{O}$  isomers detected in these experiments were propanal, 1-propenol, and acetone. The 1-propenol isomer was produced from the carbon monoxide–ethane ice and tentatively in the carbon monoxide–methane system at an abundance of  $2.36 \pm 0.94 \times 10^{-4}$  molecules  $\text{eV}^{-1}$  and  $1.52 \pm 0.61 \times 10^{-4}$  molecules  $\text{eV}^{-1}$ , respectively. Here, the propanal isomer was detected in yields of  $8.84 \pm 2.65 \times 10^{-4}$  molecules  $\text{eV}^{-1}$ ,  $1.11 \pm 0.33 \times 10^{-3}$  molecules  $\text{eV}^{-1}$ ,  $1.25 \pm 0.38 \times 10^{-4}$  molecules  $\text{eV}^{-1}$ , and  $3.18 \pm 0.95 \times 10^{-5}$  molecules  $\text{eV}^{-1}$  *via* the carbon monoxide–ethane ice and tentatively in the carbon monoxide–methane, –ethylene, and –acetylene systems, respectively. Lastly, acetone was produced at yields of  $5.44 \pm 1.63 \times 10^{-4}$  molecules  $\text{eV}^{-1}$ ,  $1.06 \pm 0.32 \times 10^{-4}$  molecules  $\text{eV}^{-1}$ , and  $2.69 \pm 0.81 \times 10^{-5}$  molecules  $\text{eV}^{-1}$  from the carbon monoxide–methane ice and tentatively in the ethylene and acetylene systems, respectively. The  $\text{C}_3\text{H}_8\text{O}$  isomers include 1-propanol, 2-propanol, and methylethyl ether. The 1-propanol and 2-propanol isomers have IE energies too similar to discriminate if both are formed. The signal corresponding to 1-propanol was observed in the carbon monoxide–ethane system and tentatively in the carbon monoxide–methane system in yields of  $1.57 \pm 0.63 \times 10^{-4}$  molecules  $\text{eV}^{-1}$  and  $2.20 \pm 0.90 \times 10^{-4}$  molecules  $\text{eV}^{-1}$ , respectively. Likewise, the 2-propanol isomer was observed in the carbon monoxide–ethane system and tentatively in the carbon monoxide–methane system in yields of  $8.69 \pm 3.48 \times 10^{-4}$  molecules  $\text{eV}^{-1}$  and  $1.20 \pm 0.50 \times 10^{-3}$  molecules  $\text{eV}^{-1}$ , respectively. Finally, the methylethyl ether isomer was only observed *via* the carbon monoxide–methane system in a yield of  $2.10 \pm 0.90 \times 10^{-5}$  molecules  $\text{eV}^{-1}$ . The  $\text{C}_4\text{H}_8\text{O}$  isomer 1-butanal was formed in a yield of  $2.00 \pm 0.80 \times 10^{-4}$  molecules  $\text{eV}^{-1}$ ,  $1.00 \pm 0.40 \times 10^{-4}$  molecules  $\text{eV}^{-1}$ , and  $5.93 \pm 2.37 \times 10^{-5}$  molecules  $\text{eV}^{-1}$  in the carbon monoxide–methane ice and tentatively in the ethane and ethylene ices, respectively. The 2-methyl-propanal isomer was also detected in

the carbon monoxide–methane ice and tentatively in the ethane and ethylene ices in yields of  $1.32 \pm 0.53 \times 10^{-4}$  molecules  $\text{eV}^{-1}$ ,  $1.00 \pm 0.40 \times 10^{-4}$  molecules  $\text{eV}^{-1}$ , and  $4.45 \pm 1.78 \times 10^{-5}$  molecules  $\text{eV}^{-1}$ , respectively. Although multiple isomers were detected for the  $\text{C}_3\text{H}_2\text{O}$ ,  $\text{C}_3\text{H}_4\text{O}$ , and  $\text{C}_2\text{H}_4\text{O}_2$  there is no available PI cross section information available to calculate the corresponding yields of these isomers, except for the  $\text{C}_3\text{H}_4\text{O}$  isomer propenal as previously stated above.

The branching ratios of these structural isomers detected here can also be used to better understand the chemistry from which they were formed. Through a thermodynamic equilibrium mechanism the branching ratio of these isomers will be controlled *via* the equilibrium constant  $K$ . Here,  $K$  corresponds to the yield of the isomers *via*  $K = [\text{isomer1}]/[\text{isomer2}] = \exp(-\Delta G/RT)$ , utilizing the ideal gas constant ( $R$ ), a specific temperature ( $T$ ), and the difference of the isomers' Gibbs free energies ( $\Delta G$ ). Utilizing this calculation the theoretical thermal equilibrium ratios were determined at temperatures of 10 K and 200 K; this higher temperature was chosen as it defines the maximum temperature where any sublimation signal related to these isomers was still observed. Calculating this value for acetaldehyde *versus* vinyl alcohol reveals branching ratios of  $3.80 \pm 0.76 \times 10^{249}$  (10 K) and  $1.94 \pm 0.39 \times 10^{11}$  (200 K). The ethanol to dimethyl ether isomer ratio should be formed at  $1.5 \times 10^{261}$  (10 K) and  $1.14 \times 10^{13}$  (200 K). The propanal *versus* 1-propenol calculations correspond to  $6.34 \pm 1.27 \times 10^{88}$  (10 K) and  $2.75 \pm 0.55 \times 10^4$  (200 K) for propanal to (*E*)-1-propenol, and  $4.8 \pm 0.96 \times 10^{62}$  (10 K) as well as  $1.4 \pm 0.28 \times 10^3$  (200 K) for propanal *versus* (*Z*)-1-propenol due to the energy differences of the 1-propenol conformers. The acetone and 1-propenol isomers should be produced with a ratio of  $9.1 \pm 1.82 \times 10^{255}$  (10 K) along with  $6.28 \pm 1.26 \times 10^{12}$  (200 K). Meanwhile, the acetone *versus* propanal ratio was calculated to be  $1.44 \pm 0.29 \times 10^{167}$  (10 K) and  $2.28 \pm 0.46 \times 10^8$  (200 K). The 1-propanol *versus* 2-propanol ratio was determined to be  $2.3 \pm 0.4 \times 10^{90}$  (10 K) and  $3.3 \pm 0.6 \times 10^4$  (200 K). The 1-propanol and methylethyl ether isomers will have a ratio of  $8.5 \pm 0.7 \times 10^{196}$  (10 K) and  $7.0 \pm 0.6 \times 10^9$  (200 K), but the 2-propanol to methylethyl ether ratio was determined to be  $2.0 \pm 0.1 \times 10^{287}$  (10 K) as well as  $2.3 \pm 0.1 \times 10^{14}$  (200 K). Finally, the ratio of the 2-methyl-propanal to 1-butanal isomer was calculated to be  $1.9 \pm 0.1 \times 10^{157}$  (10 K) and  $7.3 \pm 0.3 \times 10^7$  (200 K). However, a large discrepancy is observed upon comparison of these thermodynamic ratios with the experimentally derived ratios across each of the systems studied (Table 5). The experimental ratios display a considerable overproduction of all isomers from 3 to 286 orders of magnitude. This vast inconsistency proves that these isomers are not formed under thermal equilibrium conditions, but instead through non-equilibrium processes within the ices (see Section 3.4).

### 3.4. Energetics

Next, formation pathways to general COMs containing the functional groups that were confirmed to form *via* the detection of the specific isomers discussed previously are analyzed. Although the FTIR analysis provided proof for the development of

Table 5 Experimental branching ratios of detected isomers

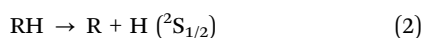
Isomer	CO-CH <sub>4</sub>	CO-C <sub>2</sub> H <sub>6</sub>	CO-C <sub>2</sub> H <sub>4</sub>	CO-C <sub>2</sub> H <sub>2</sub>
Acetaldehyde : ethenol	6.8 ± 3.8	0.9 ± 0.5	0.5 ± 0.3	<sup>a</sup>
Ethanol : dimethyl ether	42.0 ± 23.5	<sup>a</sup>	<sup>a</sup>	<sup>a</sup>
Propanal : 1-propenol	7.0 ± 3.9	3.8 ± 2.1	<sup>a</sup>	<sup>a</sup>
Acetone : 1-propenol	3.6 ± 2.0	<sup>a</sup>	<sup>a</sup>	<sup>a</sup>
Propanal : acetone	2.0 ± 1.1	<sup>a</sup>	1.2 ± 0.7	1.2 ± 0.7
2-Propanol : 1-propanol	5.5 ± 3.1	5.6 ± 3.1	<sup>a</sup>	<sup>a</sup>
1-Propanol : methylethyl ether	11 ± 6	N.D.	<sup>a</sup>	<sup>a</sup>
2-Propanol : methylethyl ether	57 ± 32	N.D.	<sup>a</sup>	<sup>a</sup>
1-Butanal : 2-methyl-propanal	1.5 ± 0.8	1.0 ± 0.6	1.3 ± 0.6	<sup>a</sup>

<sup>a</sup> No ratio could be calculated due to the non-detection of an isomer(s) in that system.

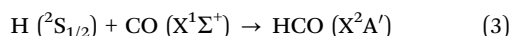
functional groups linked with carbonyl containing molecules – aldehydes and ketones – even at 5 K, the FTIR data were incapable of identifying individual COMs due to coinciding absorptions of the functional groups. Due to these complications, kinetic profiles tracking the formation of individual COMs could not be extracted and this discussion of possible reaction mechanisms needs to be verified *via* future experiments. The formation of aldehydes (RCHO), with R being an alkane, alkene, or alkyne hydrocarbon group, can be accounted for *via* the reaction of a single carbon monoxide and alkane, alkene, or alkyne molecule (reaction (1)).



However, the overall reaction (1) is frequently thermodynamically unfavorable at 5 K due to its endoergicity and is typically not a barrierless reaction.<sup>21,41,66</sup> Consequently, an alternative energy source is needed, such as secondary electrons produced in the track of GCRs within interstellar ices, to initiate the reaction beginning with the rupture of a carbon–hydrogen bond of alkanes, alkenes, or alkynes (reaction (2)).<sup>10,21,22,24,32,33,66,91,107,108</sup>



Here, the carbon–hydrogen bond cleavage is an endoergic process of typically 380–560 kJ mol<sup>−1</sup> (3.94–5.77 eV)<sup>46,53,54,109</sup> for methane, ethane, ethylene and acetylene, and several electron volts of energy can be supplied, *via* the electrons processing the ice, to the hydrocarbon molecule causing this bond rupture (Table 1). Thus, reaction (2) produces a hydrocarbon radical (R) and a suprathermal hydrogen atom (H) that contains excess energy capable of overcoming reaction barriers to addition (*E<sub>b</sub>*) such as with ground state carbon monoxide in reaction (3) (*E<sub>b</sub>* = 11 kJ mol<sup>−1</sup>, 0.11 eV; Δ<sub>R</sub>G = −56 kJ mol<sup>−1</sup>, −0.59 eV) producing the formyl radical (HCO).<sup>10,21,41,66</sup>

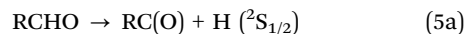


It is important to point out that the formyl radical was observed in each of the carbon monoxide–hydrocarbon systems and verified with isotopic shifts (Table 2 and Table S1, ESI†). Next, the hydrocarbon radicals (R), such as methyl (CH<sub>3</sub>), ethyl (C<sub>2</sub>H<sub>5</sub>), vinyl (C<sub>2</sub>H<sub>3</sub>), ethynyl (C<sub>2</sub>H), 1-propyl (1-C<sub>3</sub>H<sub>7</sub>), and 2-propyl (2-C<sub>3</sub>H<sub>7</sub>) radicals, can then barrierlessly recombine in the ice with formyl radicals (reaction (4a)); Δ<sub>R</sub>G = −340 ± 20 kJ mol<sup>−1</sup>, −3.5 ± 0.2 eV<sup>41,46,109</sup> to form the detected

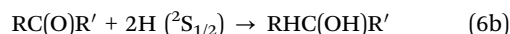
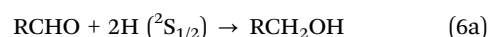
aldehydes: acetaldehyde, propanal, propenal, propynal, 1-butanal, and 2-methyl-propanal, respectively. Similarly, two formyl radicals can recombine barrierlessly as well to form the detected glyoxal isomer (reaction (4b))



Furthermore, these aldehydes can produce ketones (RC(O)R') *via* another carbon–hydrogen bond breaking, thus forming an aldehyde type radical (reaction (5a)), which can then recombine barrierless with another hydrocarbon radical (reaction (5b)).

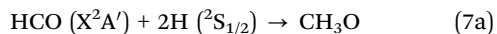


Here, reactions (5) can account for the production of acetone for example. Alternatively, the aldehyde products (reaction (6a)), as well as ketones (reaction (6b)), can be hydrogenated, *via* suprathermal hydrogen atoms, leading to alcohols (Δ<sub>R</sub>G = −470 ± 20 kJ mol<sup>−1</sup>, −4.9 ± 0.2 eV).<sup>41</sup>



For example, reactions (6) can explain the production of several detected alcohols *via* the hydrogenation of ketene, acetaldehyde, propenal, propanal, acetone, and glyoxal, which produces ethenol, ethanol, 1-propenol, 1-propanol, 2-propanol, and glycolaldehyde and/or ethane-1,2-diol, respectively. The ketene, cyclopropanone, and cyclopropenone molecules are likely formed through excitation pathways *via* the interaction of excited carbon monoxide or the respective excited methane, ethylene, or acetylene hydrocarbon unit, but further experiments exploring the reaction dynamics of these pathways are needed.<sup>33,66,91</sup> The excitation of the reactants is again possible *via* the energy deposited into the ice from the energetic electrons. The products containing excess energy can then be stabilized by the surrounding ice matrix. Finally, ethers may be formed from a methanol precursor, which could be formed *via* the successive hydrogenation of the formyl radical to produce the methoxy radical (CH<sub>3</sub>O) (reaction (7a)); Δ<sub>R</sub>G = −440 ± 20 kJ mol<sup>−1</sup>, −4.6 ± 0.2 eV.<sup>41</sup> The methoxy radical can then barrierlessly recombine with a hydrocarbon radical forming an ether type molecule (reaction (7b)); Δ<sub>R</sub>G = −350 ± 20 kJ mol<sup>−1</sup>, −3.7 ± 0.2 eV.<sup>41</sup>





For instance, the recombination of the methanol based radical with a methyl or ethyl radical produces dimethyl ether and methylethyl ether, respectively.

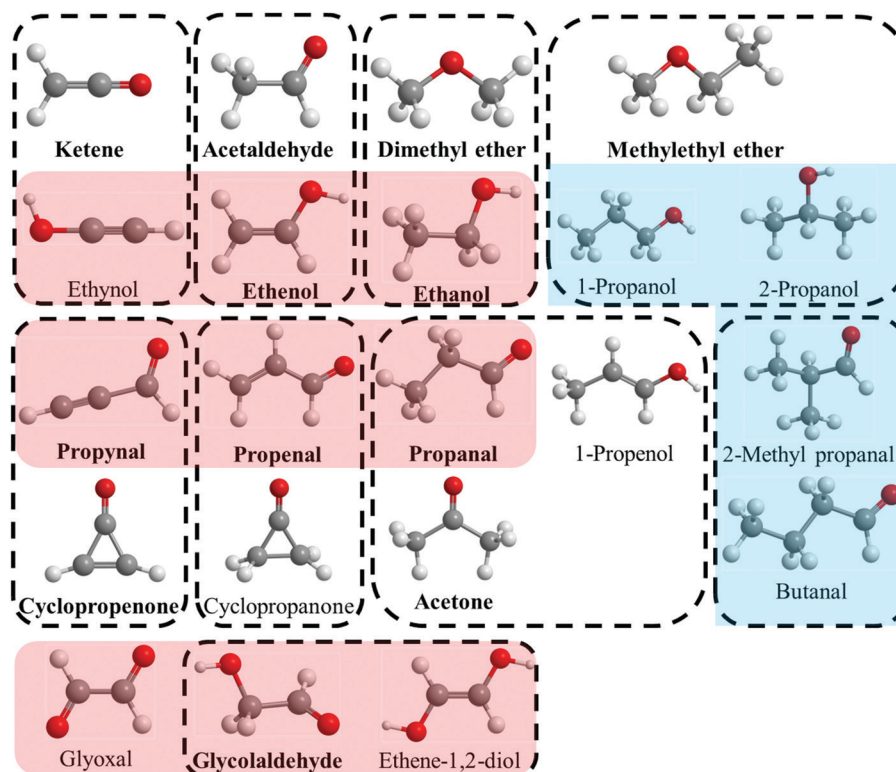
These schematic reactions are able to account for the production of each of the 21 specific isomers observed in this manuscript. As previously discussed, the experimental branching ratios derived from the present experiments strongly support these non-equilibrium pathways outlined above, and suggest that tunneling is not a dominating formation pathway in the current experiments. This conclusion is further supported by the similarity in product yields between the hydrogen and deuterium substituted systems, which would not be possible *via* the difference in the tunneling capabilities of the hydrogen and deuterium atoms. Briefly, the only remaining functional groups detected in purely carbon, hydrogen, and oxygen atom bearing COMs in the ISM are the ester ( $\text{RC(O)OR}'$ ) and acid ( $\text{RC(O)OH}$ ) groups, and both have multiple oxygen atoms incorporated into the functional groups. Note that the only pathway to obtain multiple oxygen atoms into a single molecule discussed here was *via* the recombination of two formyl radicals (reaction (4b)), which does not produce a molecule with two oxygen atoms connected to the same carbon atom. Therefore, it is unlikely that either the ester or acid functional groups are formed in any

significant abundance from these reactants. However, these groups can be formed *via* other reactants known to be present in ISM ices *via* studies on the formation of these types of molecules utilizing ices containing water<sup>83</sup> or carbon dioxide<sup>86</sup> with hydrocarbons.

## 4. Conclusions

Our studies were able to confirm the formation of at least 21 distinct isomers, which can be associated with the molecular formulae  $\text{C}_2\text{H}_2\text{O}$ ,  $\text{C}_2\text{H}_4\text{O}$ ,  $\text{C}_2\text{H}_6\text{O}$ ,  $\text{C}_3\text{H}_2\text{O}$ ,  $\text{C}_3\text{H}_4\text{O}$ ,  $\text{C}_3\text{H}_6\text{O}$ ,  $\text{C}_3\text{H}_8\text{O}$ ,  $\text{C}_4\text{H}_8\text{O}$ ,  $\text{C}_2\text{H}_2\text{O}_2$ , and  $\text{C}_2\text{H}_4\text{O}_2$  (Fig. 16 and Table 4). The  $\text{C}_2\text{H}_2\text{O}$  group was confirmed *via* the detection of ketene ( $\text{H}_2\text{CCO}$ ) and tentatively ethynol ( $\text{HCCOH}$ ), the  $\text{C}_2\text{H}_4\text{O}$  group was verified through the observation of ethenol ( $\text{CH}_2\text{CHOH}$ ) and acetaldehyde ( $\text{CH}_3\text{CHO}$ ), and the  $\text{C}_2\text{H}_6\text{O}$  group was established *via* the detection of ethanol ( $\text{CH}_3\text{CH}_2\text{OH}$ ) and dimethyl ether ( $\text{CH}_3\text{OCH}_3$ ). Interestingly, ketene,<sup>110</sup> ethenol,<sup>111</sup> acetaldehyde,<sup>1</sup> ethanol,<sup>112</sup> and dimethyl ether<sup>113</sup> have all been observed in the ISM.<sup>1</sup>

Next, the  $\text{C}_3\text{H}_2\text{O}$  group was ratified *via* the identification of propynal ( $\text{HCCCHO}$ ) and cyclopropanone ( $\text{c-C}_3\text{H}_2\text{O}$ ), the  $\text{C}_3\text{H}_4\text{O}$  group was corroborated from the assignment of propenal ( $\text{CH}_2\text{CHCHO}$ ) and cyclopropanone ( $\text{c-C}_3\text{H}_4\text{O}$ ), the  $\text{C}_3\text{H}_6\text{O}$  group was proven with the recognition of 1-propanol ( $\text{CH}_2\text{CHCH}_2\text{OH}$ ), propanal ( $\text{CH}_3\text{CH}_2\text{CHO}$ ), and acetone ( $\text{CH}_3\text{C(O)CH}_3$ ), and the  $\text{C}_3\text{H}_8\text{O}$  group was revealed as a product *via* the detection of



**Fig. 16** Carbon, hydrogen, and oxygen containing molecules formed in carbon monoxide–hydrocarbon mixtures exposed to ionizing radiation *via* PI-ReTOF-MS; COMs detected in the ISM are designated in bold. Molecules grouped in red define C2 alcohols, C3 carbonyls, and C3-alcohols/carbonyls (top to bottom) with various degrees of saturation (left to right). Molecules grouped in blue share a common (iso)propyl ( $\text{C}_3\text{H}_7$ ) moiety in alcohols and aldehydes. Structural isomers and/or tautomers are circled in dashed lines.



1-propanol ( $\text{CH}_3\text{CH}_2\text{CH}_2\text{OH}$ ) and/or 2-propanol ( $\text{CH}_3\text{CH}(\text{OH})\text{CH}_3$ ), and methylethyl ether ( $\text{CH}_3\text{COC}_2\text{H}_5$ ). Propynal,<sup>114</sup> cyclopropenone,<sup>115</sup> propenal,<sup>116</sup> propanal,<sup>116</sup> acetone,<sup>117</sup> and methylethyl ether<sup>118</sup> have all been detected in the ISM.<sup>1</sup> The only isomers detected here that have not been observed in the ISM are the cyclopropanone and 1-/2-propanol isomers.

The  $\text{C}_4\text{H}_8\text{O}$  group was confirmed *via* the detection of 1-butanol ( $\text{H}_3\text{C}(\text{CH}_2)_2\text{CHO}$ ) and 2-methyl-propanal ( $\text{CH}_3\text{CH}(\text{CH}_3)\text{CHO}$ ), but neither of these isomers has been observed in the ISM to date.<sup>1</sup> Finally, the  $\text{C}_2\text{H}_2\text{O}_2$  group was authenticated *via* the detection of glyoxal ( $\text{HC}(\text{O})\text{CHO}$ ), and the  $\text{C}_2\text{H}_4\text{O}_2$  group was validated by the observation of glycolaldehyde ( $\text{CH}_2(\text{OH})\text{CHO}$ ) and ethene-1,2-diol ( $\text{CH}(\text{OH})\text{CHOH}$ ). From these groups only the glycolaldehyde<sup>119</sup> isomer has been detected in the ISM so far.<sup>1</sup>

Here, a homologous series of saturated alcohols was confirmed *via* the C2 and C3 alcohols ethanol, and 1-propanol and/or 2-propanol, respectively (Fig. 16). From these alcohol COMs, ethanol has been detected in the ISM.<sup>1</sup> It is worth pointing out that this is the first evidence of a C3 alcohol *via* the detection of 1-propanol and/or 2-propanol.<sup>1,41</sup> Furthermore, these isomers contain unique structural carbon chains, with 2-propanol having a branched carbon chain, while 1-propanol is a straight carbon chain. Interestingly, these types of unique carbon chains have been observed in the ISM already *via* the analogous nitrogen containing COMs propyl cyanide ( $\text{CH}_3\text{CH}_2\text{CH}_2\text{CN}$ ) and isopropyl cyanide ( $\text{CH}_3\text{CH}(\text{CH}_3)\text{CN}$ ).<sup>120</sup> These similarities suggest that 1-propanol and 2-propanol may also be useful tracers of the hydrocarbon chemistry taking place in the ISM if detected. Also, the related C2 and C3 unsaturated alcohols were detected *via* ethynol, ethenol, and 1-propenol. These unsaturated alcohols are capable of undergoing tautomerization, which form the structural isomers ketene, acetaldehyde, and propanal *via* the hydrogen shift of ethynol, ethenol, and 1-propenol, respectively (Fig. 16). From these six COMs, ethenol, acetaldehyde, and propanal were all detected in the ISM.<sup>1</sup> Finally, the dimethyl ether and methylethyl ether molecules are also related to these alcohol molecules as they are structural isomers of ethanol and 1-propanol and 2-propanol, respectively. Here, the ether functional group is formally produced from an alcohol precursor *via* the recombination of a methoxy ( $\text{CH}_3\text{O}$ ) or an ethoxy ( $\text{C}_2\text{H}_5\text{O}$ ) radical with an alkyl radical. Both of these ether type COMs, dimethyl ether and methylethyl ether, are present in the ISM.<sup>1</sup>

Similarly, a homologous series of C2, C3, and C4 saturated aldehydes was also detected from the carbon monoxide-hydrocarbon mixtures. The C2 aldehyde group is confirmed by the assignment of acetaldehyde; the C3 aldehyde propanal was observed along with its ketone isomer acetone, and C4 aldehydes were probed *via* 1-butanol and 2-methyl-propanal. Also, the unsaturated aldehydes propenal and propynal were produced from these ice analogues. These detections confirm that all degrees of unsaturation are synthesized in the form of alkyne ( $\text{C}_2\text{H}$ ), alkene ( $\text{C}_2\text{H}_2$ ), and alkyl ( $\text{C}_2\text{H}_3$ ) functional groups from propynal, propenal, and propanal, respectively (Fig. 16). These findings have significant implications as all of the C2 and C3 aldehydes and ketones detected from these experiments

are observed in the ISM, but the C4 aldehydes, 1-butanol and 2-methyl-propanal, have remained elusive to astronomical detection.<sup>1</sup> However, 1-butanol and 2-methyl-propanal are also carriers of straight and branched propyl groups, respectively, which have been observed in the analogous COMs propyl cyanide ( $\text{CH}_3\text{CH}_2\text{CH}_2\text{CN}$ ) and isopropyl cyanide ( $\text{CH}_3\text{CH}(\text{CH}_3)\text{CN}$ ), where the HCO functional group is replaced with a cyano moiety (Fig. 16).<sup>120</sup> Similarly to 1-propanol and 2-propanol, these COMs would be useful tracers for the production of analogous COMs with different functional groups.

The exotic cyclic molecules cyclopropenone and cyclopropanone have also been observed here along with their respective aldehyde isomers propynal and propenal (Fig. 16). Although both  $\text{C}_3\text{H}_2\text{O}$  isomers, propynal and cyclopropenone, have been observed in the ISM, only the  $\text{C}_3\text{H}_4\text{O}$  isomer propenal, but not cyclopropanone has been confirmed.<sup>1</sup> The similarity of these systems suggests that cyclopropanone is also a likely COM awaiting detection in the ISM.

Finally, glyoxal, glycolaldehyde, and ethene-1,2-diol were observed in the present experiments, which are all COMs containing two oxygen atoms, but only glycolaldehyde – the sugar related molecule – has been confirmed in the ISM.<sup>1</sup> Interestingly, only glycolaldehyde has been observed in the ISM. However, similarly to the previously mentioned aldehyde and alcohol groups the diol isomer, ethene-1,2-diol, is a possible tautomer of glycolaldehyde (Fig. 16). Furthermore, the varying degrees of unsaturation detected in the aldehyde and alcohol groups show that the unsaturated relative, glyoxal, is also a likely ISM constituent.

These isomers show that certain functional groups are preferentially formed based on the reactant ice mixture. The isomers show that carbonyl ( $\text{C}=\text{O}$ ), alcohol ( $\text{O}-\text{H}$ ), and ether ( $\text{C}-\text{O}-\text{C}$ ) functional groups were the only types confirmed to be produced. Also, these specific identifications had varying degrees of unsaturation, as well as unique structures including straight carbon chains, branched carbon chains and even cyclic carbon rings. Interestingly, a single detection existed for molecules containing two carbonyls (glyoxal), one carbonyl and one alcohol (glycolaldehyde), and two alcohols (ethane-1,2-diol), and suggests that these molecules may be closely related to one another and observable in the ISM in future surveys.

The ester ( $\text{RC}(\text{O})\text{OR}'$ ) and acid ( $\text{RC}(\text{O})\text{OH}$ ) functional groups have been detected in interstellar COMs, but were not definitively detected in these experiments. Interestingly, the ethylene oxide ( $\text{c}-\text{C}_2\text{H}_4\text{O}$ )<sup>121</sup> and propylene oxide ( $\text{c}-\text{C}_3\text{H}_6\text{O}$ )<sup>122</sup> isomers have been detected in the ISM, but were not formed in the present experiments. However, similar experiments utilizing carbon dioxide mixed with methane, ethylene, and propene produced acetic acid,<sup>123,124</sup> ethylene oxide,<sup>22</sup> and propylene oxide,<sup>12</sup> respectively. These results show that even a minor change of the reactants can produce a new array of structural isomers. Although the present chemical systems, which only represent a simplified model ISM ice, have been previously investigated, the lack of sensitive analytical techniques utilized has not allowed a complete understanding of the chemistry occurring. Therefore, it is necessary to continue to exploit these

powerful analytical tools to explore the complex and unconventional chemistry occurring in ISM ices.<sup>24</sup>

The COMs consisting solely of carbon, hydrogen, and oxygen atoms currently detected in the ISM show a vast diversity in their chemical complexity (Fig. 1). Interestingly, these studies provide evidence that among these observed molecules more than half can be formed upon interaction of carbon monoxide–methane, –ethane, –ethylene, or –acetylene ices with energetic electrons (Table 4). It should be noted that several molecules detected in the present study, but not yet in the ISM could be due to the lack of spectra to search the ISM for the respective molecule rather than the lack of the molecule. Also, the isomers not observed in the ISM, but detected in the present experiments are likely produced in the ISM as well, and can be used to guide searches for these molecules in the ISM. Concurrently, with the aid of the Atacama Large Millimeter/Submillimeter Array (ALMA), the detection of new COMs of varying complexity will continue to grow, and an understanding of these data will require advanced experimental laboratory techniques as exposed here. These results also provide understanding of the link between the origin and evolution of comets and the interstellar material that created them. The recent mission to comet 67P/Churyumov-Gerasimenko, via the Rosetta mission, detected COMs incorporating the carbonyl functional groups including acetaldehyde, acetone, propanal, and glycolaldehyde.<sup>125</sup> Furthermore, analysis of meteorites, such as the Murchison meteorite, has revealed the production of 29 different aldehydes and ketones including, for example, formaldehyde, acetaldehyde, propanal, butanal, and acetone.<sup>126</sup> These detections fulfill the chemical cycle from interstellar clouds via star-forming regions to our solar system, which ultimately brings us closer to eventually predicting where in the Galaxy molecular precursors linked to the Origins of Life might have been synthesized.

## Conflicts of interest

There are no conflicts to declare.

## Acknowledgements

RIK and MJA thank the US National Science Foundation (AST-1800975) for support to conduct the experiments and data analysis. The experimental apparatus was financed by the W. M. Keck Foundation through an equipment grant.

## Notes and references

- 1 B. A. McGuire, *Astrophys. J., Suppl. Ser.*, 2018, **239**, 17.
- 2 E. Herbst, *Int. Rev. Phys. Chem.*, 2017, **36**, 287–331.
- 3 E. Herbst, *Phys. Chem. Chem. Phys.*, 2014, **16**, 3344–3359.
- 4 M. J. Mottl, B. T. Glazer, R. I. Kaiser and K. J. Meech, *Geochemistry*, 2007, **67**, 253–282.
- 5 V. Wakelam, J. C. Loison, E. Herbst, B. Pavone, A. Bergeat, K. Béroff, M. Chabot, A. Faure, D. Galli, W. D. Geppert, D. Gerlich, P. Gratier, N. Harada, K. M. Hickson, P. Honvault, S. J. Klippenstein, S. D. L. Picard, G. Nyman, M. Ruaud, S. Schlemmer, I. R. Sims, D. Talbi, J. Tennyson and R. Wester, *Astrophys. J., Suppl. Ser.*, 2015, **217**, 20–26.
- 6 T. Vasyunina, A. I. Vasyunin, E. Herbst, H. Linz, M. Voronkov, T. Britton, I. Zinchenko and F. Schuller, *Astrophys. J.*, 2014, **780**, 19.
- 7 E. Herbst and E. F. van Dishoeck, *Annu. Rev. Astron. Astrophys.*, 2009, **47**, 427–480.
- 8 T. J. Millar, E. Herbst and S. B. Charnley, *Astrophys. J.*, 1991, **369**, 147–156.
- 9 N. Adams, D. Smith, K. Giles and E. Herbst, *Astron. Astrophys.*, 1989, **220**, 269–271.
- 10 M. J. Abplanalp, S. Gozem, A. I. Krylov, C. N. Shingledecker, E. Herbst and R. I. Kaiser, *Proc. Natl. Acad. Sci. U. S. A.*, 2016, **113**, 7727–7732.
- 11 A. Occhiogrosso, A. Vasyunin, E. Herbst, S. Viti, M. D. Ward, S. D. Price and W. A. Brown, *Astron. Astrophys.*, 2014, **564**, 1–9.
- 12 A. Bergantini, M. J. Abplanalp, P. Pokhilko, A. I. Krylov, C. N. Shingledecker, E. Herbst and R. I. Kaiser, *Astrophys. J.*, 2018, **860**, 108.
- 13 A. C. A. Boogert, P. A. Gerakines and D. C. B. Whittet, *Annu. Rev. Astron. Astrophys.*, 2015, **53**, 541–581.
- 14 C. N. Shingledecker, J. Tennis, R. L. Gal and E. Herbst, *Astrophys. J.*, 2018, **861**, 20.
- 15 C. N. Shingledecker, R. Le Gal and E. Herbst, *Phys. Chem. Chem. Phys.*, 2017, **19**, 11043–11056.
- 16 R. I. Kaiser and K. Roessler, *Astrophys. J.*, 1998, **503**, 959–975.
- 17 R. I. Kaiser, S. Maity and B. M. Jones, *Phys. Chem. Chem. Phys.*, 2014, **16**, 3399–3424.
- 18 C. N. Shingledecker and E. Herbst, *Phys. Chem. Chem. Phys.*, 2018, **20**, 5359–5367.
- 19 C. Sagan and B. N. Khare, *Nature*, 1979, **277**, 102–107.
- 20 R. I. Kaiser, *Chem. Rev.*, 2002, **102**, 1309–1358.
- 21 C. J. Bennett, C. S. Jamieson, Y. Osamura and R. I. Kaiser, *Astrophys. J.*, 2005, **624**, 1097–1115.
- 22 C. J. Bennett, Y. Osamura, M. D. Lebar and R. I. Kaiser, *Astrophys. J.*, 2005, **634**, 698–711.
- 23 Y. S. Kim, C. J. Bennett, C. Li-Hsieh, K. O. Brien and R. I. Kaiser, *Astrophys. J.*, 2010, **711**, 744–756.
- 24 M. J. Abplanalp, M. Förstel and R. I. Kaiser, *Chem. Phys. Lett.*, 2016, **644**, 79–98.
- 25 M. H. Moore, B. Donn, R. Khanna and M. F. A'Hearn, *Icarus*, 1983, **54**, 388–405.
- 26 P. A. Gerakines, M. H. Moore and R. L. Hudson, *J. Geophys. Res.*, 2001, **106**, 33381–33385.
- 27 R. I. Kaiser, A. Gabrysch and K. Roessler, *Rev. Sci. Instrum.*, 1995, **66**, 3058–3066.
- 28 A. M. Turner, M. J. Abplanalp, T. J. Blair, R. Dayuha and R. I. Kaiser, *Astrophys. J., Suppl. Ser.*, 2018, **234**, 6.
- 29 M. J. Abplanalp, B. M. Jones and R. I. Kaiser, *Phys. Chem. Chem. Phys.*, 2018, **20**, 5435–5468.
- 30 R. I. Kaiser, S. Maity and B. M. Jones, *Angew. Chem., Int. Ed.*, 2015, **54**, 195–200.
- 31 S. Maity, R. I. Kaiser and B. M. Jones, *Phys. Chem. Chem. Phys.*, 2015, **17**, 3081–3114.

- 32 S. Maity, R. I. Kaiser and B. M. Jones, *Faraday Discuss.*, 2014, **168**, 485–516.
- 33 S. Maity, R. I. Kaiser and B. M. Jones, *Astrophys. J.*, 2014, **789**, 36–49.
- 34 L. Zhou, S. Maity, M. Abplanalp, A. Turner and R. I. Kaiser, *Astrophys. J.*, 2014, **790**, 38–47.
- 35 R. I. Kaiser, P. Jansen, K. Petersen and K. Roessler, *Rev. Sci. Instrum.*, 1995, **66**, 5226–5231.
- 36 G. Tarczay, M. Förstel, P. Maksyutenko and R. I. Kaiser, *Inorg. Chem.*, 2016, **55**, 8776–8785.
- 37 P. Maksyutenko, M. Förstel, P. Crandall, B.-J. Sun, M.-H. Wu, A. H. H. Chang and R. I. Kaiser, *Chem. Phys. Lett.*, 2016, **658**, 20–29.
- 38 NIST Standard Reference Database Number 69, <http://webbook.nist.gov/chemistry/ie-ser/>, (February 21, 2017).
- 39 C. Zhu, R. Frigge, A. M. Turner, M. J. Abplanalp, B.-J. Sun, Y.-L. Chen, A. H. H. Chang and R. I. Kaiser, *Phys. Chem. Chem. Phys.*, 2019, **21**, 1952–1962.
- 40 A. Bergantini, S. Góbi, M. J. Abplanalp and R. I. Kaiser, *Astrophys. J.*, 2018, **852**, 70.
- 41 M. J. Abplanalp, S. Góbi, A. Bergantini, A. M. Turner and R. I. Kaiser, *ChemPhysChem*, 2018, **19**, 556–560.
- 42 S. Góbi, P. B. Crandall, P. Maksyutenko, M. Förstel and R. I. Kaiser, *J. Phys. Chem. A*, 2018, **122**, 2329–2343.
- 43 C. Zhu, R. Frigge, A. M. Turner, R. I. Kaiser, B.-J. Sun, S.-Y. Chen and A. H. H. Chang, *Chem. Commun.*, 2018, **54**, 5716–5719.
- 44 R. Frigge, C. Zhu, A. M. Turner, M. J. Abplanalp, A. Bergantini, B.-J. Sun, Y.-L. Chen, A. H. H. Chang and R. I. Kaiser, *Astrophys. J.*, 2018, **862**, 84.
- 45 R. Frigge, C. Zhu, A. M. Turner, M. J. Abplanalp, B.-J. Sun, Y.-S. Huang, A. H. H. Chang and R. I. Kaiser, *Chem. Commun.*, 2018, **54**, 10152–10155.
- 46 M. J. Abplanalp, S. Góbi and R. I. Kaiser, *Phys. Chem. Chem. Phys.*, 2019, **21**, 5378–5393.
- 47 G. Tarczay, M. Förstel, S. Góbi, P. Maksyutenko and R. I. Kaiser, *ChemPhysChem*, 2017, **18**, 882–889.
- 48 M. Förstel, Y. A. Tsegaw, P. Maksyutenko, A. M. Mebel, W. Sander and R. I. Kaiser, *ChemPhysChem*, 2016, **17**, 2726–2735.
- 49 R. I. Kaiser and P. Maksyutenko, *J. Phys. Chem. C*, 2015, **119**, 14653–14668.
- 50 B. M. Jones and R. I. Kaiser, *J. Phys. Chem. Lett.*, 2013, **4**, 1965–1971.
- 51 R. I. Kaiser and K. Roessler, *Astrophys. J.*, 1997, **475**, 144–154.
- 52 C. J. Bennett, C. S. Jamieson, Y. Osumura and R. I. Kaiser, *Astrophys. J.*, 2006, **653**, 792–811.
- 53 M. J. Abplanalp and R. I. Kaiser, *Astrophys. J.*, 2017, **836**, 195–226.
- 54 M. J. Abplanalp and R. I. Kaiser, *Astrophys. J.*, 2016, **827**, 132–161.
- 55 W. Zheng, D. Jewitt, Y. Osumura and R. I. Kaiser, *Astrophys. J.*, 2008, **674**, 1242–1250.
- 56 W. Zheng, D. Jewitt and R. I. Kaiser, *Astrophys. J.*, 2006, **648**, 753.
- 57 R. I. Kaiser, A. M. Stockton, Y. S. Kim, E. C. Jensen and R. A. Mathies, *Astrophys. J.*, 2013, **765**, 111–119.
- 58 C. J. Bennett, S. J. Brotton, B. M. Jones, A. K. Misra, S. K. Sharma and R. I. Kaiser, *Anal. Chem.*, 2013, **85**, 5659–5665.
- 59 B. M. Jones, R. I. Kaiser and G. Strazzulla, *Astrophys. J.*, 2014, **788**, 170.
- 60 B. M. Jones, R. I. Kaiser and G. Strazzulla, *Astrophys. J.*, 2014, **781**, 85–96.
- 61 Y. A. Tsegaw, S. Góbi, M. Förstel, P. Maksyutenko, W. Sander and R. I. Kaiser, *J. Phys. Chem. A*, 2017, **121**, 7477–7493.
- 62 S. Góbi, A. Bergantini and R. I. Kaiser, *Astrophys. J.*, 2016, **832**, 164.
- 63 P. Groner, I. Stolkin and H. H. Gunthard, *J. Phys. E: Sci. Instrum.*, 1973, **6**, 122–123.
- 64 A. M. Turner, M. J. Abplanalp, S. Y. Chen, Y. T. Chen, A. H. H. Chang and R. I. Kaiser, *Phys. Chem. Chem. Phys.*, 2015, **17**, 27281–27291.
- 65 A. M. Turner, M. J. Abplanalp and R. I. Kaiser, *Astrophys. J.*, 2016, **819**, 97.
- 66 M. J. Abplanalp, A. Borsuk, B. M. Jones and R. I. Kaiser, *Astrophys. J.*, 2015, **814**, 45–61.
- 67 P. A. Gerakines and R. L. Hudson, *Astrophys. J.*, 2015, **805**, L20.
- 68 R. Hudson, P. Gerakines and M. Moore, *Icarus*, 2014, **243**, 148–157.
- 69 R. L. Hudson, R. F. Ferrante and M. H. Moore, *Icarus*, 2014, **228**, 276–287.
- 70 P. A. Gerakines, W. A. Schutte, J. M. Greenberg and E. F. van Dishoeck, *Astron. Astrophys.*, 1995, **296**, 810–818.
- 71 A. M. Turner, A. Bergantini, M. J. Abplanalp, C. Zhu, S. Góbi, B.-J. Sun, K.-H. Chao, A. H. H. Chang, C. Meinert and R. I. Kaiser, *Nat. Commun.*, 2018, **9**, 3851–3859.
- 72 P. Maksyutenko, L. G. Muzangwa, B. M. Jones and R. I. Kaiser, *Phys. Chem. Chem. Phys.*, 2015, **17**, 7514–7527.
- 73 M. Förstel, P. Maksyutenko, B. M. Jones, B.-J. Sun, S.-H. Chen, A. H. H. Chang and R. I. Kaiser, *ChemPhysChem*, 2015, **16**, 3139–3142.
- 74 G. Strazzulla and R. E. Johnson, in *Comets in the Post-Halley Era*, ed. R. L. Newburn, Jr., M. Neugebauer and J. Rahe, Springer Netherlands, Dordrecht, 1991, pp. 243–275.
- 75 M. H. Moore and R. L. Hudson, *Proc. IAU*, 2006, **1**, 247.
- 76 M. H. Moore and R. L. Hudson, *Proc. IAU*, 2005, **1**, 247–260.
- 77 D. Drouin, A. R. Couture, D. Joly, X. Tastet, V. Aimez and R. Gauvin, *Scanning*, 2007, **29**, 92–101.
- 78 G. J. H. van Nes, PhD thesis, University of Groningen, 1978.
- 79 R. K. McMullan, A. Kvik and P. Popelier, *Acta Crystallogr., Sect. B: Struct. Sci.*, 1992, **48**, 726–731.
- 80 S. Góbi, M. Förstel, P. Maksyutenko and R. I. Kaiser, *Astrophys. J.*, 2017, **835**, 241.
- 81 S. Góbi, A. Bergantini and R. I. Kaiser, *Astrophys. J.*, 2017, **838**, 84.
- 82 S. Góbi, A. Bergantini, A. M. Turner and R. I. Kaiser, *J. Phys. Chem. A*, 2017, **121**, 3879–3890.
- 83 A. Bergantini, P. Maksyutenko and R. I. Kaiser, *Astrophys. J.*, 2017, **841**, 96.

- 84 M. Förstel, A. Bergantini, P. Maksyutenko, S. Göbi and R. I. Kaiser, *Astrophys. J.*, 2017, **845**, 83.
- 85 M. Förstel, P. Maksyutenko, A. M. Mebel and R. I. Kaiser, *Astrophys. J.*, 2016, **818**, L30.
- 86 A. Bergantini, R. Frigge and R. I. Kaiser, *Astrophys. J.*, 2018, **859**, 59.
- 87 R. I. Kaiser and P. Maksyutenko, *Chem. Phys. Lett.*, 2015, **631–632**, 59–65.
- 88 M. Förstel, P. Maksyutenko, B. M. Jones, B. J. Sun, A. H. H. Chang and R. I. Kaiser, *Chem. Commun.*, 2016, **52**, 741–744.
- 89 R. I. Kaiser, G. Eich, A. Gabrysch and K. Roessler, *Astrophys. J.*, 1997, **484**, 487–498.
- 90 B. M. Jones, C. J. Bennett and R. I. Kaiser, *Astrophys. J.*, 2011, **734**, 78–90.
- 91 L. Zhou, R. I. Kaiser, L. G. Gao, A. H. H. Chang, M. C. Liang and Y. L. Yung, *Astrophys. J.*, 2008, **686**, 1493–1502.
- 92 C. S. Jamieson and R. I. Kaiser, *Chem. Phys. Lett.*, 2007, **440**, 98–104.
- 93 G. A. Guirgis, B. R. Drew, T. K. Gounev and J. R. Durig, *Spectrochim. Acta, Part A*, 1998, **54**, 123–143.
- 94 W. Coleman and B. M. Gordon, *Appl. Spectrosc.*, 1987, **41**, 1159–1162.
- 95 W. Coleman and B. M. Gordon, *Appl. Spectrosc.*, 1987, **41**, 1169–1172.
- 96 X. K. Zhang, E. G. Lewars, R. E. March and J. M. Parnis, *J. Phys. Chem.*, 1993, **97**, 4320–4325.
- 97 G. Socrates, *Infrared and Raman characteristic group frequencies: tables and charts*, John Wiley & Sons, 2004.
- 98 B. Yang, J. Wang, T. A. Cool, N. Hansen, S. Skeen and D. L. Osborn, *Int. J. Mass Spectrom.*, 2012, **309**, 118–128.
- 99 J. I. M. Pastoors, A. Bodi, P. Hemberger and J. Bouwman, *Chem. – Eur. J.*, 2017, **23**, 13131–13140.
- 100 T. A. Cool, K. Nakajima, T. A. Mostefaoui, F. Qi, A. McIlroy, P. R. Westmoreland, M. E. Law, L. Poisson, D. S. Peterka and M. Ahmed, *J. Chem. Phys.*, 2003, **119**, 8356–8365.
- 101 G. Bieri, L. Åsbrink and W. von Niessen, *J. Electron Spectrosc. Relat. Phenom.*, 1982, **27**, 129–178.
- 102 T. A. Cool, J. Wang, K. Nakajima, C. A. Taatjes and A. McIlroy, *Int. J. Mass Spectrom.*, 2005, **247**, 18–27.
- 103 F. Goulay, A. J. Trevitt, J. D. Savee, J. Bouwman, D. L. Osborn, C. A. Taatjes, K. R. Wilson and S. R. Leone, *J. Phys. Chem. A*, 2012, **116**, 6091–6106.
- 104 J. C. Traeger, *Int. J. Mass Spectrom.*, 1985, **66**, 271–282.
- 105 T. Butscher, F. Duvernay, P. Theule, G. Danger, Y. Carissan, D. Hagebaum-Reignier and T. Chiavassa, *Mon. Not. R. Astron. Soc.*, 2015, **453**, 1587–1596.
- 106 J. P. Porterfield, J. H. Baraban, T. P. Troy, M. Ahmed, M. C. McCarthy, K. M. Morgan, J. W. Daily, T. L. Nguyen, J. F. Stanton and G. B. Ellison, *J. Phys. Chem. A*, 2016, **120**, 2161–2172.
- 107 C. J. Bennett and R. I. Kaiser, *Astrophys. J.*, 2007, **661**, 899–909.
- 108 M. Förstel, P. Maksyutenko, B. M. Jones, B. J. Sun, H. C. Lee, A. H. H. Chang and R. I. Kaiser, *Astrophys. J.*, 2016, **820**, 117.
- 109 M. N. Ryazantsev, A. Jamal, S. Maeda and K. Morokuma, *Phys. Chem. Chem. Phys.*, 2015, **17**, 27789–27805.
- 110 B. Turner, *Astrophys. J.*, 1977, **213**, L75–L79.
- 111 B. E. Turner and A. J. Apponi, *Astrophys. J.*, 2001, **561**, L207–L210.
- 112 B. Zuckerman, B. Turner, D. Johnson, F. Clark, F. Lovas, N. Fourikis, P. Palmer, M. Morris, A. Lilley and J. Ball, *Astrophys. J.*, 1975, **196**, L99–L102.
- 113 L. Snyder, D. Buhl, P. Schwartz, F. Clark, D. Johnson, F. Lovas and P. Giguere, *Astrophys. J.*, 1974, **191**, L79.
- 114 W. M. Irvine, R. D. Brown, D. M. Cragg, P. Friberg, P. D. Godfrey, N. Kaifu, H. E. Matthews, M. Ohishi, H. Suzuki and H. Takeo, *Astrophys. J.*, 1988, **335**, L89–L93.
- 115 J. M. Hollis, J. R. Anthony, P. R. Jewell and F. J. Lovas, *Astrophys. J.*, 2006, **642**, 933.
- 116 J. M. Hollis, P. Jewell, F. Lovas, A. Remijan and H. Møllendal, *Astrophys. J.*, 2004, **610**, L21.
- 117 F. Combes, M. Gerin, A. Wootten, G. Włodarczak, F. Clausset and P. Encrenaz, *Astron. Astrophys.*, 1987, **180**, L13–L16.
- 118 B. Tercero, J. Cernicharo, A. López, N. Brouillet, L. Kolesníková, R. Motiyenko, L. Margulès, J. Alonso and J.-C. Guillemin, *Astron. Astrophys.*, 2015, **582**, L1.
- 119 J. M. Hollis, F. J. Lovas and P. R. Jewell, *Astrophys. J.*, 2000, **540**, L107–L110.
- 120 A. Belloche, R. T. Garrod, H. S. Müller and K. M. Menten, *Science*, 2014, **345**, 1584–1587.
- 121 J. Dickens, W. M. Irvine, M. Ohishi, M. Ikeda, S. Ishikawa, A. Nummelin and Å. Hjalmarsen, *Astrophys. J.*, 1997, **489**, 753.
- 122 B. A. McGuire, P. B. Carroll, R. A. Loomis, I. A. Finneran, P. R. Jewell, A. J. Remijan and G. A. Blake, *Science*, 2016, **352**, 1449.
- 123 A. Bergantini, C. Zhu and R. I. Kaiser, *Astrophys. J.*, 2018, **862**, 140.
- 124 C. J. Bennett, T. Hama, Y. S. Kim, M. Kawasaki and R. I. Kaiser, *Astrophys. J.*, 2011, **727**, 27.
- 125 K. Altwegg, H. Balsiger, J. J. Berthelier, A. Bieler, U. Calmonte, S. A. Fuselier, F. Goesmann, S. Gasc, T. I. Gombosi, L. Le Roy, J. de Keyser, A. Morse, M. Rubin, M. Schuhmann, M. G. G. T. Taylor, C. Y. Tzou and I. Wright, *Mon. Not. R. Astron. Soc.*, 2017, **469**, S130–S141.
- 126 J. C. Aponte, D. Whitaker, M. W. Powner, J. E. Elsila and J. P. Dworkin, *ACS Earth Space Chem.*, 2019, **3**, 463–472.